Cellular automorphisms and self duality

Lowell Abrams[*‡] and Daniel Slilaty[†‡]

August 3, 2013

Dedicated to John B. Conway on the occasion of his retirement.

Abstract

We catalog up to a type of reducibility all cellular automorphisms of the sphere, projective plane, torus, Klein bottle, and three-crosscaps (Dyck's) surface. We also show how one can obtain all self-dual embeddings in a surface S given a catalog of all irreducible cellular automorphisms in S.

[*]Department of Mathematics, The George Washington University, Washington, DC 20052. Email: labrams@gwu.edu

[†]Department of Mathematics and Statistics, Wright State University, Dayton, OH 45435. Email: daniel.slilaty@wright.edu.

[‡]Much of the work in this paper was completed during several visits between the two authors which were funded by the Department of Mathematics of The George Washington University and the Department of Mathematics and Statistics of Wright State University.

1 Introduction

A graph G is said to be *cellularly embedded* in a closed surface S if the complement of G in S is a disjoint union of regions homeomorphic to a disk; these regions are the *faces* of the embedding. Figure 1.1 illustrates two examples of cellular embeddings in the torus. (Ignore the asterisks for now.) Note that each face of an embedding of G in S is bounded by a closed walk in G.

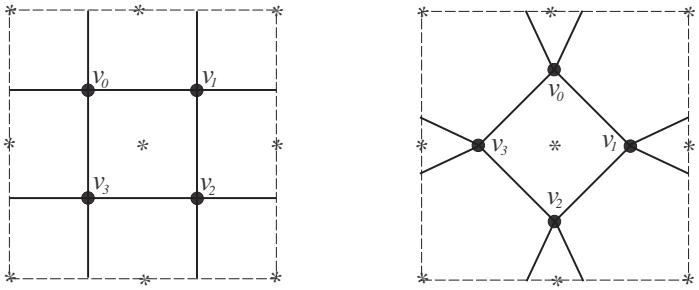

Figure 1.1.

Given a graph G cellularly embedded in a closed surface S, an automorphism of G is called a *cellular automorphism of G in S* when, loosely speaking, it takes facial boundary walks to facial boundary walks. These are often called *map automorphisms*. In Figure 1.1 a cellular automorphism of order 4 can be defined by sending each vertex v_i to v_{i+1} and mapping the edges accordingly. The asterisks indicate points fixed by some power of the automorphism less than 4. Note that any cellular automorphism of G in S induces an automorphism of the surface S itself, but that our use of the term "cellular automorphism" is essentially tied to the cellular structure given by the graph embedding. Thus the two different graph embeddings in Figure 1.1 give rise to two different cellular automorphisms even though the point-wise action on the torus is the same.[1]

Our first task in this paper is to elucidate some of the basic properties of cellular automorphisms and to define a notion of reduction of cellular automorphisms suitable for construction of complete catalogs of irreducible cellular automorphisms of a given surface. More specifically, "reduction" here involves deletion and contraction of orbits of edges, *i.e.*, graph minors compatible with the action of the automorphism. We verify the completeness of our catalogs with theorems of the following general form: *If φ is a cellular automorphism of G in S then φ reduces to a power of one of the following cellular automorphisms from our catalog for S.* We give complete catalogs in this way of all irreducible cellular automorphisms of the

[1]It is worth noting that cellular automorphisms of embedded graphs in S and elements of the mapping class group of S [9] are, in general, not related. In the mapping class group of the sphere, for example, the only nontrivial element is isotopic to the antipodal map, while nontrivial cellular automorphisms of graphs in the sphere can have various other forms (see Section 4). Also, it is known [16, 21] that the mapping class group of an orientable surface S of genus at least 1 is generated by Dehn twists. A Dehn twist, however, is performed locally around a simple closed curve, and therefore faces of an embedded graph which are not incident to this curve are fixed. By taking a facial subdivision if necessary, it follows that any such action on an embedded graph induces the identity cellular automorphism of the surface (see Proposition 2.2).

sphere (Section 4), projective plane (Section 5), torus (Section 6.1), Klein bottle (Section 7.1), and three-crosscaps surface, also known as *Dyck's surface* (Section 8.1). Note that we are essentially cataloguing automorphism/cellular-structure pairs. These are the main results of the first part of the paper.

Given graph G cellularly embedded in surface S, we define the *dual graph* G^* along with the dual embedding in S as follows: The vertices of G^* are the "centers" of the faces of G in S, and each edge e^* corresponds bijectively to an edge e of G and connects the vertices of G^* corresponding to the face(s) on either side of e. The embedding of G in S is *self-dual* if the cellular structure of vertices, edges and faces given by G in S is isomorphic to the cellular structure given by G^* in S; this implies that G and G^* are isomorphic graphs, but generally asserts more than that. There is a very close connection between self-duality and cellular automorphisms of quadrangular-faced embeddings in surfaces; this was explained by Archdeacon and Richter in [8] and we review it in Section 9.1.

Our second task in this paper is to provide procedures sufficient for constructing all possible self-dual graph embeddings in any closed surface S given a catalog of all irreducible cellular automorphisms in S. Our main results here are Constructions 9.14, 9.19, and 9.32 along with Theorems 9.15, 9.20, and 9.33. Given our catalogs, our procedures characterize all self-dual embeddings in the sphere, projective plane, torus, Klein bottle, and Dyck's surface. Self-dual embeddings in the sphere were previously characterized from three different perspectives by Archdeacon and Richter in [8], Servatius and Servatius in [30], and again by Servatius and Servatius in [31]. Self-dual embeddings in the projective plane were characterized by Archdeacon and Negami in [7].

Our key advance in this work is the development of an extendable framework designed to characterize exhaustively all cellular automorphisms and self-dual embeddings of any given surface. The remainder of this introduction surveys some of the extensive previous work relating to cellular automorphisms and self-duality, as well as highlighting some connections to other topics.

Tucker [41] proved that if a finite group Γ acts on a surface S then some Cayley graph G_Γ of Γ cellularly embeds in S such that every element of Γ induces a cellular automorphism of G_Γ in S. Note that Γ necessarily acts transitively on the vertices of G_Γ. Thomassen [39] uses the combinatorial restrictions imposed by vertex-transitivity to list all but finitely many of the vertex-transitive graphs which embed in the torus or Klein bottle. Pellicer and Weiss [28] also use such combinatorial restrictions to classify all vertex-transitive cellular embeddings in surfaces of non-negative Euler characteristic in terms of Schläfli symbols and various polyhedral constructions. (They further categorize these embeddings in terms of numbers of orbits of flags.) These two works [28, 39] are those most closely related to the first portion of this paper.

Our results in the first part of this paper differ from those in [28, 39] in several ways. Primarily, we give explicit depictions of the cellular actions of individual automorphisms rather than focusing on combinatorial structures implied by a transitive group action. (The highly structured grid rotations discussed in Section 6.1 are a good example of curiosities that can arise from this perspective.) Our approach has a notion of minimality and as a result many (although not all) of our minimal cellular automorphisms are vertex transitive. Nevertheless we do not rely on any initial presumption of transitivity. We also incorporate a detailed analysis of fixed points. Our approach is to a great extent motivated by the application in the second half of this paper of cellular automorphisms to the study of self-dual graph embeddings.

Our study of cellular automorphisms fundamentally involves consideration of their quotient spaces, which are essentially 2-dimensional instances of what Thurston termed "good orbifolds" in [40]. Conway and Huson discuss 2-dimensional orbifolds in [14], and in particular provide there an interesting notational scheme. The Thurston approach, using the notation from [14], is applied by Conway, Burgiel and Goodman-Strauss in [13] to derive the symmetry groups of the plane and sphere. Using similar techniques, Gross and Tucker [18, 6.3.3] classify all groups of symmetries acting on the torus. Motivated by questions from the study of Riemann surfaces Breuer and also Broughton, Kimura, Kuribayashi, and Kuribayashi [11, 12, 19, 20] implicitly use orbifolds to catalog and investigate all groups of orientation-preserving symmetries acting pseudofreely on the orientable surfaces of genus 2 through 48. Again, our interest here is not in classifying entire groups of symmetries acting on a given surface, but rather in classifying and cataloguing the ways in which an irreducible cellular structure in a 2-dimensional orbifold lifts back to the original surface and induces a

cellular automorphism.

Yet another tack different from the one taken here is surveyed by Širáň and Tucker [35], who present an almost completely group-theoretic approach to the study of vertex-transitive cellular automorphisms.

A well-established direction in the study of cellular automorphisms considers lifting a cellular automorphism of an embedded graph to a cellular automorphism of a covering graph in a covering surface. The covering construction of particular interest here is the voltage-graph lifting construction [18, §4.1,2]. Archdeacon, Gvozdjak, and Širáň in [5] and Širáň in [34] have observed that to lift a cellular automorphism through a voltage-graph lifting construction requires some notion of compatibility of the voltage assignment with the cellular automorphism; these sources each provide such compatibility conditions and use them to exhibit interesting examples. The lifting question in the case of graph coverings (not necessarily embeddings) has also been addressed. In [22] Malnič, Nedela, and Škoviera develop a unifying generalization called "voltage spaces" of the various types of voltage assignments and present corresponding criteria for lifting automorphisms. We use techniques from [22] in Section 3.3.3. In earlier work Surowski makes use, for a similar purpose, of the cohomology of a graph with values in a given group as an analogue of a voltage assignment [38].

Self-duality has been of interest since the discovery of the Platonic solids. More recently, Servatius and Servatius [32] point out three notions of self-duality for a graph G cellularly embedded in a surface S. First, *graph self-duality* refers to the existence of a graph isomorphism between G and its dual G^* in S. Second, *map self-duality* indicates the existence of a cellular isomorphism of G in S to G^* in S. (This is the type of duality we focus on in this paper.) Third, *matroid self-duality* applies when G and G^* have isomorphic cycle matroids. In general these three notions are distinct, but for 3-connected plane graphs they are equivalent by a result of Whitney [43].

Note that most of the results on self-duality surveyed below focus on self-dual embeddings for a given class of graphs in different surfaces. We, however, catalogue all different map-self-dual embeddings for a given surface, like what was done for the sphere in [8, 30, 31] and for the projective plane in [7].

One popular approach to self-duality has been to devise specific constructions that produce self-dual embeddings. In [3] Archdeacon surveys three techniques for constructing self-dual polyhedra, two of which can be used to construct involutory self-dual polyhedra, and the other of which, called the *addition construction*, provides a means to combine two graph-self-dual embeddings to obtain a third. The addition construction is used by Archdeacon and Hartsfield in [6] to construct graph-self-dual embeddings of complete bipartite graphs and by Archdeacon in [4] to construct graph-self-dual embeddings of complete multipartite graphs. Servatius and Christopher [29] offer two constructions for combining any plane graph with its dual to produce a map-self-dual plane graph. In [30] Servatius and Servatius show how all map-self-dual plane embeddings can be constructed by iteratively applying particular operations they call δ-expansions to one of a few basic plane graphs.

Another popular topic is self-duality for embedded Cayley graphs and Cayley maps, such as in White [42] and Stahl [36], which deal with graph-self-duality, and Anderson and Richter [2] which addresses map-self-duality.

The special case of cellular automorphisms and self-duality in just the torus itself has many interesting connections to geometry in the plane. A *wallpaper isometry* is an isometry of the plane that preserves a regular square or hexagonal grid. Drawing on work of Coxeter and Moser [15], Gross and Tucker show that any finite group of automorphisms of the torus is a quotient of a group of wallpaper isometries [18, p. 295]. Our work elaborates on this relationship between the torus and the plane in the following way. Any plane graph which is invariant under some wallpaper isometry is called a *plane lattice*. Since the plane is the universal cover of the torus, an isometry that leaves a plane lattice invariant projects down to a cellular automorphism on the torus. (Note, though, that this projection is certainly not unique.) Conversely, any cellular automorphism of the torus can be lifted to a cellular automorphism of a plane graph via the Map-Extension Theorem [23, Ch.5]. Although it is not *a priori* obvious that the automorphism of the plane can be chosen to be an isometry, it does follow from our catalog by checking each automorphism individually. As such, our characterization of all cellular automorphisms on the torus can be viewed as a characterization

of all projections of isometries of plane lattices down to the torus.

Given that any cellular automorphism of the torus can be lifted to a plane lattice, any self-dual embedding in the torus can be lifted to a self-dual plane lattice. Conversely, any self-dual plane lattice maps down to a self-dual embedding in the torus. As such, a characterization of all self-dual embeddings in the torus is a characterization of projections of self-dual plane lattices. A direct cataloguing of these self-dual plane lattices was accomplished by Servatius and Servatius in [33]. In that same paper the authors address the question of when the automorphism group of an infinite plane graph may be realized as a group of isometries of the plane.

Interestingly, self-dual plane lattices are also of special interest in percolation theory. Bollobás and Riordan prove [10, §5.4] that for any plane lattice G which is invariant under reflection through the origin, the critical bond-percolation probabilities for G and its plane dual G^* sum to 1. Thus, such a plane lattice which is self-dual will have percolation threshold exactly equal to $\frac{1}{2}$. The concept of self-duality also plays an important role in work of Ziff and Scullard [46] which exhibits exact values of percolation thresholds for many plane lattices. Partially motivated by percolation theory, Wierman [44] outlines several methods of constructing infinite self-dual graphs, although not all are lattices; he comments there [44, §4] that "it may be possible to characterize periodic infinite self-dual graphs" (*i.e.*, self-dual plane lattices) by characterizing self-dual graphs on the torus in a manner analogous to that of [8] for the sphere. In fact, this is one of the items accomplished in this paper and also in [33].

2 Cellular automorphisms

Throughout the paper we assume that the reader is familiar with the topology of surfaces, their homology groups, and curves on surfaces such as what is presented in Giblin [17] or Stillwell [37].

2.1 Graph basics

A *graph* G consists of a collection of vertices (*i.e.,* topological 0-cells), denoted by $V(G)$, and a set of edges (*i.e.,* topological 1-cells), denoted by $E(G)$, where an edge has two ends each of which is attached to a vertex. A *link* is an edge that has its ends incident to distinct vertices and a *loop* is an edge that has both of its ends incident to the same vertex. When we refer to an edge $e \in E(G)$ we presume a choice of direction along that edge. The same edge with the opposite direction is denote by $-e$. Given this direction on e we have a well defined ordering of the endpoints. The tail endpoint is referred to by $\mathbf{t}(e)$ and the head endpoint by $\mathbf{h}(e)$. Thus $\mathbf{h}(-e) = \mathbf{t}(e)$. We do not consider graphs with isolated vertices unless specifically mentioned.

A *walk* in G is a sequence of edges $w = e_1, \ldots, e_n$ such that $\mathbf{h}(e_i) = \mathbf{t}(e_{i+1})$ for each $i \in \{1, \ldots, n-1\}$. We say the *length* of w is n. If $\mathbf{h}(e_n) = \mathbf{t}(e_1)$ we say that w is *closed*. We consider any cyclic shift of a closed walk to be the same closed walk. We write $-w = -e_n, \ldots, -e_1$. For two graphs G and H an *isomorphism* $\varphi\colon G \to H$ is a bijection $\varphi\colon (V(G) \sqcup E(G)) \to (V(H) \sqcup E(H))$ where $\varphi(V(G)) = V(H)$, $\varphi(E(G)) = E(H)$, $\varphi\mathbf{h} = \mathbf{h}\varphi|_{E(G)}$, and $\varphi\mathbf{t} = \mathbf{t}\varphi|_{E(G)}$. An isomorphism naturally extends to walks in G and takes them to walks in H. In much of combinatorics, the usual notion of isomorphism on two simple graphs G and H is a bijection on the vertex sets such that two vertices in G are adjacent iff their images in H are adjacent. Our definition of isomorphism on general graphs coincides with the usual notion of isomorphism on simple graphs.

Let $C_1(G)$ denote the $\mathbb{Z}$-module $\langle e : e \in E(G)\rangle$. Given a walk $w = e_1, \ldots, e_n$ we misuse notation and also use w to refer to $\sum_i e_i$. Let $Z_1(G)$ denote the submodule of $C_1(G)$ generated by closed walks. An introduction to voltage graphs and their derived graphs can be found in [18, §2.1], but we describe these briefly here. Given a cyclic group A (in this work all groups are cyclic and written additively), an *A-voltage* assignment on graph G is a function $\sigma\colon E(G) \to A$ such that $\sigma(e) = -\sigma(-e)$. Given σ we construct the *derived graph* G^σ as follows. We have $V(G^\sigma) = V(G) \times A$ and $E(G^\sigma) = E(G) \times A$ where (x, a), for $x \in V(G)$ or $x \in E(G)$, is denoted by x_a. Then $\mathbf{t}(e_a) = \mathbf{t}(e)_a$ and $\mathbf{h}(e_a) = \mathbf{h}(e)_{a+\sigma(e)}$.

If σ is an A-voltage assignment on a graph G, we use σ_* to denote the induced $\mathbb{Z}$-module map $Z_1(G) \to \mathbb{A}$. Given $\eta\colon V(G) \to A$ define $\sigma^\eta\colon E(G) \to A$ by $\sigma^\eta(e) = \eta\mathbf{h}(e) + \sigma(e) - \eta\mathbf{t}(e)$. Evidently $\sigma_* = \sigma^\eta_*$. Conversely,

if $\sigma_* = \tau_*$ then there is an η such that $\tau = \sigma^\eta$ [45]. We use the following proposition repeatedly without further mention.

Proposition 2.1. *If σ and η are as above, then $G^\sigma \cong G^{\sigma^\eta}$.*

Proof. Define $\psi\colon (V(G^\sigma) \sqcup E(G^\sigma)) \to \big(V(G^{\sigma^\eta}) \sqcup E(G^{\sigma^\eta})\big)$ by $\psi(v_a) = v_{a+\eta(v)}$ and $\psi(e_a) = e_{a+\eta\mathbf{t}(e)}$. Clearly, ψ is bijective. Also, we have

$$\mathbf{t}\psi(e_a) = \mathbf{t}(e_{a+\eta\mathbf{t}(e)}) = \mathbf{t}(e)_{a+\eta\mathbf{t}(e)} = \psi\mathbf{t}(e_a)$$

and

$$\mathbf{h}\psi(e_a) = \mathbf{h}(e_{a+\eta\mathbf{t}(e)}) = \mathbf{h}(e)_{a+\eta\mathbf{t}(e)+\sigma^\eta(e)} = \mathbf{h}(e)_{a+\sigma(e)+\eta\mathbf{h}(e)} = \psi\mathbf{h}(e)_{a+\sigma(e)} = \psi\mathbf{h}(e_a).$$

□

When G is embedded in a closed surface S such that $S \setminus G$ is a collection of open 2-cells (called *faces*) with 1-dimensional boundaries we say that G is *cellularly* embedded in S. Note that this requires that G be connected and also excludes the embedding of a single vertex in the sphere from being termed cellular. Let $F(G)$ be the collection of faces and view each face $f \in F(G)$ as a labeled regular n-gon where n is the length of the facial boundary walk around f. An *oriented face* of G consists of a choice of face f along with a starting vertex and direction along the n-gon (in other words, it is a choice of face along with a choice of a flag of that face). If f is an oriented face and θ is an element of the dihedral group of order $2n$, then define the oriented face θf in the obvious fashion. Denote the set of oriented faces by $\vec{F}(G)$. The boundary walk in G of $f \in \vec{F}(G)$ is denoted by $\partial(f)$; this is a closed walk in G beginning at the designated starting vertex and proceeding in the specified direction along f. Note that $\partial(\theta f) = \partial(f)$ when θ is a rotation and $\partial(\theta f) = -\partial(f)$ when θ is a reflection. It is also possible (when S is the sphere) that two different oriented faces coming from distinct underlying unoriented faces have the same boundary walk. A *cellular isomorphism* from G_1 in S to G_2 in S is a bijection $\varphi\colon (V(G_1) \sqcup E(G_1) \sqcup \vec{F}(G_1)) \to (V(G_2) \sqcup E(G_2) \sqcup \vec{F}(G_2))$ satisfying the following: φ restricted to $V(G_1) \sqcup E(G_1)$ is an isomorphism from G_1 to G_2 and φ restricted to $\vec{F}(G_1)$ takes n-sided faces to n-sides faces such that for each $f \in \vec{F}(G_1)$ we have $\varphi(\theta f) = \theta\varphi(f)$ and $\varphi\partial = \partial\varphi|_{\vec{F}(G)}$. When $G_1 = G_2$ we call φ a *cellular automorphism*.

A *minor* of a graph G is a graph obtained by contractions and deletions of edges and deletions of isolated vertices. By convention isolated vertices are deleted as they occur; it is known that deletions and contractions of edges can be performed singly, together, and in different orders without affecting the resulting minor. The deletion of edge set D and contraction of edge set C is denoted by $G\backslash D/C$. A *surface minor* of a graph G cellularly embedded in a closed surface S is a minor that is connected and whose induced embedding is still cellular.

Now let S denote a surface with holes whose boundaries are pointwise disjoint, and let $[S]^\bullet$ denote the surface with those holes capped by disks. We say that G is *properly* embedded in S if G is cellularly embedded in $[S]^\bullet$ in such a way that each boundary of a hole is covered by a cycle of G. If C is a cycle covering the boundary of a hole, we call C a *hole-cycle*. A *surface minor* of G in S is a surface minor of G in $[S]^\bullet$ that is properly embedded in S.

Given G embedded in closed surface S, there is a *topological dual* embedding of a graph G^* in S. The vertices of G^* are the centers of the faces of G in S and for each edge e in G the dual edge in G^* connects the vertices in the face(s) on either side of e.

2.2 Fixed points

Given a cellular automorphism of G in a closed surface S, we denote the set of fixed points of φ by $\mathrm{fix}(\varphi)$. This is the set of points on S that are fixed by φ when we consider each face as a regular n-gon. If $C \subseteq \mathrm{fix}(\varphi)$ forms a simple closed curve on S, then we call C an *oval* of φ. Given $f \in \vec{F}(G)$, if $\varphi(f) = \theta f$ for some dihedral symmetry θ, then θ is the identity symmetry iff $\varphi(e) = e$ for every edge in $\partial(f)$ iff $\varphi(e) = e$ for some e in $\partial(f)$. When $\varphi(f) = f$ (*i.e.,* with $\theta = 1$) we say that φ *fixes* f.

Proposition 2.2. *If φ is a cellular automorphism of G in S, then given $f \in \vec{F}(G)$ and e on $\partial(f)$, φ is uniquely determined by $\varphi(f)$ and $\varphi(e)$. In particular, φ fixes some $f \in \vec{F}(G)$ iff φ is the identity map.*

Proof. Given $\varphi(f)$ and $\varphi(e)$, the remaining values of $\varphi(e')$ for all other e' in $\partial(f)$ are uniquely determined. Then for any $f' \in \vec{F}(G)$ adjacent to f, $\varphi(f')$ is uniquely determined. The rest of φ then follows inductively by the fact that G^* is connected when G is cellularly embedded. □

Proposition 2.3. *If a cellular automorphism φ of G in S is not the identity map, then fix(φ) is a disjoint union of ovals and isolated points where*

(1) an isolated fixed point is either at a vertex of G, the midpoint of an edge of G, or the center of a face of G;

(2) for any $e \in E(G)$, fix(φ) $\cap\, e$ is either all of e or the midpoint of e; and

(3) for any $f \in \vec{F}(G)$, fix(φ) $\cap\, f$ is either an isolated point at the center of f or a line segment connecting two antipodal points on the boundary of f.

Proof. Let $x \in \mathrm{fix}(\varphi)$. If x is in the interior of some $f \in \vec{F}(G)$, then $\varphi(f) = \theta f$ for some θ which is a reflection or nontrivial rotation. In the former case $\mathrm{fix}(\varphi) \cap f$ is a line segment connecting two antipodal points on the boundary of f and in the latter case x is an isolated fixed point at the center of f. If x is in the interior of some $e \in E(G)$, then x is the midpoint of e when $\varphi(e) = -e$ or $e \cap \mathrm{fix}(\varphi) = e$ when $\varphi(e) = e$.

We now have that $\mathrm{fix}(\varphi)$ is a collection of isolated points as in (1) along with a collection of line segments. Since the action of φ around any line segment is a reflection, each endpoint of these line segments connects to exactly one other such line segment. This gives us our desired conclusion. □

Write $|\varphi|$ to denote the order of φ.

Proposition 2.4. *If φ is a cellular automorphism of G in S and $|\varphi| > 2$, then fix(φ) is a collection of isolated points on S.*

Proof. By way of contradiction suppose that $x \in \mathrm{fix}(\varphi)$ is part of an oval. In that case the intersection of $\mathrm{fix}(\varphi)$ and a very small neighborhood around x is a line segment going through x. The map φ^2 fixes this whole neighborhood and so, by Proposition 2.3, φ^2 is the identity. □

Given $|\varphi| = n$, let $\overline{\mathrm{fix}}(\varphi) = \mathrm{fix}(\varphi) \cup \mathrm{fix}(\varphi^2) \cup \cdots \cup \mathrm{fix}(\varphi^{n-1})$. We call $\overline{\mathrm{fix}}(\varphi)$ the set of *pseudofixed* points of φ. When $\overline{\mathrm{fix}}(\varphi)$ has no ovals (*i.e.,* contains only isolated points) then φ is called *pseudofree* and when $\overline{\mathrm{fix}}(\varphi) = \emptyset$ we call φ *free*.

Proposition 2.5. *If φ is a cellular automorphism of G in S then, for any k,*

(1) fix(φ) $\subseteq$ fix(φ^k),

(2) φ(fix(φ^k)) = fix(φ^k), and

(3) $\varphi(\overline{\mathrm{fix}}(\varphi)) = \overline{\mathrm{fix}}(\varphi)$.

Proof. That $\mathrm{fix}(\varphi) \subseteq \mathrm{fix}(\varphi^k)$ is evident. Now if $x \in \mathrm{fix}(\varphi^k)$ then $\varphi^k(\varphi(x)) = \varphi^{k+1}(x) = \varphi(\varphi^k(x)) = \varphi(x)$, which implies $\varphi(x) \in \mathrm{fix}(\varphi^k)$ and so $\varphi(\mathrm{fix}(\varphi^k)) \subseteq \mathrm{fix}(\varphi^k)$. Also $\varphi^k(\varphi^{-1}(x)) = \varphi^{k-1}(x) = \varphi^{-1}(\varphi^k(x)) = \varphi^{-1}(x)$ and so $\varphi^{-1}(x) \in \mathrm{fix}(\varphi^k)$ which implies $x \in \varphi(\mathrm{fix}(\varphi^k))$. Thus $\mathrm{fix}(\varphi^k) \subseteq \varphi(\mathrm{fix}(\varphi^k))$ which implies $\varphi(\mathrm{fix}(\varphi^k)) = \mathrm{fix}(\varphi^k)$. That $\varphi(\overline{\mathrm{fix}}(\varphi)) = \overline{\mathrm{fix}}(\varphi)$ follows from (2). □

Given an isolated pseudofixed point x, the *index* of x is $|\mathsf{orbit}_\varphi(x)|$, which is also equal to n/t where $t \geq 1$ is the smallest integer such that $\varphi^t(x) = x$. By Proposition 2.5(3) and continuity, φ maps isolated pseudofixed points to isolated pseudofixed points and ovals to ovals. Given oval O, the smallest integer t such that $\varphi^t(O) = O$ is the *index* of the oval O. (Of course, t must divide $|\varphi|/2$.) Propositions 2.6 and 2.7 now follow.

Proposition 2.6. *If φ is a cellular automorphism of G in S, then $\overline{fix}(\varphi)$ is a disjoint union of isolated points and ovals that satisfies the structural properties in Proposition 2.3.*

Proposition 2.7. *If $\overline{fix}(\varphi)$ contains ovals $O_1, \ldots, O_t$, then φ induces a permutation on this set of ovals of order dividing $|\varphi|/2$.*

Given an oval O_i of φ of index m, $\varphi^m|_{O_i}$ is a well-defined dihedral action on O_i and so is either a rotation of O_i or a reflection of O_i. Proposition 2.8 tells us that this action is rotation rather than reflection when the oval has an annular neighborhood. Proposition 5.2 is the analogous result for when the oval has a Möbius neighborhood.

Proposition 2.8. *Let φ be a cellular automorphism of G in S whose set of pseudofixed points $\overline{fix}(\varphi)$ contains an oval O with an annular neighborhood in S. If m is the index of O, then we get the following.*

(1) The action of φ^m restricted to O itself is rotation, say of order r, rather than reflection.

(2) The action of φ^m restricted to a small annular neighborhood around O is rotation of odd order r followed by reflection.

(3) $|\varphi| = 2rm$

Proof. (1) If the action of φ^m on O itself is a reflection of O, then φ^{2m} fixes O. Furthermore, φ^{2m} fixes a thin annular neighborhood of O because either φ^m includes reflection of faces around O or does not. Thus φ^{2m} fixes any face incident to O and so φ^{2m} is the identity by Proposition 2.2. This however contradicts the fact that O is an oval because if $|\varphi^m| = 2$, then φ^m must fix O and not perform a reflection on O.

(2) Let $k = |\varphi|/2$. Since φ^k fixes O, the minimality of m implies that $m|k$. Since the action of φ^k on a thin annular neighborhood around O is reflection through O, the action of φ^m on the thin annular neighborhood around O must include a reflection along with the rotation. Furthermore, the order of the rotation must be odd.

(3) This follows by the minimality of m and Proposition 2.2. □

Proposition 2.9. *If φ is a non-pseudofree involutory cellular automorphism of G in S and the ovals of φ separate S then the ovals of φ separate S into two connected components.*

Proof. Because of the reflecting action of φ across the ovals, they must separate S into an even number of components, say $A_1, \ldots, A_k$ and $B_1, \ldots, B_k$ where φ exchanges A_i and B_i. But then the ovals on A_i connect only to the ovals on B_i. Connectivity of S now implies that $k = 1$. □

2.3 Minors, augmentations, and induced automorphisms

2.3.1 Orbit minors

Let φ be an automorphism of G. Given $C, D \subset E(G)$ with $\mathsf{orbit}_\varphi(C) \cap \mathsf{orbit}_\varphi(D) = \emptyset$ we call the minor $H = G/\mathsf{orbit}_\varphi(C)\backslash\mathsf{orbit}_\varphi(D)$ an *orbit minor* of G with respect to φ. The orbit minor is called *nontrivial* when it has at least one edge. The automorphism induced on H from Proposition 2.10 we shall denote by $\varphi|_H$.

Proposition 2.10. *Let φ be an automorphism on G and let $H = G/\mathsf{orbit}_\varphi(C)\backslash\mathsf{orbit}_\varphi(D)$ be an orbit minor. If π is the projection map from $G\backslash\mathsf{orbit}_\varphi(D)$ to H, then $\pi\varphi\pi^{-1}$ is a well-defined automorphism on H.*

Proof. Note that $E(H) = E(G) \setminus \mathsf{orbit}_\varphi(D \cup C)$ and that φ restricts to a well defined permutation of $E(H) \subseteq E(G)$ since we are deleting full orbits of edge-sets. If follows that $(\pi\varphi\pi^{-1})|_{E(H)} = \varphi|_{E(H)}$. Now for each vertex v in H, $\pi^{-1}(v)$ is either a single vertex or corresponds to a connected component of the subgraph of G on $\mathsf{orbit}_\varphi(C)$. As such $\pi\varphi\pi^{-1}(v)$ is well defined. For each edge e in H, there is a well-defined edge $e' = \pi^{-1}(e)$ such that the endpoint functions $\mathbf{h}_H$ and $\mathbf{h}_G$ satisfy $\pi\mathbf{h}_G(e') = \mathbf{h}_H\pi(e')$ and

$\mathbf{h}_G\pi^{-1}(e) \in \pi^{-1}\mathbf{h}_H(e)$. These along with the fact that $\pi\varphi\pi^{-1}(v)$ is well defined on the vertices of H yields the following which tells us that that $\pi\varphi\pi^{-1}$ is a well-defined automorphism on H.

$$\mathbf{h}_H\pi\varphi\pi^{-1}(e) = \mathbf{h}_H\pi\varphi(e') = \pi\mathbf{h}_G\varphi(e') = \pi\varphi\mathbf{h}_G(e') = \pi\varphi\mathbf{h}_G\pi^{-1}(e) = \pi\varphi\pi^{-1}\mathbf{h}_H(e)$$

□

2.3.2 Surface orbit minors

Let φ be a cellular automorphism of G in S and let $C, D \subset E(G)$ be such that

(M1) $\mathsf{orbit}_\varphi(C) \cap \mathsf{orbit}_\varphi(D) = \emptyset$,

(M2) the subgraph of $\mathsf{orbit}_\varphi(C)$ in G is acyclic,

(M3) no connected component of $\mathsf{orbit}_\varphi(C)$ intersects two connected components of $\overline{\mathrm{fix}}(\varphi)$,

(M4) $G\backslash\mathsf{orbit}_\varphi(D)$ is connected and cellularly embedded in S,

(M5) the points of $\overline{\mathrm{fix}}(\varphi)$ on S satisfy the structural criterion in Proposition 2.6 with respect to the induced embedding of $G/\mathsf{orbit}_\varphi(C)\backslash\mathsf{orbit}_\varphi(D)$.

In this case we call $G/\mathsf{orbit}_\varphi(C)\backslash\mathsf{orbit}_\varphi(D)$ a *surface orbit minor* with respect to φ. The cellular automorphism of H in S given in Proposition 2.11 we will denote by $\varphi|_H$.

Proposition 2.11. *Let φ be a cellular automorphism of G in S and let $H = G/\mathsf{orbit}_\varphi(C)\backslash\mathsf{orbit}_\varphi(D)$ be a surface orbit minor. If ρ is the projection map of $F(G)$ to $F(G\backslash\mathsf{orbit}_\varphi(D))$ and the identity map on $G \setminus \mathsf{orbit}_\varphi(D)$ and π is the projection map from $G\backslash\mathsf{orbit}_\varphi(D)$ to H and the identity map on $F(G\backslash\mathsf{orbit}_\varphi(D))$, then $\pi\rho\varphi\rho^{-1}\pi^{-1}$ is a well-defined cellular automorphism on H in S.*

Write $G' = G \setminus \mathsf{orbit}_\varphi(D)$. If f is an oriented face of H then it has a designated starting vertex v with a choice of direction along the underlying 2-cell. As such while there is only a single choice of 2-cell and direction in G' for $\pi^{-1}(f)$, there may be several choices of a designated vertex. However, all of these choices necessarily belong to the connected subgraph $\pi^{-1}(v)$, so for our purposes the choice may be made arbitrarily. Thus, if θ is any dihedral symmetry of f then $\pi^{-1}(\theta f) = \theta'\pi^{-1}(f)$ for some dihedral symmetry θ'.

Note also that $\pi^{-1}\partial_H(f)$ is not defined since $\partial_H(f)$ is not simply a subgraph. In this specialized case we define $\pi^{-1}\partial_H(f)$ to be $\partial_{G'}\pi^{-1}(f)$.

Proof of Proposition 2.11. If $f_1, f_2 \in \vec{F}(G)$ share a boundary edge e, then $\varphi(f_1)$ and $\varphi(f_2)$ share the boundary edge $\varphi(e)$. As such $\rho\varphi\rho^{-1}$ is well-defined on $\vec{F}(G')$ and we get that $\partial_{G'}\rho\varphi\rho^{-1}(f) = \rho\varphi\rho^{-1}\partial_{G'}(f)$ for any $f' \in \vec{F}(G')$.

Now for any $f \in \vec{F}(H)$ we have an oriented face $f' = \pi^{-1}(f) \in \vec{F}(G')$ as discussed above; furthermore, we get that $\partial_H\pi(f') = \pi\partial_{G'}(f')$. So now

$$\partial_H\pi\rho\varphi\rho^{-1}\pi^{-1}(f) = \pi\partial_{G'}\rho\varphi\rho^{-1}\pi^{-1}(f) = \pi\rho\varphi\rho^{-1}\partial_{G'}\pi^{-1}(f) = \pi\rho\varphi\rho^{-1}\pi^{-1}\partial_H(f).$$

Similarly, for any dihedral symmetry θ we get that

$$\pi\rho\varphi\rho^{-1}\pi^{-1}(\theta f) = \theta\pi\rho\varphi\rho^{-1}\pi^{-1}(f).$$

□

By the definition of surface orbit minors and Proposition 2.11 we get Proposition 2.12.

Proposition 2.12. *If φ is a cellular automorphism of G in S and H is a surface orbit minor of G with respect to φ, then there is a bijection between $\overline{fix}(\varphi)$ and $\overline{fix}(\varphi|_H)$ preserving isolation and index.*

Proposition 2.13. *Suppose φ is a cellular automorphism of G in S. The action of φ is uniquely determined by the action of $\varphi|_H$ on any nontrivial surface orbit minor H of G and, in particular, $|\varphi| = \left|\varphi|_H\right|$.*

Proof. We need only show that our result holds for $H = G/\mathsf{orbit}_\varphi(e)$ and $H = G\backslash\mathsf{orbit}_\varphi(e)$ for a single edge e and then the result in general follows by induction.

If $H = G/\mathsf{orbit}_\varphi(e)$, then let $E_1, \ldots, E_m$ be the connected components (necessarily acyclic, by definition of surface orbit minor) of the subgraph of G on edges $\mathsf{orbit}_\varphi(e)$. The surface orbit minor H is obtained from G by contracting these subgraphs $E_1, \ldots, E_m$ and obtaining vertices $v_1, \ldots, v_m$ which form a single orbit under $\varphi|_H$. Now take a small disk neighborhood D_i around each v_i. There is an induced dihedral action φ^m on D_i and φ acts in a prescribed way on the set of disks $D_1, \ldots, D_m$. The decontraction of E_i can be made to occur inside the disk D_i and the resulting configuration must be compatible with the dihedral action φ^m; furthermore, the action of φ on the set of disks has not changed.

If $H = G\backslash\mathsf{orbit}_\varphi(e)$, then let $F_1, \ldots, F_m$ be the faces of H in which edges from $\mathsf{orbit}_\varphi(e)$ were deleted. There is an induced dihedral action φ^m on any orientation $\vec{F}_i$ of F_i. So now $|\varphi|/m$ edges of $\mathsf{orbit}_\varphi(e)$ are added to $\vec{F}_i$ to obtain G in a way that is compatible with the dihedral action φ^m on $\vec{F}_i$.

In each of the two previous paragraphs, $|\varphi| = \left|\varphi|_H\right|$ by Proposition 2.2. □

Proposition 2.14. *If φ is a cellular automorphism of G_1 in S, G_2 in S is a surface orbit minor of G_1 in S with respect to φ, and G_3 is a surface orbit minor of G_2 in S with respect to φ, then G_3 is a surface orbit minor of G_1 in S with respect to φ.*

Proof. Say that $G_{i+1} = G_i/\mathsf{orbit}_\varphi(C_i)\backslash\mathsf{orbit}_\varphi(D_i)$. That (M1), (M3), and (M4) hold for $\mathsf{orbit}_\varphi(C_1 \cup C_2)$ and $\mathsf{orbit}_\varphi(D_1 \cup D_2)$ is immediate. That (M2) holds follows from the fact that if $\mathsf{orbit}_\varphi(C_1 \cup C_2)$ contains a cycle yet $\mathsf{orbit}_\varphi(C_1)$ is acyclic in G_1, then $\mathsf{orbit}_\varphi(C_2)$ must contain a cycle in G_2. That (M5) holds comes from the fact that G_3 in S is a surface orbit of G_2 in S which is a surface orbit minor of G_1 in S. □

2.3.3 Augmentation

Given an order-n cellular automorphism φ of G in S, it will become necessary later to move all of the isolated points of $\overline{\mathrm{fix}}(\varphi)$ off of G and include all of the ovals in G. We do this by a process we call *augmentation* in which we take φ on G in S and construct a graph $\overline{G}$ in S, described below, on which φ naturally induces a cellular automorphism which we also denote by φ. We call $\overline{G}$ the *augmentation* of G.

For each isolated pseudofixed point in the center of an edge (loop or link) of G, we replace the edge with the configuration shown in Figure 2.15 to obtain graph G'. There is a natural induced action of φ on G' in S and there is no isolated pseudofixed point of φ on the midpoint of an edge in G'. If there are no isolated pseudofixed points in the centers of edges of G, then let $G' = G$.

For isolated pseudofixed points at vertices of G' we replace small neighborhoods around these vertices with configurations as shown in Figure 2.15 to obtain a graph G''. Note that the cycles resulting from these replacements are pairwise vertex disjoint. Again, there is a natural induced action of φ on G'' in S and each isolated pseudofixed point of φ is now in the center of a face of G''. If there are no isolated pseudofixed points at the vertices of G', then let $G'' = G'$.

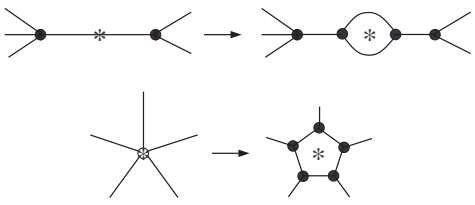

Figure 2.15.

If O is an oval of φ on G'' in S, then for each segment g of O in the interior of a face of G'' in S, replace g with the appropriate configuration as shown in Figure 2.16. Do this for all such segments and let $\overline{G}$ be the graph obtained. If there are no such segments, then let $\overline{G} = G''$. There is a natural induced action of φ on $\overline{G}$ in S and all ovals of φ are now cycles in $\overline{G}$. We call these cycles *oval-cycles*.

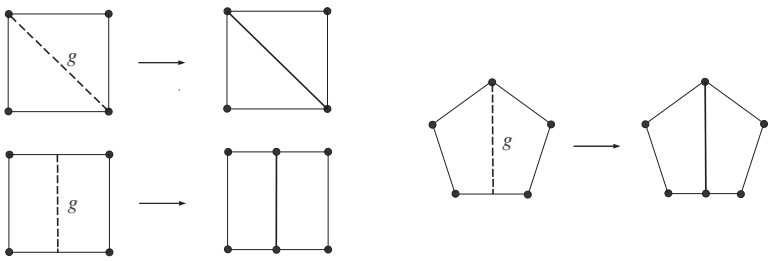

Figure 2.16.

If φ is a cellular automorphism of G in S and if $\overline{G} \neq G$, then we say that φ is *augmentable*.

2.3.4 Reducing cellular automorphisms

Given two cellular automorphisms φ of G in S and ψ of H in S, we say that φ *reduces to* ψ (which we denote by $\varphi \rightsquigarrow \psi$) when there is a surface orbit minor K of G and a cellular isomorphism $\eta\colon K \to H$ such that $\eta\varphi|_K = \psi\eta$. We say that φ is *irreducible* when there is no nontrivial surface orbit minor of G in S.

Proposition 2.17. *Let φ be a cellular automorphism of G in S.*

- *If φ is pseudofree, then there is a surface orbit minor H of $\overline{G}$ in S such that $\varphi|_H$ is irreducible.*
- *If φ is not pseudofree, then there is a surface orbit minor H of $\overline{G}$ in S such that $\overline{H} = H$ and any reduction of $\varphi|_H$ is obtained after deleting edges on oval cycles and so is augmentable.*

Proof. For the first part, delete as many orbits of edges as possible and then contract as many orbits of edges as possible. For the second part, since φ takes oval cycles to oval cycles we can delete as many orbits of non-oval edges as possible and then contract as many orbits of edges, including oval edges, as possible. □

A non-pseudofree cellular automorphism φ of G in S whose reductions are all obtained by deleting edges on oval cycles (as in the second part of Proposition 2.17) is said to be *oval-irreducible*. So now our definitions of augmentability, reductions, and irreducibility along with Propositions 2.12 and 2.13 tell us that we can effectively describe all cellular automorphisms of S and their pseudofixed points by a complete catalog of all irreducible and oval-irreducible cellular automorphisms of non-augmentable embeddings in S.

3 Quotients and lifts

Given a topological space X and automorphism φ of X, we denote the quotient space by $X/\langle\varphi\rangle$. Given a cellular automorphism of G in a closed surface S, Proposition 2.6 implies that $S/\langle\varphi\rangle$ is a surface with holes where the boundaries of the holes correspond to the orbits of the ovals of $\overline{\mathrm{fix}}(\varphi)$. To ensure that $G/\langle\varphi\rangle$ is a graph we need only require that φ have no pseudofixed point in the center of an edge. (The existence of such pseudofixed points would require the use of "half edges.") Given the projection $\pi\colon S \to S/\langle\varphi\rangle$, let $B = \pi(\overline{\mathrm{fix}}(\varphi))$. The isolated points in B are called the *branch points* of π. In [18] isolated points of $\overline{\mathrm{fix}}(\varphi)$ are called "prebranch points" of π. Of course we refer to these as the isolated pseudofixed points of φ.

3.1 Graph constructions

Suppose that σ is a $\mathbb{Z}_n$-voltage assignment on G. So now G^σ has an associated graph automorphism $\beta_\sigma\colon G^\sigma \to G^\sigma$ given by $\beta_\sigma(v_b) = v_{b+1}$ and $\beta_\sigma(e_b) = e_{b+1}$. Note that β_σ is a free graph automorphism, that is, there are no points on G^σ that are fixed by any power of β_σ. We call this the *basic automorphism* of G^σ associated to σ. Proposition 3.1 is an elaboration of Theorem 2.4.5 of [18] for cyclic groups.

Proposition 3.1. *If φ is a free automorphism of a connected graph G, then there is a $\mathbb{Z}_{|\varphi|}$-voltage assignment σ on $G/\langle\varphi\rangle$ and a graph isomorphism $\psi\colon (G/\langle\varphi\rangle)^\sigma \to G$ such that $\psi\beta_\sigma = \varphi\psi$ up to reversal of orientations on loops.*

Lemma 3.2. *If φ is a free automorphism of a graph G and C is a cycle in G, then $C/\langle\varphi\rangle$ contains a cycle.*

Proof. If C is a loop, then the result follows because φ is free. Suppose then that C has length at least 2 and let π denote the projection $G \to G/\langle\varphi\rangle$. Suppose for the sake of contradiction that $\pi(C)$ is acyclic. Then $\pi(C)$ is a forest, so has a vertex v' of degree 1. Let e' be the edge in $\pi(C)$ incident to v', let v_0 be a vertex in $\pi^{-1}(v') \cap C$ and let e_0 and e_1 be the edges of C incident to v_0. Thus $\pi(e_0) = \pi(e_1) = e'$, which implies $\varphi^k(e_0) = e_1$ for some $k < |\varphi|$. Since v_0 is not pseudofixed, we must have $\varphi^k(v_0) = v_1$ where v_1 is the other vertex incident to e_1. But then $e' = \pi(e_1)$ is a loop, a contradiction. □

Proof of Proposition 3.1. Let π denote the covering map $G \to G/\langle\varphi\rangle$, and let $n = |\varphi|$. Note that $G/\langle\varphi\rangle$ is connected and let T be a spanning tree in $G/\langle\varphi\rangle$. We claim that $\pi^{-1}(T)$ consists of n vertex-disjoint copies of T. This can be shown inductively on subtrees $S_0 \subset \cdots \subset S_m$ where S_0 is a single vertex, $S_m = T$ and S_i has i edges. In the base case, since φ is free, $\pi^{-1}(S_0)$ is n distinct vertices, which is n distinct copies of S_0. Now assume that $\pi^{-1}(S_i)$ is n vertex-disjoint copies of S_i and consider the single edge e_{i+1} in $E(S_{i+1}) \setminus E(S_i)$. Since φ is free, $\pi^{-1}(e_{i+1})$ is n distinct copies of e_{i+1} and these must all have one endpoint on corresponding vertices in the components of $\pi^{-1}(S_i)$. The other end must be unattached because otherwise the symmetry provided by φ will yield a cycle in $\pi^{-1}(S_{i+1})$, which by Lemma 3.2 yields a cycle in S_{i+1}, a contradiction. Hence $\pi^{-1}(S_{i+1})$ is n vertex-disjoint copies of S_{i+1}.

For any vertices $u, v \in V(G)$ in the same component of $\pi^{-1}(T)$, there is a uv-path γ connecting them in that component and so for any k we have that $\varphi^k(\gamma)$ is a $\varphi^k(u)\varphi^k(v)$-path in a component of $\pi^{-1}(T)$. Therefore, if we arbitrarily choose one component of $\pi^{-1}(T)$ and call it T_0, then φ induces a labeling $T_1, \ldots, T_{n-1}$ on the remaining components of $\pi^{-1}(T)$ where for any vertex $v \in T_i$ and any k we have $\varphi^k(v) \in T_{i+k}$.

Let e be any edge of $G/\langle\varphi\rangle$ not in T. Write $\pi^{-1}(e) = \{e_0, \ldots, e_{n-1}\}$ where $\mathbf{t}(e_i) \in T_i$, and so $\varphi^k(e_0) = e_k$. Now if $\mathbf{h}(e_0) \in T_j$, then we have that

$$\mathbf{h}(e_k) = \mathbf{h}\varphi^k(e_0) = \varphi^k\mathbf{h}(e_0) \in T_{j+k}.$$

So now define a $\mathbb{Z}_n$-voltage assignment σ on $G/\langle\varphi\rangle$ by $\sigma(e) = 0$ for all edges e in T, and for all edges $e \notin T$ define $\sigma(e) = j$, where $\mathbf{h}(e_0) \in T_j$.

Now consider the derived graph $(G/\langle\varphi\rangle)^\sigma$. The spanning tree T in $G/\langle\varphi\rangle$ lifts to n vertex-disjoint copies of T and, since the voltage on every edge in T is zero, the subscripts on the vertices in each copy of T are all the same. Let H_i be the copy of T whose vertices all have subscript i. So now define $\psi\colon (G/\langle\varphi\rangle)^\sigma \to G$ by taking each vertex in H_i to its corresponding vertex in T_i. The definition of σ guarantees that this is an isomorphism. Now β_σ takes each vertex and incident edges in H_i to the corresponding vertex and incident edges in H_{i+1} as φ takes each vertex and edges in T_i to the corresponding vertex and edges in T_{i+1}. Thus $\psi\beta_\sigma = \varphi\psi$ up to reversal of orientations on loops. □

3.2 Pseudofree constructions

Let φ be a cellular automorphism of G in S of order n. When φ is pseudofree, the quotient $S/\langle\varphi\rangle$ is again a surface; its connections with voltage graphs and derived embeddings are discussed in detail in [18, §§4.1–4.2]. One proposition from there that we will use repeatedly is the following. A *Möbius walk* is a closed walk with an odd number of orientation reversals along it, that is, a closed walk with a non-orientable neighborhood.

Proposition 3.3. *If G is embedded in a nonorientable surface S and is given voltage assignment σ, then the following are equivalent.*

(1) The derived surface S^σ is nonorientable.

(2) There is a Möbius walk w of G in S with $\sigma_*(w) = 0$.

(3) There is a Möbius walk w of G in S with $\sigma_*(w)$ of odd order in the voltage group.

Proposition 3.4. *Suppose that φ is a pseudofree cellular automorphism of G in S and $\pi\colon S \to S/\langle\varphi\rangle$ is the corresponding projection map. If $\pi(\overline{G})/C\backslash D$ is a surface minor such that $C \cap D = \emptyset$, C is acyclic in $\pi(\overline{G})$, and each branch point of π is the center of its own face, then $\overline{G}/\pi^{-1}(C)\backslash\pi^{-1}(D)$ is a surface orbit minor of $\overline{G}$ in S.*

Proof. Let $n = |\varphi|$. Because every pseudofixed point of φ is in the center of a face of $\overline{G}$ and is not on $\overline{G}$, φ is free on $\overline{G}$. Proposition 3.1 gives us a $\mathbb{Z}_n$-voltage assignment σ on $\pi(\overline{G})$ and an isomorphism $\psi\colon (\pi(\overline{G}))^\sigma \to \overline{G}$ such that $\psi\beta_\sigma = \varphi\psi$.

Now we verify that conditions (M1)–(M5) hold. Because $C \cap D = \emptyset$, we get that $\pi^{-1}(C) \cap \pi^{-1}(D) = \emptyset$. Because C is acyclic in $\pi(\overline{G})$, Lemma 3.2 gives us that $\pi^{-1}(C)$ is acyclic in G. Because all of the pseudofixed points of φ are off of G, we get condition (M3). Because the embedding of G in S is isomorphic to a derived embedding from a voltage-graph construction we get properties (M4) and (M5). □

Proposition 3.5. *If φ, G, S, $H = \pi(\overline{G})/C\backslash D$, and $\tilde{H} = \overline{G}/\pi^{-1}(C)\backslash\pi^{-1}(D)$ are as given in Proposition 3.4, then $\tilde{H}/\langle\varphi|_{\tilde{H}}\rangle = H$.*

Proof. Given that $\tilde{H}$ is defined by contracting and deleting the orbits of edges corresponding to the edges contracted and deleted in the quotient, we get our desired result. □

A standard technique An argument that we shall use repeatedly in the derivation of our catalogs of cellular automorphisms is as follows. Given a pseudofree cellular automorphism φ of G in S we also have the φ-action on $\overline{G}$ in S. Given the quotient $\overline{G}/\langle\varphi\rangle$ in $S/\langle\varphi\rangle$, we choose a surface minor H of $\overline{G}/\langle\varphi\rangle$ satisfying the conditions in Proposition 3.4. By Proposition 3.4, H corresponds to a surface orbit minor $\tilde{H}$ of $\overline{G}$ in S. Since all of the pseudofixed points of $\varphi|_{\tilde{H}}$ are off of $\tilde{H}$, $\varphi|_{\tilde{H}}$ is free on H. This fact along with Proposition 3.5 allows us to apply Proposition 3.1 to get a $\mathbb{Z}_{|\varphi|}$-voltage assignment σ on $\tilde{H}/\langle\varphi|_{\tilde{H}}\rangle$ that reconstructs $\tilde{H}$ and $\varphi|_{\tilde{H}}$. We can then conclude that $\varphi \rightsquigarrow \beta_\sigma$.

Another tool we use is the Riemann-Hurwitz Equation; see for example [18, §4.2.4]. The *deficiency* of a branch point x is defined to be $n - |\pi^{-1}(x)|$ and denoted by $\mathrm{def}(x)$.

Theorem 3.6 (Riemann-Hurwitz Equation (Form 1))**.** *Let S be a closed surface. If $\pi : \widetilde{S} \to S$ is an n-sheeted covering map with set Y of isolated branch points, then*

$$\chi(\widetilde{S}) = n\chi(S) - \sum_{y\in Y} \mathrm{def}(y).$$

A second useful form for the Reimann-Hurwitz equation arises when π is defined by a voltage-graph lifting construction using group $\mathcal{G}$. In this case, the branch points of π are isolated, $n = |\mathcal{G}|$, and for each $y \in Y$ there is an integer $v_y \mid n$ such that $|\pi^{-1}(y)| = n/v_y$. We call v_y the *order* of y and note that if y is contained in the face f of the voltage graph embedded in S and g is the net voltage around the face walk of f, then $v_y = |g|$.

Theorem 3.7 (Riemann-Hurwitz Equation (Form 2))**.** *If $\pi : \widetilde{S} \to S$ is an n-sheeted covering map defined by a voltage-graph lifting construction using group $\mathcal{G}$ of order n and Y is the set of isolated branch points, then*

$$\chi(\widetilde{S}) = n\left(\chi(S) - \sum_{y\in Y}\left(1 - \frac{1}{v_y}\right)\right).$$

3.3 Nonpseudofree constructions

We utilize two different constructions for reducing nonpseudofree cellular automorphisms to pseudofree ones: the cutting construction and the folding quotient.

3.3.1 The cutting construction

Let φ be a non-pseudofree cellular automorphism of G in S. If the ovals of φ do not separate S, then cut $\overline{G}$ together with S along its oval cycles to make two copies of each oval cycle having an annular neighborhood and one copy of double the length of each oval cycle having a Möbius neighborhood. This results in a graph $G^{\circlearrowleft}$ properly embedded in surface $S^{\circlearrowleft}$ with hole cycles being the new cycles produced by cutting. The action of φ naturally induces a cellular automorphism $\varphi^{\circlearrowleft}$ on $G^{\circlearrowleft}$ in $[S^{\circlearrowleft}]^{\bullet}$ that is pseudofree, has the same order as φ, and takes capped faces to capped faces.

As an example consider the embedding G' in the torus shown in Figure 3.8 with free order-12 cellular automorphism φ defined by $i \mapsto (i+1)$. Cut out the circular faces shown and then paste the i^{th} hole to the $(i+6)^{th}$ hole by identifying the points corresponding by φ to obtain a graph G embedded in the non-orientable surface S of characteristic -12. We now have that φ is naturally defined on G in S and is an order-12 non-pseudofree cellular automorphism with $G^{\circlearrowleft} = G'$.

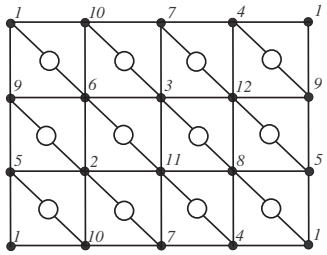

Figure 3.8.

3.3.2 Folding quotients and unfolding lifts

Given a non-pseudofree involutory cellular automorphism φ of G in closed surface S, let $\pi\colon S \to S/\langle\varphi\rangle$ be the corresponding projection map. We now get that $\pi(S)$ is a surface with holes and $\pi(\overline{G})$ is properly embedded in $\pi(S)$ where the hole-cycles are isomorphic copies of the oval cycles and the image of each isolated fixed point of φ is the center of a face of $\pi(\overline{G})$ in $\pi(S)$. We call this quotient a *folding quotient*.

Proposition 3.9 is an analogue of the Riemann-Hurwitz equation for nonpseudofree involutory cellular automorphisms.

Proposition 3.9. *If φ is an involutory cellular automorphism of G in S, s is the number of ovals in fix(φ), r is the number of isolated fixed points, and π the corresponding projection map, then $\pi(S)$ has s holes and*

$$\chi([\pi(S)]^{\bullet}) = \frac{\chi(S)}{2} + \frac{r}{2} + s.$$

Proof. Since for $\overline{G}$ in S the isolated fixed points are in the centers of faces and the numbers of vertices and edges in oval cycles are equal we have that

$$\begin{aligned}
\chi([\pi(S)]^{\bullet}) &= \chi(\pi(S)) + s \\
&= |V(\pi(\overline{G}))| - |E(\pi(\overline{G}))| + |F(\pi(\overline{G}))| + s \\
&= \tfrac{|V(\overline{G})|}{2} - \tfrac{|E(\overline{G})|}{2} + \tfrac{|F(\overline{G})|+r}{2} + s \\
&= \tfrac{\chi(S)}{2} + \tfrac{r}{2} + s
\end{aligned}$$

□

Let G be properly embedded in a compact surface S with holes and let $\sigma\colon E(G) \to \mathbb{Z}_2$ be a voltage assignment. Consider the usual derived embedding of G^{σ} in $([S]^{\bullet})^{\sigma}$. Observe that $([S]^{\bullet})^{\sigma}$ is either a closed surface or a disjoint union of two homeomorphic closed surfaces. If C is a hole-cycle of G in S, then if $\sigma_*(C) = 0$ we get that C lifts to two cycles C_0 and C_1 in G^{σ}, each bounding a face in $([S]^{\bullet})^{\sigma}$. If $\sigma_*(C) = 1$ then C lifts to a single cycle C' bounding a face in $([S]^{\bullet})^{\sigma}$ having twice the length of C. In the former case

we remove the two open faces bounded by C_0 and C_1 and then identify the corresponding vertices and edges of C_0 and C_1; this results in a cycle with an annular neighborhood (see Figure 3.10).

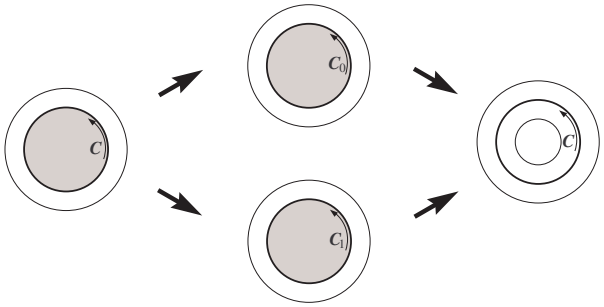

Figure 3.10.

In the latter case we remove the face bounded by C' and identify the boundary with itself via the antipodal map; this results in a cycle with a Möbius neighborhood (see Figure 3.11). These operations yield a graph $\widehat{G}^\sigma$ embedded in a closed surface which we denote by $\widehat{S}^\sigma$. We call $\widehat{G}^\sigma$ in $\widehat{S}^\sigma$ the *unfolding lift* of G from σ. Note that $(\widehat{G}^\sigma)^\circlearrowleft$ in $(\widehat{S}^\sigma)^\circlearrowleft$ is the same as G^σ in $([S]^\bullet)^\sigma$ when $([S]^\bullet)^\sigma$ is connected. (We do not allow the cutting construction when the ovals separate the surface.)

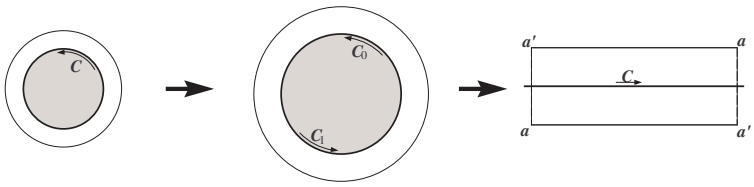

Figure 3.11.

Let G be properly embedded in a compact surface S with holes. We label the vertices of G^σ in $([S]^\bullet)^\sigma$ as with the usual voltage-graph lifting construction. The vertices of $\widehat{G}^\sigma$ in $\widehat{S}^\sigma$ that arise from vertex identifications are then relabeled by removing the subscripts. The basic automorphism β_σ on G^σ in $([S]^\bullet)^\sigma$ (whether connected or not) naturally induces a cellular automorphism of $\widehat{G}^\sigma$ which we also call β_σ which is an involution with oval-cycles being the lifts of the hole-cycles. Proposition 3.12 illustrates β_σ in the case that $\sigma_* = 0$.

Proposition 3.12. *Let G^σ be an unfolding lift of G embedded in S with at least one hole. If $\sigma_* = 0$ then $\widehat{S}^\sigma$ consists of two copies of G in S identified along the holes, and β_σ reflects the copies of G across the boundary of the holes.*

Proof. If $\sigma_* = 0$ then, up to isomorphism, we may assume that $\sigma = 0$ as well, and so S^σ consists of two disjoint copies of G in S. After identifying holes the assertion follows. □

Proposition 3.13 is the analogue of Proposition 3.1 for involutory cellular automorphisms.

Proposition 3.13. *Suppose φ is an involutory cellular automorphism of G in S with at least one oval. There is a $\mathbb{Z}_2$-voltage assignment σ on $H = \overline{G}/\langle\varphi\rangle$ in $S/\langle\varphi\rangle$ and an isomorphism $\psi\colon \widehat{H}^\sigma \to \overline{G}$ such that $\psi\beta_\sigma = \varphi\psi$.*

Proof. Suppose that the ovals separate S. By Proposition 2.9 the ovals separate S into two homeomorphic components, so setting $\sigma \equiv 0$ gives the desired conclusion by Proposition 3.12.

Suppose now that the ovals do not separate S. Consider $G^\circlearrowleft$ in $[S^\circlearrowleft]^\bullet$ and the corresponding $\varphi^\circlearrowleft$ action on this embedding. We must have that $G^\circlearrowleft/\langle\varphi^\circlearrowleft\rangle = \overline{G}/\langle\varphi\rangle$; we call this graph H, and note that H is embedded in $[S^\circlearrowleft]^\bullet/\langle\varphi^\circlearrowleft\rangle = [S/\langle\varphi\rangle]^\bullet$. Now by Proposition 3.1, there is a $\mathbb{Z}_2$-voltage assignment σ on H and a graph isomorphism $\psi_0\colon H^\sigma \to G^\circlearrowleft$ such that $\psi_0\beta_\sigma = \varphi\psi_0$. Now ψ_0 naturally induces an isomorphism $\psi\colon \widehat{H}^\sigma \to G$ such that $\psi\beta_\sigma = \varphi\psi$. □

Proposition 3.14 is the analogue of Proposition 3.4 for involutory cellular automorphisms.

Proposition 3.14. *Suppose that φ is an involutory cellular automorphism of G in S with at least one oval and $\pi\colon S \to S/\langle\varphi\rangle$ is the corresponding projection map. If $\pi(\overline{G})/C\backslash D$ is a surface minor in $\pi(S)$ such that*

(i) $C \cap D = \emptyset$,

(ii) each connected component of C in $\pi(\overline{G})$ intersects at most one hole-cycle,

(iii) C is acyclic in $\pi(\overline{G})$ and the only cycles in the union of C with the hole-cycles of $\pi(\overline{G})$ are the hole-cycles themselves, and

(iv) each image of an isolated fixed point is the center of its own face,

then $\overline{G}/\pi^{-1}(C)\backslash\pi^{-1}(D)$ is a surface orbit minor of $\overline{G}$ in S.

Proof. Proposition 3.13 gives us a $\mathbb{Z}_2$-voltage assignment σ on $\pi(\overline{G})$ and an isomorphism $\psi\colon \widehat{\pi(\overline{G})^\sigma} \to \overline{G}$ such that $\psi\beta_\sigma = \varphi\psi$. Now condition (i) in the quotient yields condition (M1). Condition (ii) in the quotient and the fact that $\overline{G}$ touches none of the isolated fixed points yields condition (M3). Condition (iii) in the quotient guarantees that $\pi^{-1}(C)$ is acyclic in G by the following argument. First, if Z is a cycle in $\pi^{-1}(C)$, then Z must intersect an oval cycle H in $\overline{G}$ because the corresponding edge set in $\pi(\overline{G})^\sigma$ is acyclic by Lemma 3.2. Thus there is a path γ in Z which is edge disjoint from H yet has both endpoints in H. However now $\pi(\gamma \cup H) \subset C \cup \pi(H)$ contains a cycle that is not a hole-cycle, a contradiction of (iii). Thus we have condition (M2) for $\overline{G}$. Because the embedding of $\pi(\overline{G})$ in $\pi(S)$ is proper and satisfies (iv) and because the embedding of $\overline{G}$ in S is isomorphic to a derived embedding from an unfolding-lift construction we get properties (M4) and (M5). □

Proposition 3.15. *If φ, G in S, $H = \pi(\overline{G})/C\backslash D$, and $\tilde{H} = \overline{G}/\pi^{-1}(C)\backslash\pi^{-1}(D)$ are as given in Proposition 3.14, then $\tilde{H}/\langle\varphi|_{\tilde{H}}\rangle = H$.*

Proof. By the same reasoning as in Proposition 3.5. □

3.3.3 Lifting cellular automorphisms to unfolding lifts

Let G be a connected graph, φ a free automorphism of G, and σ a $\mathbb{Z}_2$-voltage assignment on G such that for any closed walk w, $\sigma_*(w) = \sigma_*(\varphi(w))$. Choose a base vertex b in G and for each other vertex v, let w_v be a vb-walk. In the derived graph G^σ, the walk w_v lifts to two walks $w_{v,i}$ for $i \in \mathbb{Z}_2$ from v_i to $b_{\sigma(w_v)+i}$. For $a \in \mathbb{Z}_2$, define $\varphi^\uparrow_{\sigma,a}$ on the vertices of G^σ by first setting $\varphi^\uparrow_{\sigma,a}(b_i) = c_{i+a}$ where $\varphi(b) = c$ and then setting $\varphi^\uparrow_{\sigma,a}(v_i) = u_{i+\sigma_*(w_v)+a+\sigma_*(\varphi(w_v))}$ where $\varphi(v) = u$ (see Figure 3.16). Proposition 3.17(1) tells us that $\varphi^\uparrow_{\sigma,a}$ is an automorphism on G^σ and that this definition on the vertices completely determines the action on the edges.

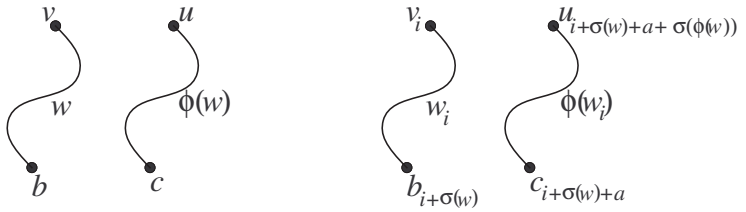

Figure 3.16.

Proposition 3.17. *Let $\varphi^\uparrow_{\sigma,a}$ be as defined above, $n = |\varphi|$, and π be the projection map from G^σ to G.*

(1) $\varphi^\uparrow_{\sigma,a}$ is a well-defined automorphism of G^σ that is independent of the choice of b and the w_v's and satisfies $\varphi\pi = \pi\varphi^\uparrow_{\sigma,a}$.

(2) $|\varphi^\uparrow_{\sigma,a}| \in \{n, 2n\}$ and $\varphi^\uparrow_{\sigma,a}$ is free on G^σ.

(3) If n is odd, then there is $a \in \mathbb{Z}_2$ such that $|\varphi^\uparrow_{\sigma,a}| = 2n$ and $|\varphi^\uparrow_{\sigma,a+1}| = n$.

(4) If n is even, then $|\varphi^\uparrow_{\sigma,a}| = |\varphi^\uparrow_{\sigma,a+1}|$; furthermore $|\varphi^\uparrow_\sigma| = 2n$ iff for every $v\varphi(v)$-walk w in G, $\sigma_*(w, \varphi(w), \ldots, \varphi^{n-1}(w)) = 1$.

(5) If φ is a cellular automorphism of G in S, then $\varphi^{\uparrow}_{\sigma,a}$ induces a cellular automorphism of G^{σ} in S^{σ}.

Proof. (1) This is immediately implied by the results in [22, §5].
(2) By [22, Props. 5.1,5.2], $(\varphi^{\uparrow}_{\sigma,a})^n$ either exchanges the two vertices in each fiber or is the identity map. Also, we must have that $n \leq |\varphi^{\uparrow}_{\sigma,a}| \leq 2n$ which then gives us that $|\varphi^{\uparrow}_{\sigma,a}| \in \{n, 2n\}$. Now suppose by way of contradiction that x is a point in G^{σ}, necessarily either a vertex or center of an edge, that is fixed by $(\varphi^{\uparrow}_{\sigma,a})^k \neq \mathrm{id}$. This implies that $\pi(x)$ is fixed by φ^k and so since φ is free we must have that $k = n$ and $|\varphi^{\uparrow}_{\sigma,a}| = 2n$. By [22, Prop. 5.1], however, $(\varphi^{\uparrow}_{\sigma,a})^n$ has no fixed points.
(3) Let β be the automorphism of G^{σ} that exchanges the vertices in each fiber. As in the proof of (2) above, $|\varphi^{\uparrow}_{\sigma,a}|$ is determined by whether $(\varphi^{\uparrow}_{\sigma,a})^n$ is β or the identity. Evidently $\beta\varphi^{\uparrow}_{\sigma,a} = \varphi^{\uparrow}_{\sigma,a+1}$ and β commutes with these maps as well. Thus $(\varphi^{\uparrow}_{\sigma,a})^n, (\varphi^{\uparrow}_{\sigma,a+1})^n \in \{\mathrm{id}, \beta\}$ and, because n is odd, we have

$$(\varphi^{\uparrow}_{\sigma,a+1})^n = \left(\beta\varphi^{\uparrow}_{\sigma,a}\right)^n = \beta^n \left(\varphi^{\uparrow}_{\sigma,a}\right)^n = \beta \left(\varphi^{\uparrow}_{\sigma,a}\right)^n \neq \left(\varphi^{\uparrow}_{\sigma,a}\right)^n.$$

(4) Similar to the proof of (3) we have that $(\varphi^{\uparrow}_{\sigma,a})^n = (\varphi^{\uparrow}_{\sigma,a+1})^n$ and so $|\varphi^{\uparrow}_{\sigma,a}| = |\varphi^{\uparrow}_{\sigma,a+1}|$. Now given a closed walk $\gamma = w, \varphi(w), \ldots, \varphi^{n-1}(w)$ for some $v\varphi(v)$-walk w in G, we have $(\varphi^{\uparrow}_{\sigma,a})^n(v_i) = v_{i+na+\sigma_*(\gamma)} = v_{i+\sigma_*(\gamma)}$ because n is even. Thus $(\varphi^{\uparrow}_{\sigma,a})^n = \mathrm{id}$ when $\sigma_*(\gamma) = 0$ and $(\varphi^{\uparrow}_{\sigma,a})^n = \beta$ when $\sigma_*(\gamma) = 1$.
(5) Given an oriented face f of G in S (with starting vertex v), there are two oriented faces of G^{σ} in S^{σ} that project down to f. We denote these by $f^{\uparrow}_0$ and $f^{\uparrow}_1$ with starting vertices v_0 and v_1, respectively. Note that the underlying unoriented faces of $f^{\uparrow}_0$ and $f^{\uparrow}_1$ may be the same, in which case $f^{\uparrow}_0$ and $f^{\uparrow}_1$ differ by a 180° rotation. Suppose that $g = \varphi(f)$ and $w = \varphi(v)$. If $\varphi^{\uparrow}_{\sigma,a}(v_i) = w_j$ then define $\varphi^{\uparrow}_{\sigma,a}(f^{\uparrow}_i) = g^{\uparrow}_j$. These definitions and the fact that $\varphi^{\uparrow}_{\sigma,a}$ is an automorphism give us that $\theta\varphi^{\uparrow}_{\sigma,a}(f^{\uparrow}_i) = \varphi^{\uparrow}_{\sigma,a}(\theta f^{\uparrow}_i)$ for a dihedral symmetry θ, and since $\partial\varphi = \varphi\partial$ we also have $\partial\varphi^{\uparrow}_{\sigma,a}(f^{\uparrow}_i) = \varphi^{\uparrow}_{\sigma,a}\partial(f^{\uparrow}_i)$. □

Proposition 3.18. *If G is properly embedded in a surface S with holes, φ is a cellular automorphism of G in $[S]^{\bullet}$ that takes capped faces to capped faces, and σ is a $\mathbb{Z}_2$-voltage assignment on G satisfying $\sigma(\varphi(w)) = \sigma(w)$ for all closed walks w, then $\varphi^{\uparrow}_{\sigma,a}$ induces a cellular automorphism of $\widehat{G}^{\sigma}$ in $\widehat{S}^{\sigma}$. Furthermore, if $|\varphi^{\uparrow}_{\sigma,a}| = 2|\varphi|$, then $\varphi^{\uparrow}_{\sigma,a}$ is non-pseudofree with oval cycles being the lifts of the hole cycles.*

Proof. The first part follows from Proposition 3.17(5) and the fact that φ takes capped faces of G in S to capped faces. Now if $|\varphi^{\uparrow}_{\sigma,a}| = 2|\varphi| = 2k$, then $(\varphi^{\uparrow}_{\sigma,a})^k$ on G^{σ} in S^{σ} is the basic automorphism β_{σ}. So then $(\varphi^{\uparrow}_{\sigma,a})^k$ on $\widehat{G}^{\sigma}$ in $\widehat{S}^{\sigma}$ performs reflections around the lifts of the hole-cycles of G in S. □

3.3.4 Induced actions on quotients and their fixed points

If φ is a non-pseudofree cellular automorphism of G in S where $|\varphi| = 2k$ and $G = \overline{G}$ then we define $\varphi^{\downarrow}$ on the graph $G/\langle\varphi^k\rangle$ in $S/\langle\varphi^k\rangle$ as follows. First note that the points of $S/\langle\varphi^k\rangle$ are the orbits in S under the action of φ^k. These orbits are of the form $\{x\}$ where $x \in \mathrm{fix}(\varphi^k)$ and $\{x, \varphi^k(x)\}$ where $x \notin \mathrm{fix}(\varphi^k)$, so we define $\varphi^{\downarrow}(\{x\}) = \{\varphi(x)\}$ and $\varphi^{\downarrow}(\{x, \varphi^k(x)\}) = \{\varphi(x), \varphi^{k+1}(x)\}$. The map $\varphi^{\downarrow}$ is well defined because, by Proposition 2.5, $\varphi(x) \in \mathrm{fix}(\varphi^k)$ iff $x \in \mathrm{fix}(\varphi^k)$.

Proposition 3.19. *The map $\varphi^{\downarrow}$ is an order-k pseudofree cellular automorphism of $G/\langle\varphi^k\rangle$ in $[S/\langle\varphi^k\rangle]^{\bullet}$ which maps capped faces to capped faces, and furthermore all isolated pseudofixed points of $\varphi^{\downarrow}$ are images of isolated pseudofixed points of φ and are all off of $G/\langle\varphi^k\rangle$.*

Proof. Let $\pi\colon S \to S/\langle\varphi^k\rangle$ be the quotient map sending each point to its orbit. First we claim that $\varphi^{\downarrow}\pi = \pi\varphi$. To see this, let $x \in S$. If $x \in \mathrm{fix}(\varphi^k)$ then $\varphi^{\downarrow}\pi(x) = \varphi^{\downarrow}(\{x\}) = \{\varphi(x)\} = \pi\varphi(x)$. If $x \notin \mathrm{fix}(\varphi^k)$ then $\varphi^{\downarrow}\pi(x) = \varphi^{\downarrow}(\{x, \varphi^k(x)\}) = \{\varphi(x), \varphi^{k+1}(x)\} = \pi\varphi(x)$.

Because φ on G in S has no pseudofixed points in the centers of edges or pseudofixed segments in the interiors of faces, $G/\langle\varphi^k\rangle$ is a graph and $\varphi^{\downarrow}$ on $G/\langle\varphi^k\rangle$ takes vertices to vertices and edges to edges. We now claim that $\varphi^{\downarrow}$ defines an automorphism on $G/\langle\varphi^k\rangle$. Denote the head and tail functions on $G/\langle\varphi^k\rangle$ by $\mathbf{h}^{\downarrow}$ and

$\mathbf{t}^\downarrow$. Note that $\mathbf{h}^\downarrow\pi = \pi\mathbf{h}$ and $\mathbf{t}^\downarrow\pi = \pi\mathbf{t}$. Now we get that $\varphi^\downarrow\mathbf{h}^\downarrow = \mathbf{h}^\downarrow\varphi^\downarrow$ and $\varphi^\downarrow\mathbf{t}^\downarrow = \mathbf{t}^\downarrow\varphi^\downarrow$ (which makes $\varphi^\downarrow$ an automorphism of $G/\langle\varphi^k\rangle$) because for each $\pi(e)$ we get that

$$\varphi^\downarrow\mathbf{h}^\downarrow\pi(e) = \varphi^\downarrow\pi\mathbf{h}(e) = \pi\varphi\mathbf{h}(e) = \pi\mathbf{h}\varphi(e) = \mathbf{h}^\downarrow\pi\varphi(e) = \mathbf{h}^\downarrow\varphi^\downarrow\pi(e).$$

Given a walk $e_1, \ldots, e_n$ in G, we write $\pi(e_1, \ldots, e_n)$ for $\pi(e_1), \ldots, \pi(e_n)$; this is a walk in $G/\langle\varphi^k\rangle$ because $\mathbf{h}^\downarrow\pi(e_i) = \pi\mathbf{h}(e_i) = \pi\mathbf{t}(e_{i+1}) = \mathbf{t}^\downarrow\pi(e_{i+1})$. If we denote the facial boundary function on the embedding of $G/\langle\varphi^k\rangle$ in $[S/\langle\varphi^k\rangle]^\bullet$ by $\partial^\downarrow$ we get that $\partial^\downarrow\pi(f) = \pi\partial(f)$ and so for each $\pi(f)$ we get

$$\varphi^\downarrow\partial^\downarrow\pi(f) = \varphi^\downarrow\pi\partial(f) = \pi\varphi\partial(f) = \pi\partial\varphi(f) = \partial^\downarrow\pi\varphi(f) = \partial^\downarrow\varphi^\downarrow\pi(f)$$

which makes $\varphi^\downarrow$ a cellular automorphism of $G/\langle\varphi^k\rangle$ in $[S/\langle\varphi^k\rangle]^\bullet$.

That $|\varphi^\downarrow| = k$ follows from Proposition 2.2. To show that $\varphi^\downarrow$ is pseudofree, suppose by way of contradiction that O is an oval of $\varphi^\downarrow$ on $G/\langle\varphi^k\rangle$. Thus O is fixed by $(\varphi^\downarrow)^{k/2}$. The preimage of O in G, call it $\pi^{-1}(O)$, is either two copies of O or a circle of twice the length of O. Since $(\varphi^\downarrow)^{k/2}$ fixes O, it must be that the action of $\varphi^{k/2}$ exchanges the doubled parts of $\pi^{-1}(O)$ and thus φ^k fixes $\pi^{-1}(O)$. Thus the single circle or two circles of $\pi^{-1}(O)$ are ovals of φ and so O is a hole-cycle in $G/\langle\varphi^k\rangle$. Since one side of O is the hole and the other side is not and since $\varphi^\downarrow$ takes capped faces to capped faces, it cannot be that the action of $(\varphi^\downarrow)^{k/2}$ reflects around O, a contradiction.

To prove the final claim, suppose for the sake of contradiction that x is an isolated pseudofixed point of $\varphi^\downarrow$ that is not the image of a pseudofixed point of φ. If x has index $m < k$ then any $\hat{x}$ in $\pi^{-1}(x)$ in G satisfies $\varphi^{2m}(\hat{x}) = \hat{x}$, a contradiction since $2m < 2k$. □

Proposition 3.20 identifies when it is possible that $\mathrm{fix}(\varphi^\downarrow) \not\subseteq \mathrm{fix}(\varphi^k)$.

Proposition 3.20. *If φ is a cellular automorphism of G in S with $|\varphi| = 2k$ and $\mathit{fix}(\varphi^\downarrow) \not\subseteq \mathit{fix}(\varphi^k)$, then $k = 2^r - 1$ for some r.*

Proof. Say that $\{x, \varphi^k(x)\} \in \mathrm{fix}(\varphi^\downarrow)$ where $x \notin \mathrm{fix}(\varphi^k)$. Thus $\{x, \varphi^k(x)\} = \varphi^\downarrow(\{x, \varphi^k(x)\}) = \{\varphi(x), \varphi^{k+1}(x)\}$. It cannot be that $\varphi(x) = x$ because then $x \in \mathrm{fix}(\varphi)$ but $x \notin \mathrm{fix}(\varphi^k)$, a contradiction. So $\varphi^{k+1}(x) = x$ and therefore there is some minimum integer $m > 1$ with $\varphi^m(x) = x$. So now we get that $m \mid (k+1)$ and $m \mid 2k$. Let p be some prime factor of m. It cannot be that $p > 2$ because then $p \mid k$ which implies $p \nmid (k+1)$, a contradiction. It follows that $p = 2$ and so $k+1$ is a power of 2. □

Proposition 3.21. *Let φ be a non-pseudofree cellular automorphism of $G = \overline{G}$ in S of order $2k$ and $\pi\colon S \to S/\langle\varphi^k\rangle$ the associated projection map. If σ and ψ are as given in Proposition 3.13, then there is $a \in \mathbb{Z}_2$ such that $\psi(\varphi^\downarrow)^\uparrow_{a,\sigma} = \varphi\psi$.*

Proof. We claim that for any closed walk w in $\pi(G)$ we have $\sigma_*(w) = \sigma_*(\varphi^\downarrow(w))$. Now $\sigma_*(w)$ is determined by whether $\pi^{-1}(w)$ in $G \cong \widehat{G}^\sigma$ consists of two copies of w or one walk of twice the length of w. Since the automorphisms φ and $\varphi^\downarrow$ preserve walk lengths, this property for w and $\pi^{-1}(w)$ is the same for $\varphi^\downarrow(w)$ and $\pi^{-1}\varphi^\downarrow(w) = \varphi\pi^{-1}(w)$ and so $\sigma_*(w) = \sigma_*(\varphi^\downarrow(w))$ which confirms that $(\varphi^\downarrow)^\uparrow_{a,\sigma}$ is defined. Now we have that $(\varphi^\downarrow)^\uparrow_{a,\sigma}$ and $\psi^{-1}\varphi\psi$ are both lifts of $\varphi^\downarrow$ on $\widehat{\pi(G)^\sigma}$. In [22, p. 931] it is stated that all lifts of $\varphi^\downarrow$ on $\pi(G)^\sigma$ (and so also on $\widehat{\pi(G)^\sigma}$) will be related by compositions with deck transformations. Since we are using $\mathbb{Z}_2$-voltages there are exactly two deck transformations and so $(\varphi^\downarrow)^\uparrow_{0,\sigma}$ and $(\varphi^\downarrow)^\uparrow_{1,\sigma} = \beta_\sigma(\varphi^\downarrow)^\uparrow_{0,\sigma}$ are the only lifts of $\varphi^\downarrow$ and therefore one of them is equal to $\psi^{-1}\varphi\psi$. □

4 Cellular automorphisms of the sphere

Much of the information in this section is implicit in [8, §§4,5]. Denote the sphere by $\mathbf{S}$ and the projective plane by $\mathbf{P}$.

Rotations $\mathcal{R}_{k,\mathbf{S}}$ Given a cycle of length $k > 1$ with vertices $v_1, \ldots, v_k$ embedded in the sphere with faces F_1 and F_2, we define the cellular automorphism $\mathcal{R}_{k,S}$ of order k by $v_i \mapsto v_{i+1}$ and $F_i \mapsto F_i$. Note that $\mathcal{R}_{k,\mathbf{S}}$ is pseudofree with two isolated fixed points and is irreducible.

Rotation reflections $\mathcal{RR}_{2k,\mathbf{S}}$ Given a cycle of length $2k \geq 2$ with vertices $v_1, \ldots, v_{2k}$ embedded in the sphere with faces F_1 and F_2, we define the cellular automorphism $\mathcal{RR}_{2k,\mathbf{S}}$ by $v_i \mapsto v_{i+1}$ and $F_1 \mapsto F_2$. Note that the pointwise action of $\mathcal{RR}_{2,\mathbf{S}}$ on the sphere is the usual antipodal map and this is a free cellular automorphism. For $2k \geq 4$, $\mathcal{RR}_{2k,\mathbf{S}}$ is pseudofree with two isolated pseudofixed points. Also, $\mathcal{RR}_{2k,\mathbf{S}}$ is irreducible.

Oval rotation reflections $\mathcal{ORR}_{4k+2,\mathbf{S}}$ Given a cycle of length $2k+1 \geq 1$ with vertices $v_1, \ldots, v_{2k+1}$ embedded in the sphere with faces F_1 and F_2, we define the cellular automorphism $\mathcal{ORR}_{4k+2,\mathbf{S}}$ by $v_i \mapsto v_{i+1}$ and $F_1 \mapsto F_2$. This is not pseudofree and the cycle on $v_1, \ldots, v_{2k+1}$ is the oval cycle. Also, $\mathcal{ORR}_{4k+2,\mathbf{S}}$ is oval irreducible.

Theorem 4.1 tells us that this catalog of non-augmentable cellular automorphisms of $\mathbf{S}$ is complete up to reducibility.

Theorem 4.1. *If φ is a cellular automorphism of G in $\mathbf{S}$ with $\overline{G} = G$, then φ reduces to one of $(\mathcal{R}_{k,\mathbf{S}})^i$, $(\mathcal{RR}_{2k,\mathbf{S}})^i$, and $(\mathcal{ORR}_{4k+2,\mathbf{S}})^i$ for some i.*

The following Proposition, appearing in [8, Lemma 2.5], is based on [18, Theorems 6.3.1 and 6.3.2]; we use it in the proof of Theorem 4.1.

Proposition 4.2. *Suppose φ is an order-n pseudofree cellular automorphism of G in $\mathbf{S}$. Then one of the following holds:*

(1) $\mathbf{S}/\langle\varphi\rangle$ is the sphere and there are exactly two branch points,

(2) $\mathbf{S}/\langle\varphi\rangle$ is the projective plane, there is exactly one branch point, and $n > 2$, or

(3) $\mathbf{S}/\langle\varphi\rangle$ is the projective plane, there are no branch points, and $n = 2$.

Proof of Theorem 4.1. Let $n = |\varphi|$ and let π denote the projection $\mathbf{S} \to \mathbf{S}/\langle\varphi\rangle$. Suppose first that φ is pseudofree. In Case (1) of Proposition 4.2, it follows from Theorem 3.6 that both branch points of $\pi(\mathbf{S})$ have deficiency $n-1$ and hence are images of fixed points, call them f_1 and f_2. Thus we can contract a spanning tree and delete loops in $\pi(G)$ to get a surface minor H consisting of a single loop separating $\pi(f_1)$ and $\pi(f_2)$. The corresponding surface orbit minor $\tilde{H}$ of G in $\mathbf{S}$ given by Proposition 3.4 is connected and so is an n-cycle separating f_1 and f_2. Because the pseudofixed points of $\varphi|_{\tilde{H}}$ are not on the cycle $\tilde{H}$ the action of $\varphi|_{\tilde{H}}$ on $\tilde{H}$ is rotation rather than reflection and since f_1 and f_2 are fixed, $\varphi|_{\tilde{H}} = (\mathcal{R}_{n,\mathbf{S}})^i$ for some i.

In Case (2) of Proposition 4.2, it follows from Theorem 3.6 that the branch point b has deficiency $n-2$ and so is the image of two pseudofixed points b_1 and b_2. Since $\varphi(b_1) = b_2$ we now get that $n = 2k \geq 4$ for some k. Since $\pi(G)$ is cellularly embedded in $\pi(\mathbf{S}) = \mathbf{P}$, we can contract a spanning tree in $\pi(G)$ and delete loops to get a surface minor H consisting of a single loop e embedded noncontractibly which has b in the center of the single face of the embedding. Let $\tilde{H}$ be the surface orbit minor of G in $\mathbf{S}$ given by Proposition 3.4; by Proposition 3.1 there is a $\mathbb{Z}_{2k}$-voltage assignment σ on H such that $H^\sigma \cong \tilde{H}$ and $\beta_\sigma = \varphi|_{\tilde{H}}$ up to this isomorphism. Since the facial walk bounding b is $w = e, e$ and since the deficiency of b is $n-2$ we get that $|\sigma_*(w)| = |2\sigma(e)| = n/2 = k$. Thus $\langle 2\sigma(e)\rangle = \langle 2\rangle$ and so up to automorphism of $\mathbb{Z}_{2k}$, $\sigma(e) = 1$. Thus $H^\sigma \cong \tilde{H}$ is a $2k$-cycle and again the action of $\varphi|_{\tilde{H}}$ on $\tilde{H}$ must be rotation rather than reflection. So now since $\varphi(b_1) = b_2$ we get that $\varphi|_{\tilde{H}} = (\mathcal{RR}_{2k,\mathbf{S}})^i$ for some odd i.

In Case (3) of Proposition 4.2, we again take H in $\pi(\mathbf{S})$ to be a single loop e with endpoint v embedded noncontractibly. By Proposition 3.1, there is a $\mathbb{Z}_2$-voltage assignment σ on H such that $H^\sigma \cong \tilde{H}$ and $\beta_\sigma = \varphi|_{\tilde{H}}$ up to this isomorphism. We must then have that H^σ is a 2-cycle and since φ has no fixed points we get that $\varphi|_{\tilde{H}} = \mathcal{RR}_{2,\mathbf{S}}$.

Suppose now that φ is not pseudofree and so $n = 2k$ by Proposition 2.8. If O is an oval cycle in G then since we are in the sphere, O must be the only oval cycle in G and so evidently $\varphi^k \rightsquigarrow \mathcal{ORR}_{2,\mathbf{S}}$. Proposition 2.8 now implies that $\varphi \rightsquigarrow (\mathcal{ORR}_{4t+2,\mathbf{S}})^i$ for some odd i. □

5 Cellular automorphisms of the projective plane

Rotations $\mathcal{R}_{2k,\mathbf{P}}$ Consider a cycle of length k with edges $e_1, \ldots, e_k$ embedded as a noncontractible closed curve in $\mathbf{P}$. This is a single-faced embedding whose lone facial boundary walk is $w = e_1, \ldots, e_k, e_1, \ldots, e_k$. We define the cellular automorphism $\mathcal{R}_{2k,\mathbf{P}}$ to be the rotation of the single face by $\frac{180^\circ}{k}$, which gives $e_i \mapsto e_{i+1}$. Notice that $\mathcal{R}_{2k,\mathbf{P}}$ has a fixed point in the center of its single face and has oval cycle $e_1, \ldots, e_k$ and so is not pseudofree. Notice also that if $k = 2m + 1 \geq 3$ then $(\mathcal{R}_{2k,\mathbf{P}})^2$ is pseudofree with a single pseudofixed point. The cellular automorphism $\mathcal{R}_{2k,\mathbf{P}}$ is oval-irreducible and if $k = 2m + 1 \geq 3$ then $(\mathcal{R}_{2k,\mathbf{P}})^2$ is irreducible.

Theorem 5.1 tells us that this catalog of non-augmentable cellular automorphisms of $\mathbf{P}$ is complete up to reducibility.

Theorem 5.1. *Let φ be an order-n cellular automorphism of G in the projective plane with $\overline{G} = G$.*

(1) If φ is pseudofree, then $\varphi \rightsquigarrow (\mathcal{R}_{2n,\mathbf{P}})^{2i}$ for n odd and some i.

(2) If φ is not pseudofree, then $n = 2k$ and $\varphi \rightsquigarrow (\mathcal{R}_{2k,\mathbf{P}})^i$ for some i.

Note that Theorem 5.1 implies that there are no even-order pseudofree cellular automorphisms of $\mathbf{P}$. Proposition 5.2 is an analogue of Proposition 2.8 for ovals with Möbius neighborhoods.

Proposition 5.2. *Let φ be a cellular automorphism of G in S whose set of pseudofixed points $\overline{fix}(\varphi)$ contains an oval O with a Möbius neighborhood in S. If m is the index of O, then we get the following.*

(1) The action of φ^m restricted to O itself is rotation rather than reflection.

(2) If r is the order of the rotation action of φ^m restricted to O, then $|\varphi| = 2rm$

Proof. Extend G to a graph G' with sufficiently high representativity so that the faces incident to O form a Möbius band M with O along its core. So now since $\varphi^m(O) = O$, we also get that φ^m is a cellular automorphism of $G'|_M$ in $[M]^\bullet$. The action of φ^m on O is thus a rotation by Theorem 5.1. Furthermore, if r is the order of this rotation, then φ^{rm} is the first power of φ that fixes O pointwise. As such $rm = |\varphi|/2$. □

Proof of Theorem 5.1. Let $n = |\varphi|$ and let π denote the projection $\mathbf{P} \to \mathbf{P}/\langle\varphi\rangle$. First we assume that φ is pseudofree. We begin with numerical arguments to show that $\pi(\mathbf{P})$ is the projective plane and that π has a single branch point of deficiency $n - 1$. Let Y be the set of branch points of π. Theorem 3.6 yields $1 = n\chi(\pi(\mathbf{P})) - \sum_{y\in Y} \text{def}(y)$ so $\chi(\pi(\mathbf{P})) > 0$, and $\pi(\mathbf{P})$ is either the sphere or projective plane. The former is impossible, since orientable surfaces can only lift to orientable surfaces. It follows that $\chi(\pi(\mathbf{P})) = 1$ and so we have $1 = n - \sum_{y\in Y} \text{def}(y)$, *i.e.,*

$$\sum_{y\in Y} \text{def}(y) = n - 1. \tag{1}$$

Now Theorem 3.7 gives

$$\frac{1}{n} \;=\; 1 - |Y| + \sum_y \frac{1}{v_y} \;\leq\; 1 - |Y| + \frac{|Y|}{2} \;=\; 1 - \frac{|Y|}{2}.$$

It follows that $|Y| \leq 2 - 2/n$ and so $|Y| \leq 1$. Now $|Y| \neq 0$ as this would contradict (1) and so there is a single branch point which by (1) has deficiency $n - 1$ and is therefore the image of a fixed point, call it y.

Since $\pi(G)$ in $\pi(\mathbf{P})$ is a cellular embedding, we can contract a spanning tree in $\pi(G)$ and then delete loops to obtain a surface minor H consisting of a single loop e embedded non-contractibly. Let $\tilde{H}$ be the surface orbit minor of G in $\mathbf{P}$ corresponding to H as in Proposition 3.4. Proposition 3.1 gives us that $\tilde{H}$ is

a $\mathbb{Z}_n$-voltage lift of a loop and so by connectedness $\tilde{H}$ is an n-cycle and must be embedded non-contractibly. Since the single face of $\tilde{H}$ in $\mathbf{P}$ contains the fixed point y, the action of $\varphi|_{\tilde{H}}$ on this single face must be a rotation of order n (rather than a reflection) and so $\varphi|_{\tilde{H}} = (\mathcal{R}_{2n,\mathbf{P}})^j$ for some j such that $n \notin \langle j \rangle \subset \mathbb{Z}_{2n}$ and $|\langle j \rangle| = n$. Since $\langle 2 \rangle$ is the only subgroup of $\mathbb{Z}_{2n}$ of order n, we now get that n is odd and j is even and is relatively prime to n.

Now assume that φ is not pseudofree. If φ is an involution, then Proposition 3.9 yields

$$\chi([\pi(\mathbf{P})]^\bullet) = \frac{1}{2} + s + \frac{r}{2} \leq 2.$$

Now since $s \geq 1$ and $\chi([\pi(\mathbf{P})]^\bullet)$ must be a positive integer, we get that $s = 1$ and $r = 1$. If φ has $|\varphi| = 2k$, then φ also has just one oval. This oval must be embedded noncontractibly and so does not separate $\mathbf{P}$, and thus we get that $[\mathbf{P}^\circlearrowleft]^\bullet$ is the sphere with a single capped face f. It follows that $\varphi^\circlearrowleft$ has a fixed point in f and therefore by Theorem 4.1, $\varphi^\circlearrowleft$ reduces to $(\mathcal{R}_{2k,\mathbf{S}})^i$ for some i. Evidently, since $\overline{G} = G$, φ reduces to $(\mathcal{R}_{2k,\mathbf{P}})^i$. □

6 Cellular automorphisms of the torus

6.1 A catalogue of cellular automorphisms of the torus

We note that the definitions in this section are all up to choice of basis for homology. Changes in basis are accomplished through Dehn twists, which do not change the cellular structure.

Grid rotations $\mathcal{GR}_{n,a,b,\mathbf{T}}$ Suppose that $a, b \in \{1, \ldots, n-1\} \subset \mathbb{Z}$, $\langle a, b \rangle = \mathbb{Z}_n$, $\langle a \rangle \neq \mathbb{Z}_n$, and $\langle b \rangle \neq \mathbb{Z}_n$. Without loss of generality say that $a > b$. Then there is $r, s \in \mathbb{Z}$ such that $g = ra + sb = \gcd(a, b)$. Choose r and s so that $|r| + |s|$ is as small as possible. Since every linear combination of a and b is a multiple of g and since $\langle a, b \rangle = \mathbb{Z}_n$, we get that $\langle g \rangle = \mathbb{Z}_n$.

Note that in $\mathbb{Z}_n$, $|a| = \frac{n}{\gcd(a,n)}$ and $|b| = \frac{n}{\gcd(b,n)}$ and so since $\mathbb{Z}_n = \langle a, b \rangle = \langle a \rangle + \langle b \rangle$ we get that

$$n = \frac{|a||b|}{|\langle a \rangle \cap \langle b \rangle|} = \frac{n^2}{\gcd(a,n)\gcd(b,n)|\langle a \rangle \cap \langle b \rangle|}$$

and so

$$|\langle a \rangle \cap \langle b \rangle| = \frac{n}{\gcd(a,n)\gcd(b,n)}$$

is an integer, call it t. We define the (n, a, b)-*torus-grid* as follows. We first take the disjoint union of $\gcd(a, n)$ copies of $C_{|a|}$ in the $(1, 0)$-homology class. This disjoint union contains n vertices. We can add the edges of $\gcd(b, n)$ disjoint $|b|$-cycles in the $(1, t)$ homology class where each $|a|$-cycle and each $|b|$-cycle intersect in t vertices. For example, the first graph in Figure 6.1 is the $(30, 5, 3)$-torus-grid.

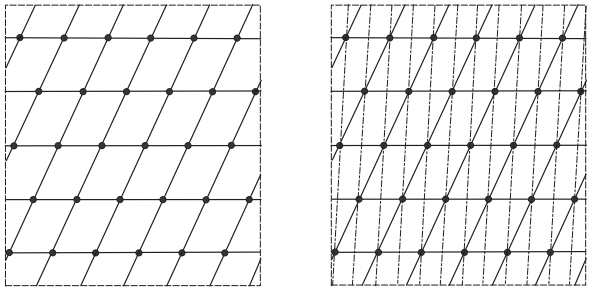

Figure 6.1.

As in Figure 6.1, we can render the (n, a, b)-torus-grid in the unit square where the $|a|$-cycles are horizontal and equally spaced and the $|b|$-cycles are $t \gcd(b, n)$ equally spaced lines of slope t. Note that each slanted line segment of the parallelograms formed in this rendering has rise $= \frac{1}{\gcd(a,n)}$ and run $= \frac{1}{t\gcd(a,n)}$. Thus,

given any vertex u in the grid, if we move r vertices to the right along u's $|a|$-cycle to vertex v and then move s vertices up along v's $|b|$-cycle to vertex w, the line in the unit square from v to w has slope

$$\frac{\frac{s}{\gcd(a,n)}}{\frac{r}{t\gcd(b,n)} + \frac{s}{t\gcd(a,n)}}.$$

So now since $g = ra + sb$ generates $\mathbb{Z}_n$, repeating this move n times will visit every vertex in the graph exactly once and the line segments described above connecting each successive pair will form a simple-closed curve in the homology class given by the above slope. This is the cellular automorphism $\mathcal{GR}_{n,a,b,\mathbf{T}}$. The second graph in Figure 6.1 is the $(30, 5, 3)$-torus-grid along with dashed lines of slope 12 representing the $(1, 12)$-homology class along which the rotation is taken.

Note that the grid rotation $\mathcal{GR}_{n,a,b,\mathbf{T}}$ is free and irreducible.

Spiral rotations $\mathcal{SR}_{n,g,\mathbf{T}}$ Given any $n \geq 2$, let $g \in \{0, \ldots, n-1\}$. Define the (n, g)-*torus-spiral* to be the embedded graph shown in Figure 6.2. Say that F_t is the oriented face with $\partial(F_t) = e_t, f_{t+1}, -e_{t+g}, -f_t$. Define the cellular automorphism $\mathcal{SR}_{n,g,\mathbf{T}}$ by $e_t \mapsto e_{t+1}$ with $\partial(F_t) \mapsto \partial(F_{t+1})$. Note that the spiral rotation $\mathcal{SR}_{n,g,\mathbf{T}}$ is free and irreducible.

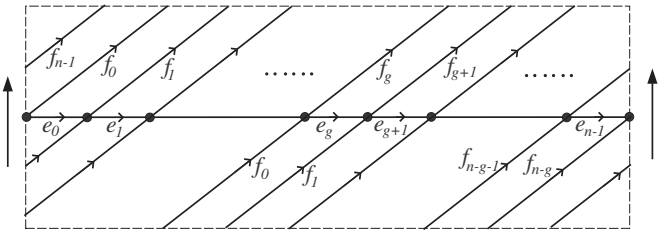

Figure 6.2.

Rotation reflections $\mathcal{LRR}_{2k,\mathbf{T}}$, $\mathcal{SRR}_{4k,\mathbf{T}}$, $\mathcal{ZRR}_{2k,0,\mathbf{T}}$, and $\mathcal{ZRR}_{4k,2k,\mathbf{T}}$ Define the $(2k, 0)$-torus-reflection-spiral to be the embedding obtained from the $(2k, 0)$-torus-spiral by reversing the loops f_{2j} and now say that F_t is the oriented face with $\partial(F_t) = e_t, f_{t+1}, -e_t, f_t$. Given the $(2k, 0)$-torus-reflection-spiral, define the cellular automorphism $\mathcal{LRR}_{2k,\mathbf{T}}$ by $e_t \mapsto e_{t+1}$ and $\partial(F_t) \mapsto \partial(F_{t+1})$. Note that $\mathcal{LRR}_{2k,\mathbf{T}}$ is free and irreducible

Define the $(4k, 2k)$-torus-reflection-spiral to be the embedding in Figure 6.3 and let F_t be the oriented face with $\partial(F_t) = e_t, f_{t+1}, -e_{t+2k}, f_{t+2k}$. Notice the shearing indicated by the labeling of the identified edges along the horizontal lines. We define the cellular automorphism $\mathcal{SRR}_{4k,\mathbf{T}}$ by $e_t \mapsto e_{t+1}$ and $\partial(F_t) \mapsto \partial(F_{t+1})$. Note that $\mathcal{SRR}_{4k,\mathbf{T}}$ is free and irreducible.

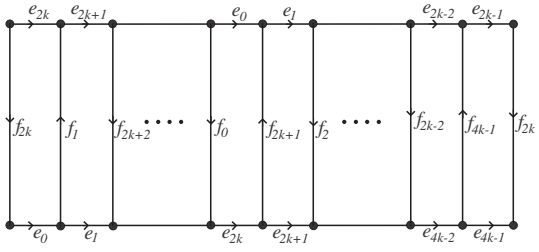

Figure 6.3.

Define the $(2k, 0)$-torus-reflection-zigzag to be the embedding shown on the left in Figure 6.4. Let F_t be the oriented face having $\partial(F_t) = e_t, e_{t+1}, -f_{t+1}, -f_t$. We define the cellular automorphism $\mathcal{ZRR}_{2k,0,\mathbf{T}}$ by $e_t \mapsto e_{t+1}$ and $\partial(F_t) \mapsto \partial(F_{t+1})$. Note that $\mathcal{ZRR}_{2k,0,\mathbf{T}}$ is free and irreducible.

Define the $(4k, 2k)$-torus-reflection-zigzag to be the embedding shown on the right of Figure 6.4. The edges oriented outwards from vertex i are e_i and f_i and so the upper zigzag cycle is $e_0, e_1, e_2, \ldots, e_{4k-1}$ and the lower zigzag cycle is $f_{2k}, f_1, f_{2k+2}, f_3, \ldots, f_0, f_{2k+1}, \ldots, f_{2k-2}, f_{4k-1}$. Let F_t be the oriented face with $\partial(F_t) = e_t, e_{t+1}, -f_{t+2k+1}, -f_t$ and define the cellular automorphism $\mathcal{ZRR}_{4k,2k,\mathbf{T}}$ by $\partial(F_t) \mapsto \partial(F_{t+1})$. Note that $\mathcal{ZRR}_{4k,2k,\mathbf{T}}$ is free and irreducible.

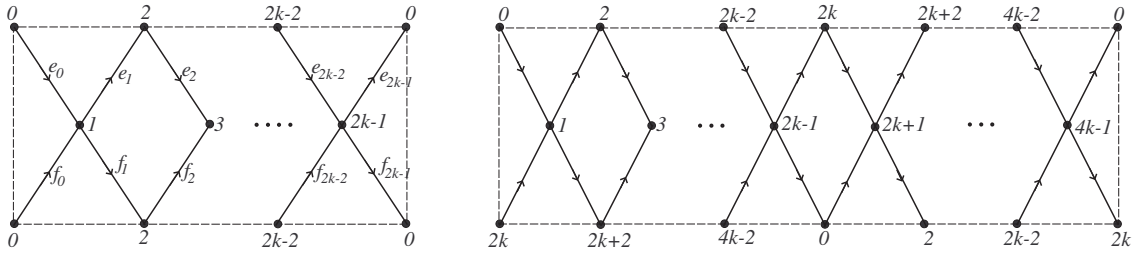

Figure 6.4.

Pseudofree automorphisms The first three embeddings shown in Figure 6.5 depict the cellular automorphisms $\mathcal{P}_{6,1:1,2:2,3:3,\mathbf{T}}$, $\mathcal{P}'_{6,1:1,2:2,3:3,\mathbf{T}}$, and $\mathcal{P}''_{6,1:1,2:2,3:3,\mathbf{T}}$, respectively. Each is described by rotating the hexagonal rendering of the torus by 60°. The second row of Figure 6.5 contains two different renderings of the same embedding in the torus; the automorphism $\mathcal{P}_{3,3:1,\mathbf{T}}$ is described by rotating the hexagonal rendering 120°. The two embeddings in the third row of Figure 6.5 depict the cellular automorphisms $\mathcal{P}_{4,2:1,2:2,\mathbf{T}}$ and $\mathcal{P}'_{4,2:1,2:2,\mathbf{T}}$, respectively. Each is described by rotating the square rendering of the torus by 90°. In the last row of Figure Figure 6.5, the first two pictures are different renderings of the same embedding and the last two pictures are different renderings of the same embedding. The cellular automorphism $\mathcal{P}_{2,4:1,\mathbf{T}}$ is defined by rotating the first hexagonal rendering by 180° and also by rotating the first rectangular rendering by 180°. The cellular automorphism $\mathcal{P}'_{2,4:1,\mathbf{T}}$ is defined by rotating the second hexagonal rendering by 180° and also by rotating the second rectangular rendering by 180°.

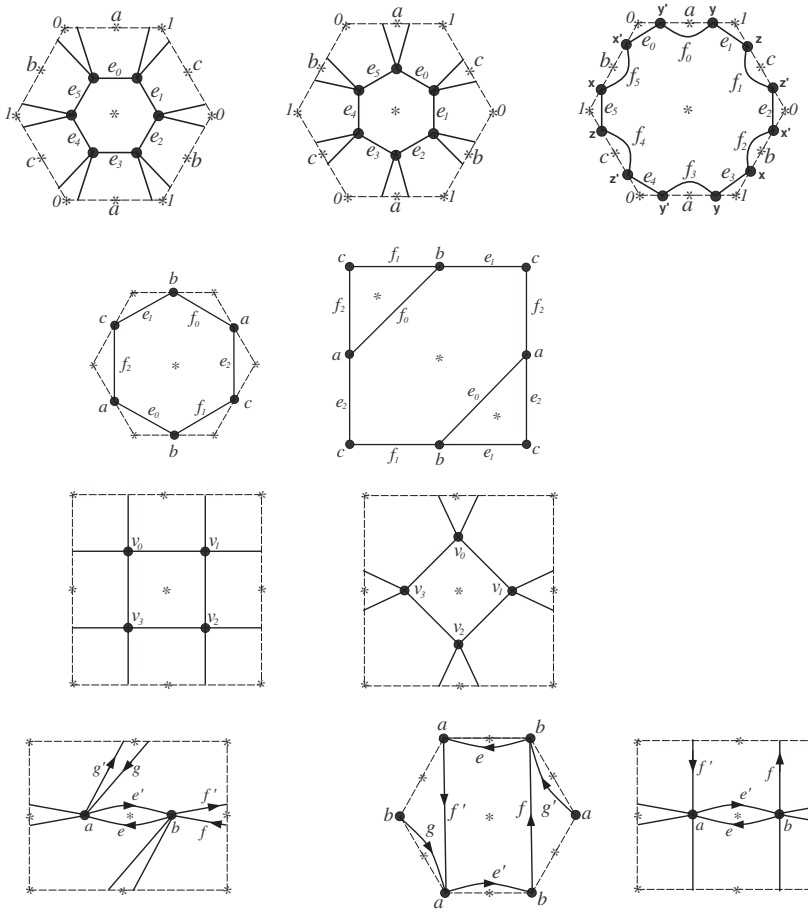

Figure 6.5.

One can check the following:

- $(\mathcal{P}_{6,1:1,2:2,3:3,\mathbf{T}})^2 \rightsquigarrow \mathcal{P}_{3,3:1,\mathbf{T}}$ and $(\mathcal{P}'_{6,1:1,2:2,3:3,\mathbf{T}})^2 \rightsquigarrow \mathcal{P}_{3,3:1,\mathbf{T}}$ by contracting one orbit of spoke edges and deleting the other orbit of spoke edges.

- $(\mathcal{P}''_{6,1:1,2:2,3:3,\mathbf{T}})^2 \rightsquigarrow \mathcal{P}_{3,3:1,\mathbf{T}}$ by contracting one orbit of f-edges and deleting the other orbit of f-edges.
- $(\mathcal{P}_{6,1:1,2:2,3:3,\mathbf{T}})^3 \rightsquigarrow \mathcal{P}_{2,4:1,\mathbf{T}}$ by contracting two orbits of spoke edges and deleting the third orbit of spoke edges, and $(\mathcal{P}_{6,1:1,2:2,3:3,\mathbf{T}})^3 \rightsquigarrow \mathcal{P}'_{2,4:1,\mathbf{T}}$ by contracting $\{e_1, e_2, e_4, e_5\}$ and deleting one orbit of spoke edges not around a.
- $(\mathcal{P}'_{6,1:1,2:2,3:3,\mathbf{T}})^3 \rightsquigarrow \mathcal{P}_{2,4:1,\mathbf{T}}$ by contracting $\{e_1, e_2, e_4, e_5\}$ and deleting one orbit of spoke edges, whereas $(\mathcal{P}'_{6,1:1,2:2,3:3,\mathbf{T}})^3 \not\rightsquigarrow \mathcal{P}'_{2,4:1,\mathbf{T}}$.
- $(\mathcal{P}''_{6,1:1,2:2,3:3,\mathbf{T}})^3 \rightsquigarrow \mathcal{P}_{2,4:1,\mathbf{T}}$ by contracting $\{e_0, e_1, e_3, e_4\}$ and deleting $\{e_2, e_5\}$, whereas $(\mathcal{P}''_{6,1:1,2:2,3:3,\mathbf{T}})^3 \not\rightsquigarrow \mathcal{P}'_{2,4:1,\mathbf{T}}$.
- $(\mathcal{P}_{4,2:1,2:2,\mathbf{T}})^2 \rightsquigarrow \mathcal{P}'_{2,4:1,\mathbf{T}}$, whereas $(\mathcal{P}_{4,2:1,2:2,\mathbf{T}})^2 \not\rightsquigarrow \mathcal{P}_{2,4:1,\mathbf{T}}$, and $(\mathcal{P}'_{4,2:1,2:2,\mathbf{T}})^2 \rightsquigarrow \mathcal{P}_{2,4:1,\mathbf{T}}$, whereas $(\mathcal{P}'_{4,2:1,2:2,\mathbf{T}})^2 \not\rightsquigarrow \mathcal{P}'_{2,4:1,\mathbf{T}}$.

Oval rotation reflection $\mathcal{ORR}_{4k+2,\mathbf{T}}$ The cellular automorphism $\mathcal{ORR}_{4k+2,\mathbf{T}}$ for $k \geq 1$ is defined on the left-hand embedding in Figure 6.6 by reflecting across the vertical oval-cycle $e_0, e_1, \ldots, e_{2k}$ and then rotating downwards by one edge. This maps $v_i \mapsto v_{i+1}$, $f_i \mapsto g_{i+1}$, and $g_i \mapsto f_{i+1}$ where addition in subscripts is modulo $2k+1$. For $k = 0$, the cellular automorphism $\mathcal{ORR}_{2,\mathbf{T}}$ is defined on the right-hand embedding in Figure 6.6 by reflecting across the vertical oval-cycle e, thus switching f and g. The automorphism $\mathcal{ORR}_{4k+2,\mathbf{T}}$ is oval-irreducible.

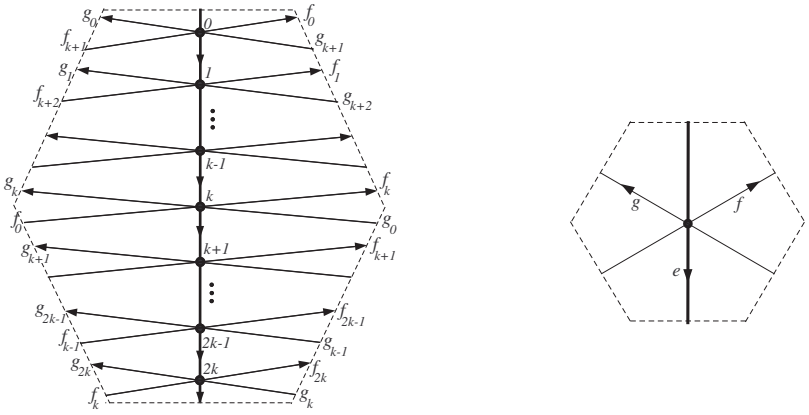

Figure 6.6.

Double-oval rotation reflection $\mathcal{OORR}_{4k+2,\mathbf{T}}$ For $k \geq 0$ we define the cellular automorphism $\mathcal{OORR}_{4k+2,\mathbf{T}}$ on the embedding in Figure 6.7 by $u_i \mapsto u_{i+1}$, $v_i \mapsto v_{i+1}$, $e_i \mapsto f_{i+1}$, and $f_i \mapsto e_{i+1}$ where addition in subscripts is modulo $2k+1$. The cycles on $u_1, \ldots, u_{2k+1}$ and $v_1, \ldots, v_{2k+1}$ are the oval cycles of $\mathcal{OORR}_{4k+2,\mathbf{T}}$ and this map is oval-irreducible.

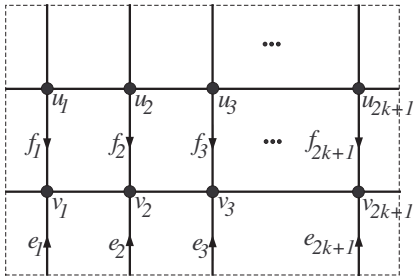

Figure 6.7.

6.2 Completeness of the catalogue

Theorem 6.8. *If φ is a free cellular automorphism of G in $\mathbf{T}$, then φ reduces to $(\mathcal{GR}_{n,a,b,\mathbf{T}})^i$, $(\mathcal{SR}_{n,g,\mathbf{T}})^i$, $(\mathcal{LRR}_{2k,\mathbf{T}})^i$, $(\mathcal{SRR}_{4k,\mathbf{T}})^i$, $(\mathcal{ZRR}_{2k,0,\mathbf{T}})^i$, or $(\mathcal{ZRR}_{4k,2k,\mathbf{T}})^i$ for some i.*

Proof. Note that $G = \overline{G}$ because φ is free. Let $n = |\varphi|$ and let π denote the projection $\mathbf{T} \to \mathbf{T}/\langle\varphi\rangle$. Here $\chi(\pi(\mathbf{T})) = 0/n = 0$ and so $\pi(\mathbf{T})$ is either the torus or Klein bottle. Let these be Cases 1 and 2, respectively.

Case 1 Since the embedding of $\pi(G)$ in $\pi(\mathbf{T}) = \mathbf{T}$ is cellular, we can contract a spanning tree and delete loops to obtain a surface minor H of $\pi(G)$ in $\pi(T)$ that consists of one vertex and two loops, say e and f, where, up to Dehn twists, we can say that e and f are in homology classes $(1,0)$ and $(0,1)$. Let $\tilde{H}$ be the surface orbit minor of G given in Proposition 3.4 and let σ be a $\mathbb{Z}_n$-voltage assignment from Proposition 3.1 that recovers $\tilde{H}$ and $\varphi|_{\tilde{H}}$ aside from the action of $\varphi|_{\tilde{H}}$ on loops. Without loss of generality either $|\sigma(e)| = n$ or $|\sigma(e)|, |\sigma(f)| < n$. Let these be Cases 1.1 and 1.2, respectively.

Case 1.1 Because the boundary walk on the one face of H in $\pi(\mathbf{T})$ is $e, f, -e, -f$, we get that $H^\sigma \cong \tilde{H}$ is the $(n, \sigma(f))$-torus-spiral (see Figure 6.2) where we consider $\sigma(f)$ as an integer from $\{0, \ldots, n-1\}$. Label the edges as in Figure 6.2. Note that the loop e lifts to the n-cycle C and that f lifts to $f_0, \ldots, f_{n-1}$. Now since φ is free, the action of $\varphi|_{\tilde{H}}$ on just the cycle C is rotation rather than reflection. Thus $\varphi|_{\tilde{H}}(e_j) = e_{j+i}$ for some i relatively prime to n and so we must have that $\varphi|_{\tilde{H}}(\partial(F_j)) = \partial(F_{j+i})$ and thus $\varphi|_{\tilde{H}}$ is $(\mathcal{SR}_{n,\sigma(f),\mathbf{T}})^i$ for some i relatively prime to n.

Case 1.2 Let $a = \sigma(e)$ and $b = \sigma(f)$. By assumption $\mathbb{Z}_n \neq \langle a\rangle$ and $\mathbb{Z}_n \neq \langle b\rangle$. However, since $\tilde{H} \cong H^\sigma$ is connected, we must have that $\langle a, b\rangle = \mathbb{Z}_n$ and so $\gcd(a, b)$ generates $\mathbb{Z}_n$. Without loss of generality we suppose $a, b \in \{1, 2, \ldots, n-1\}$ and $a > b$. Now e in H lifts to $\frac{n}{|a|} = \gcd(a, n)$ cycles of length $|a|$ in $H^\sigma \cong \tilde{H}$ and so these cycles must collectively contain all n vertices of $\tilde{H}$; the analogous result holds for f. Thus each $C_{|a|}$-cycle and each $C_{|b|}$-cycle intersect in $t = |\langle a\rangle \cap \langle b\rangle|$ vertices. So now since each vertex is in the intersection of a unique pair of cycles, we get that $n = t \gcd(a, n) \gcd(b, n)$. Thus $H^\sigma \cong \tilde{H}$ is the (n, a, b)-torus-grid. Note that a and b are both nonzero and so there are no loops and no two faces with the same boundary walk and therefore the basic automorphism β_σ completely determines $\varphi|_{\tilde{H}}$. If P is a $v_j v_{j+1}$-path in H^σ (recall that $v_{j+1} = \beta_\sigma(v_j)$) that moves x edges along an $|a|$-cycle and y edges along a $|b|$-cycle, then $\beta_\sigma(P)$ is the corresponding $v_{j+1}v_{j+2}$-path which also moves x edges along an $|a|$-cycle and y edges along a $|b|$-cycle. We see that $xa + yb$ must be a generator for $\mathbb{Z}_n$ and since we must have that $xa + yb = i \gcd(a, b)$ we get that $\varphi|_{\tilde{H}}$ is $(\mathcal{GR}_{n,a,b,\mathbf{T}})^i$ for some i relatively prime to n.

Case 2 Since the embedding of $\pi(G)$ in $\pi(\mathbf{T}) = \mathbf{K}$ is cellular, we can contract a spanning tree and contract loops to obtain a surface minor H of $\pi(G)$ in $\pi(\mathbf{T})$ that consists of one vertex and two loops, say e and f. Write $\mathbb{Z} \times \mathbb{Z}_2$ for the first homology group of $\mathbf{K}$, so that representatives of the $(1,0)$ and $(1,1)$ classes have Möbius neighborhoods. Up to homeomorphism we may assume without loss of generality that e is in the $(1,0)$-homology class. Then either f is in the $(0,1)$-homology class or the $(1,1)$-homology class; see Figure 6.9.

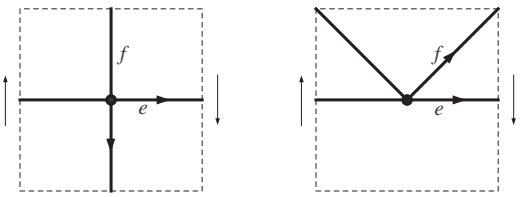

Figure 6.9.

Let these be Cases 2.1 and 2.2, respectively. In either case let $\tilde{H}$ be the surface orbit minor of G given in Proposition 3.4 and let σ be a $\mathbb{Z}_n$-voltage assignment from Proposition 3.1 that recovers $\tilde{H}$ and $\varphi|_{\tilde{H}}$ aside from the action of $\varphi|_{\tilde{H}}$ on loops.

Case 2.1 Because φ is free, σ_* is zero on facial boundary walks. Thus $\sigma_*(e, f, -e, f) = 0$ and so $2\sigma(f) = 0$, which gives $\sigma(f) \in \{0, \frac{n}{2}\}$. Since the derived embedding of H^σ is in $\mathbf{T}$ we have by Proposition 3.3 that $|\sigma(e)|$ is even and so n is even as well. Since $H^\sigma \cong \tilde{H}$ is connected we have that $\langle\sigma(e), \sigma(f)\rangle = \mathbb{Z}_n$. However since $|\sigma(e)| = 2k$ we get that $k\sigma(e) = \frac{n}{2}$ and so because $\sigma(f) \in \{0, \frac{n}{2}\}$ we have that $\mathbb{Z}_n = \langle\sigma(e), \sigma(f)\rangle = \langle\sigma(e)\rangle$. So up to automorphism of $\mathbb{Z}_n$ we get $\sigma(e) = 1$ and $\sigma(f) \in \{0, \frac{n}{2}\}$.

If $\sigma(f) = 0$, then the facial boundary walk $e, f, -e, f$ of the single face of H in $\pi(\mathbf{T})$ gives us that $H^\sigma \cong \tilde{H}$ is the $(n, 0)$-reflection-spiral (as described in Section 6.1) where e lifts to the n-cycle C of the $(n, 0)$-reflection-

spiral. Since the action of $\varphi|_{\tilde{H}}$ on the cycle C is rotation rather than reflection, $\varphi|_{\tilde{H}}(e_j) = e_{j+i}$ for some i relatively prime to $n = 2k$. Thus $\varphi|_{\tilde{H}}(\partial(F_j)) = \partial(F_{j+i})$ and so $\varphi|_{\tilde{H}}$ is $(\mathcal{LRR}_{n,\mathbf{T}})^i$ for i relatively prime to n.

If $\sigma(f) = \frac{n}{2}$, then consider the closed walk $w = f, e, \ldots, e$ in H containing $\frac{n}{2}$ copies of e. Note that $\sigma_*(w) = \sigma(f) + \frac{n}{2}\sigma(e) = 0$ so Proposition 3.3 implies that w is an annular walk. Thus $\frac{n}{2}$ is even, giving $n = 4k$ and $\sigma(f) = 2k$. Since $e, f, -e, f$ is the facial boundary walk of the single face of H in $\pi(\mathbf{T})$ we see that H^σ in $\mathbf{T}$ is the $(4k, 2k)$-reflection-spiral. Again we now have that $\varphi|_{\tilde{H}}(e_j) = e_{j+i}$ for some i relatively prime to $n = 4k$ and $\varphi|_{\tilde{H}}(\partial(F_j)) = \partial(F_{j+i})$, so $\varphi|_{\tilde{H}}$ is $(\mathcal{SRR}_{4k,\mathbf{T}})^i$ for some i relatively prime to $n = 4k$.

Case 2.2 Here the facial boundary walk of the single face of H in $\pi(\mathbf{T})$ is $e, e, -f, -f$. Since $0 = \sigma_*(e, e, -f, -f) = 2(\sigma(e) - \sigma(f))$, it follows that $\sigma(e) - \sigma(f) \in \{0, \frac{n}{2}\}$. In Case 2.2.1 we let $\sigma(e) = \sigma(f)$ and in Cases 2.2.2 we let $\sigma(e) - \sigma(f) = \frac{n}{2}$. In either case, since $\tilde{H}$ is connected, we have that $\langle \sigma(e), \sigma(f) \rangle = \mathbb{Z}_n$.

Case 2.2.1 Here we have up to automorphism of $\mathbb{Z}_n$ that $\sigma(e) = \sigma(f) = 1$. Furthermore we must also have that n is even because otherwise the closed walk $e, \ldots, e$ with n copies of e would be a Möbius walk, contradicting the orientability of $\mathbf{T}$ by Proposition 3.3. So now the facial walk $e, e, -f, -f$ of H in $\pi(\mathbf{T})$ gives us that $H^\sigma \cong \tilde{H}$ consists of two n-cycles $e_0, \ldots, e_{n-1}$ and $f_0, \ldots, f_{n-1}$ where both e_j and f_j are $v_j v_{j+1}$-links. Thus $H^\sigma \cong \tilde{H}$ is the $(2k, 0)$-reflection-zigzag as labeled in Figure 6.4. Since the action of $\varphi|_{\tilde{H}}$ on $e_0, \ldots, e_{n-1}$ must be rotation rather than reflection, we get that $\varphi|_{\tilde{H}}(e_j) = e_{j+i}$ for some i relatively prime to n. Also, $\varphi|_{\tilde{H}}(\partial(F_j)) = \partial(F_{j+i})$, so $\varphi|_{\tilde{H}}$ is $(\mathcal{ZRR}_{2k,0,\mathbf{T}})^i$ for some i relatively prime to n.

Case 2.2.2 Since $\frac{n}{2}$ is in our voltage group, n is even; furthermore, we claim that $n = 4k$. Supposing by way of contradiction that $n = 4k + 2$, it must be that exactly one of $\sigma(e)$ and $\sigma(f)$ is in the subgroup $\langle 2 \rangle$ because $\sigma(e) - \sigma(f) = \frac{n}{2} = 2k + 1 \notin \langle 2 \rangle$. Assuming that $\sigma(e) \notin \langle 2 \rangle$, we get that $|\sigma(e)|$ is even and so $\frac{|\sigma(e)|}{2}\sigma(e) = \frac{n}{2}$. Thus $\sigma(f) = \frac{n}{2} + \sigma(e) = (\frac{|\sigma(e)|}{2} + 1)\sigma(e)$ which gives us that $\mathbb{Z}_n = \langle \sigma(e), \sigma(f) \rangle = \langle \sigma(e) \rangle$. So up to some automorphism of $\mathbb{Z}_n$, $\sigma(e) = 1$ and $\sigma(f) = \frac{n}{2} + 1$. Now the closed walk $f, e, \ldots, e$ with $\frac{n}{2} - 1$ copies of e has $\sigma_*(f, e, \ldots, e) = \sigma(f) + (\frac{n}{2} - 1)\sigma(e) = 0$ and is a Möbius walk because $\frac{n}{2}$ is odd. This contradicts the orientability of $\mathbf{T}$ by Proposition 3.3 and hence $n = 4k$.

Now since $\sigma(e) - \sigma(f) = \frac{n}{2} = 2k$ we get that either $\sigma(e), \sigma(f) \in \langle 2 \rangle$ or $\sigma(e), \sigma(f) \notin \langle 2 \rangle$. Since $\langle 2 \rangle \neq \mathbb{Z}_n = \langle \sigma(e), \sigma(f) \rangle$ we get that $\sigma(e), \sigma(f) \notin \langle 2 \rangle$ and so $|\sigma(e)|$ and $|\sigma(f)|$ are both even. As in the previous paragraph we get that $(\frac{|\sigma(e)|}{2} + 1)\sigma(e) = \sigma(f)$ which yields that $\mathbb{Z}_n = \langle \sigma(e), \sigma(f) \rangle = \langle \sigma(e) \rangle$. So up to automorphism of $\mathbb{Z}_n$, $\sigma(e) = 1$ and $\sigma(f) = \frac{n}{2} + 1 = 2k + 1$. So now e lifts to a $4k$-cycle $e_0, \ldots, e_{4k-1}$ and f lifts to a $4k$-cycle $f_0, f_{2k+1}, f_2, f_{2k+3}, \ldots, f_{4k-2}, f_{2k-1}$ where e_j is a $v_j v_{j+1}$-link and f_j is a $v_j v_{2k+1+j}$-link. Since the facial boundary walk of the single face of H in $\pi(\mathbf{T})$ is $e, e, -f, -f$ we get that $\tilde{H}$ has facial boundary walks $e_j, e_{j+1}, -f_{j+2k+1}, -f_j$. It follows that $\varphi|_{\tilde{H}}(e_j) = e_{j+i}$ for some i relatively prime to $n = 4k$ and $\varphi|_{\tilde{H}}(\partial(F_j)) = \partial(F_{j+i})$, so $\varphi|_{\tilde{H}}$ is $(\mathcal{ZRR}_{4k,2k,\mathbf{T}})^i$. □

Theorem 6.10. *If φ is a cellular automorphism of $G = \overline{G}$ in $\mathbf{T}$ that is pseudofree but not free, then φ reduces to one of $\mathcal{P}_{2,4:1,\mathbf{T}}$, $\mathcal{P}'_{2,4:1,\mathbf{T}}$, $(\mathcal{P}_{3,3:1,\mathbf{T}})^i$, $(\mathcal{P}_{4,2:1,2:2,\mathbf{T}})^i$, $(\mathcal{P}'_{4,2:1,2:2,\mathbf{T}})^i$, $(\mathcal{P}_{6,1:1,2:2,3:3,\mathbf{T}})^i$, $(\mathcal{P}'_{6,1:1,2:2,3:3,\mathbf{T}})^i$, and $(\mathcal{P}''_{6,1:1,2:2,3:3,\mathbf{T}})^i$ for some i.*

Proof. Let $n = |\varphi|$, let π denote the projection $\mathbf{T} \to \mathbf{T}/\langle \varphi \rangle$, and let Y be the set of branch points of $\pi(G)$ in $\pi(\mathbf{T})$. By Theorem 3.6, $\chi(\mathbf{T}) = n\chi(\pi(\mathbf{T})) - \sum_{y \in Y} \mathrm{def}(y)$ and so $n\chi(\pi(\mathbf{T})) = \sum_{y \in Y} \mathrm{def}(y) \geq 1$ because φ is not free. Thus $\chi(\pi(\mathbf{T})) \in \{1, 2\}$ and so $\pi(\mathbf{T})$ is the projective plane or sphere. Let these be Cases 1 and 2, respectively.

Case 1 Here $n = \sum_{y \in Y} \mathrm{def}(y)$ and since each $\mathrm{def}(y) \leq n - 1$, we must have $|Y| \geq 2$. Additionally, since each $\mathrm{def}(y) = n - \frac{n}{v_y}$ where $v_y | n$ we get that each $\mathrm{def}(y) \geq n - \frac{n}{2} = \frac{n}{2}$. Thus $|Y|\frac{n}{2} \leq \sum_y \mathrm{def}(y) = n$ and so $|Y| \leq 2$ which makes $|Y| = 2$ and each $\mathrm{def}(y) = \frac{n}{2}$.

By contracting a spanning tree and deleting loops, the embedding of $\pi(G)$ in $\pi(\mathbf{T})$ has one of the two embeddings in Figure 6.11 as a surface minor, call it H. Here, we use $*$ to denote a branch point.

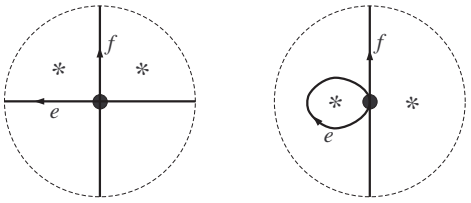

Figure 6.11.

Let $\tilde{H}$ be the surface orbit minor of G in $\mathbf{T}$ given by Proposition 3.4 and σ be a $\mathbb{Z}_n$-voltage assignment from Proposition 3.1 with $H^\sigma \cong \tilde{H}$. In the right-hand graph of Figure 6.11, since e is the facial boundary walk surrounding a branch point of deficiency $\frac{n}{2}$ we must have that $\sigma(e) = \frac{n}{2}$. The other face of the right-hand embedding has facial boundary walk f, f, e around another branch point of deficiency $\frac{n}{2}$. So it must be that $\frac{n}{2} = \sigma_*(f, f, e) = 2\sigma(f) + \frac{n}{2}$ and thus $2\sigma(f) = 0$, implying $\sigma(f) \in \{0, \frac{n}{2}\}$. However, if $\sigma(f) = \frac{n}{2}$ then the Möbius walk f, e has voltage 0, and if $\sigma(f) = 0$ then f itself is a Möbius walk of voltage 0. In either case, by Proposition 3.3 the right-hand embedding cannot lift to the orientable surface $\mathbf{T}$.

In the left-hand graph of Figure 6.11 the two facial boundaries are e, f and $e, -f$, so we have $\sigma(e)+\sigma(f) = \sigma(e) - \sigma(f) = n/2$. This implies that $2\sigma(f) = 0$, so either $\sigma(f) = 0$ and $\sigma(e) = n/2$ or $\sigma(e) = 0$ and $\sigma(f) = n/2$. Thus either e or f is a Möbius walk with voltage 0 which again, by Proposition 3.3, cannot lift to $\mathbf{T}$.

Case 2 Here $2n = \sum_{y \in Y} \mathrm{def}(y)$ and since each $\mathrm{def}(y) \leq n-1$ we must have that $|Y| \geq 3$. Additionally, since $\mathrm{def}(y) \geq \frac{n}{2}$, we get that $|Y|\frac{n}{2} \leq \sum_y \mathrm{def}(y) = 2n$ and so $|Y| \leq 4$. In Case 2.1 say $|Y| = 3$ and in Case 2.2 say $|Y| = 4$.

Case 2.1 Let $v_1 \leq v_2 \leq v_3$ be the respective orders of the three branch points. From $\mathrm{def}(y) = n - \frac{n}{v_y}$ and $2n = \sum_{y \in Y} \mathrm{def}(y)$ we get that $\frac{1}{v_1} + \frac{1}{v_2} + \frac{1}{v_3} = 1$. One can check that (v_1, v_2, v_3) is either $(3, 3, 3)$, $(2, 4, 4)$, or $(2, 3, 6)$.

Since each branch point of π is in the center of a face of $\pi(G)$ in $\pi(\mathbf{T})$ (which is the sphere) we obtain a surface minor H of $\pi(G)$ consisting of a single vertex and two loops as shown in Figure 6.12 by contracting a spanning tree and deleting loops.

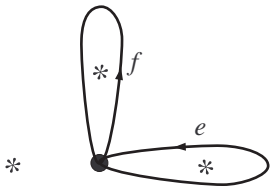

Figure 6.12.

Let $\tilde{H}$ be the surface orbit minor of G in $\mathbf{T}$ given by Proposition 3.4 and let σ be a $\mathbb{Z}_n$-voltage assignment from Proposition 3.1 with $H^\sigma \cong \tilde{H}$. If $(v_1, v_2, v_3) = (3, 3, 3)$ then $\sigma(e), \sigma(f), \sigma(e) + \sigma(f) \in \{n/3, -n/3\}$ and so $\sigma(e) = \sigma(f) = \pm n/3$. In either case, since $\tilde{H} \cong H^\sigma$ is connected we must have that $n = 3$, and one can then check that H^σ is the defining graph for $\mathcal{P}_{3,3:1,\mathbf{T}}$ and so $\varphi|_{\tilde{H}}$ is $(\mathcal{P}_{3,3:1,\mathbf{T}})^i$ for some i.

If $(v_1, v_2, v_3) = (2, 4, 4)$, then without loss of generality either $\sigma(e), \sigma(f) \in \{n/4, -n/4\}$ or $\sigma(e) = \pm n/4$ and $\sigma(f) = n/2$. In the former case, since $\sigma(e) + \sigma(f) \neq 0$, we get that $\sigma(e) = \sigma(f) = \pm n/4$. In either case, the connectedness of $\tilde{H} \cong H^\sigma$ forces $n = 4$. When $\sigma(e) = \sigma(f) = \pm n/4$ one can check that H^σ is the defining graph for $\mathcal{P}_{4,2:1,2:2,\mathbf{T}}$ and thus $\varphi|_{\tilde{H}} = (\mathcal{P}_{4,2:1,2:2,\mathbf{T}})^i$ for some i. When one of $\sigma(e), \sigma(f)$ equals $n/2$ and the other is $\pm n/4$ one can check that H^σ is the defining graph for $\mathcal{P}'_{4,2:1,2:2,\mathbf{T}}$ and thus $\varphi|_{\tilde{H}} = (\mathcal{P}'_{4,2:1,2:2,\mathbf{T}})^i$ for some i.

If $(v_1, v_2, v_3) = (2, 3, 6)$, then without loss of generality we get one of the following possibilities: $\sigma(e) = \pm n/6$ and $\sigma(f) = n/2$; $\sigma(e) = \pm n/6$ and $\sigma(f) = \pm n/3$; or $\sigma(e) = \pm n/3$ and $\sigma(f) = n/2$. In any case, the connectivity of $\tilde{H} \cong H^\sigma$ implies that $n = 6$. In each case, H^σ is the defining graph for one of $\mathcal{P}_{6,1:1,2:2,3:3,\mathbf{T}}$, $\mathcal{P}'_{6,1:1,2:2,3:3,\mathbf{T}}$, and $\mathcal{P}''_{6,1:1,2:2,3:3,\mathbf{T}}$ and so $\varphi|_{\tilde{H}}$ is one of $(\mathcal{P}_{6,1:1,2:2,3:3,\mathbf{T}})^i$, $(\mathcal{P}'_{6,1:1,2:2,3:3,\mathbf{T}})^i$, and $(\mathcal{P}''_{6,1:1,2:2,3:3,\mathbf{T}})^i$ for some i.

Case 2.2 Since each $\text{def}(y) \geq \frac{n}{2}$, $|Y| = 4$ implies that $2n = 4 \cdot \frac{n}{2} \leq \sum_y \text{def}(y) = 2n$ and so $\text{def}(y) = \frac{n}{2}$ for each branch point y and also $n = 2k$. Because π has four branch points and $\pi(\mathbf{T})$ is the sphere, we get that $\pi(G)$ has one of the two surface minors shown in Figure 6.13, call it H.

Figure 6.13.

Let $\tilde{H}$ be the surface orbit minor of G in $\mathbf{T}$ given by Proposition 3.4 and σ be a $\mathbb{Z}_n$-voltage assignment from Proposition 3.1 with $H^\sigma \cong \tilde{H}$. By connectivity of $\tilde{H}$, we have $n = 2$. If H is the left-hand graph in Figure 6.13, then the voltage on each loop must be 1. One can check that H^σ is the defining graph for $\mathcal{P}_{2,4:1,\mathbf{T}}$ and so $\varphi|_{\tilde{H}}$ is $\mathcal{P}_{2,4:1,\mathbf{T}}$.

If H is the right-hand graph in Figure 6.13, then the voltage on the innermost and outermost loops must be 1 and the voltage on the middle loop must then be 0. Thus H^σ is the defining graph for $\mathcal{P}'_{2,4:1,\mathbf{T}}$ and so $\varphi|_{\tilde{H}}$ is $\mathcal{P}'_{2,4:1,\mathbf{T}}$. □

Theorem 6.14. *If φ is a non-pseudofree involution of G in $\mathbf{T}$ with $\overline{G} = G$, then φ reduces to $\mathcal{ORR}_{2,\mathbf{T}}$ or $\mathcal{OORR}_{2,\mathbf{T}}$.*

Proof. By Proposition 3.9 we have $\chi([\pi(\mathbf{T})]^\bullet) = \frac{r}{2} + s$. Since $s \geq 1$ we have $2 \geq \frac{r}{2} + s \geq 1$. Thus $(r, s) = (0, 1)$, $(0, 2)$, or $(2, 1)$; these are Cases 1, 2, and 3, respectively.

Case 1 We have $\chi([\pi(\mathbf{T})]^\bullet) = 1$ so $\pi(\mathbf{T})$ is the Möbius band. Consider the edges of the single hole cycle in $\pi(G)$ and disregard one of them. The remaining edge set may be extended to a spanning tree T of $\pi(G)$. By contracting T and then possibly deleting some loops, we obtain a surface minor H as shown in Figure 6.15. Since T satisfies the conditions of Proposition 3.14, we get a surface orbit minor $\tilde{H}$ of G corresponding to H.

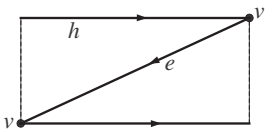

Figure 6.15.

By Proposition 3.13, there is a $\mathbb{Z}_2$-voltage assignment σ such that $\widehat{H}^\sigma \cong \tilde{H}$ and $\varphi|_{\tilde{H}} = \beta_\sigma$ up to this isomorphism. Since φ has no isolated fixed-points we have $\sigma(h) = \sigma(h) + 2\sigma(e) = \sigma_*(h, e, e) = 0$. So now either $\sigma(e) = 1$ or $\sigma(e) = 0$. We cannot have $\sigma(e) = 0$, because the unfolding lift is an orientable surface. When $\sigma(e) = 1$ we have that H^σ in $([\pi(\mathbf{T})]^\bullet)^\sigma$ is the embedding in the cylinder shown in Figure 6.16 where h_0 and h_1 are the hole cycles.

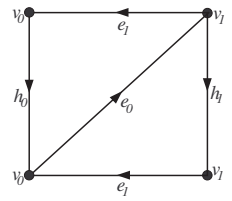

Figure 6.16.

It follows that the unfolding lift is the torus, where $h_0 = h_1$. Since h is an oval-cycle of $\varphi|_{\tilde{H}}$, $\varphi|_{\tilde{H}}$ exchanges the two faces of the embedding and so takes the facial walk h, e_0, e_1 to the facial walk h, e_1, e_0 and also takes e_0 to e_1 and e_1 to e_0. Thus $\varphi|_{\tilde{H}}$ is the automorphism $\mathcal{ORR}_{2,\mathbf{T}}$ as shown in Figure 6.6 where $h = e$, $e_1 = f$, and $e_0 = g$.

Case 2 We have $\chi([\pi(\mathbf{T})]^\bullet) = 2$ so $\pi(\mathbf{T})$ is the annulus. Disregard one edge in each of the two hole cycles and extend the remaining edges to a spanning tree T of $\pi(G)$ and then let $C = T \backslash e$ where $e \in T$ is an edge not

on either hole cycle. Now we can delete edges in $\pi(G)/C$ in $\pi(\mathbf{T})$ and then reintroduce e to obtain a surface minor H with two vertices v_1 and v_2, with loops h_1 and h_2 covering the holes, and a link e connecting v_1 and v_2. Assume the edges are oriented so that the single facial walk is $h_1, e, h_2, -e$. Since C satisfies the conditions of Proposition 3.14, we can let $\tilde{H}$ be the surface orbit minor of G corresponding to H. By Proposition 3.13 there is a $\mathbb{Z}_2$-voltage assignment σ such that $\widehat{H}^\sigma \cong \tilde{H}$ and $\varphi|_{\tilde{H}} = \beta_\sigma$ up to this isomorphism. Since φ has no isolated fixed-points we have $\sigma(h_1) + \sigma(h_2) = \sigma_*(h_1, e, h_2, -e) = 0$ and thus $\sigma(h_1) = \sigma(h_2) \in \{0, 1\}$. (Without affecting $\widehat{H}^\sigma$ we may assume that $\sigma(e) = 0$.) Since $\widehat{H}^\sigma$ is embedded in the orientable surface $\mathbf{T}$, $\sigma(h_1) = \sigma(h_2) = 0$. It follows that $\tilde{H}$ is the defining graph for $\mathcal{OORR}_{2,\mathbf{T}}$ where h_1 and h_2 are the oval cycles, so $\varphi_{\tilde{H}}$ is $\mathcal{OORR}_{2,\mathbf{T}}$.

Case 3 We have $\chi([\pi(\mathbf{T})]^\bullet) = 2$ so $\pi(\mathbf{T})$ is the disk. Let T be a spanning tree of $\pi(G)$ that includes all the edges of the single hole cycle of $\pi(G)$ save one. By contracting T and deleting loops, we obtain a surface minor H with a single vertex v, a loop h which is the hole-cycle, and an additional loop e surrounding one of the branch points as shown on the left in Figure 6.17.

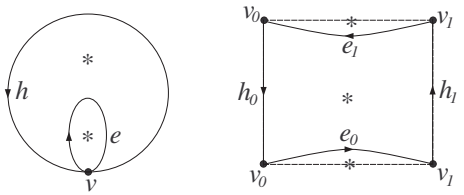

Figure 6.17.

By Proposition 3.14, there is surface orbit minor $\tilde{H}$ of G corresponding to H and by Proposition 3.13 there is a $\mathbb{Z}_2$-voltage assignment σ such that $H^\sigma \cong \tilde{H}$ and $\varphi|_{\tilde{H}} = \beta_\sigma$ up to this isomorphism. Since each face has a branch point, we have $\sigma(h) + \sigma(e) = \sigma_*(h, e) = 1$ and $\sigma(e) = 1$, and thus $\sigma(h) = 0$. The unfolding lift $\widehat{H}^\sigma$ is then embedded in $\mathbf{K}$ and not $\mathbf{T}$, a contradiction; see the right in Figure 6.17. □

Theorem 6.18. *If φ is a non-pseudofree non-involutory cellular automorphism of G in $\mathbf{T}$ with $\overline{G} = G$, then φ reduces to $(\mathcal{ORR}_{4t+2,\mathbf{T}})^i$ or $(\mathcal{OORR}_{4t+2,\mathbf{T}})^i$ for some i.*

Proof. By Proposition 2.4, we may write $n = 2k = |\varphi|$. By Theorem 6.14, φ^k reduces to either $\mathcal{OORR}_{2,\mathbf{T}}$ or $\mathcal{ORR}_{2,\mathbf{T}}$. Let these be Cases 1 and 2, respectively.

Case 1 Let π denote the projection $\mathbf{T} \to \mathbf{T}/\langle\varphi^k\rangle$ and $\pi^\downarrow$ the projection $[\pi(\mathbf{T})]^\bullet \to [\pi(\mathbf{T})]^\bullet/\langle\varphi^\downarrow\rangle$. Let O_1 and O_2 be the oval cycles of φ. Since $\varphi^k \rightsquigarrow \mathcal{OORR}_{2,\mathbf{T}}$ we get that O_1 and O_2 separate $\mathbf{T}$ into two annuli A_1 and A_2. Since φ^k exchanges A_1 and A_2 so must φ, and thus k is odd.

By Proposition 3.19 $\varphi^\downarrow$ is pseudofree and takes capped faces to capped faces. So now since $k = |\varphi^\downarrow|$ is odd, Theorem 4.1 implies that $\varphi^\downarrow \rightsquigarrow (\mathcal{R}_{k,\mathbf{S}})^i$ for some i relatively prime to k and the two fixed points of $\varphi^\downarrow$ are in the capped faces.

Now let P be a path connecting $\pi^\downarrow(O_1)$ to $\pi^\downarrow(O_2)$. As in the proof of Proposition 3.1, $(\pi^\downarrow)^{-1}(P)$ consists of k disjoint copies of P in $\pi(G)$ and thus O_1 and O_2 taken together with $(\pi^\downarrow)^{-1}(P)$ form a subdivision of the embedding on the left of Figure 6.19, call it H. Note that H is a surface orbit minor of $\pi(G)$ in the sphere obtained by deletions only, and so $\varphi^\downarrow|_H$ is defined.

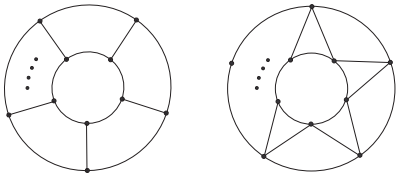

Figure 6.19.

We can now apply Proposition 3.14 to obtain a surface orbit minor $\tilde{H}$ of G corresponding to H, and by Proposition 3.13 there is a $\mathbb{Z}_2$-voltage assignment σ such that $\widehat{H}^\sigma \cong \tilde{H}$. By Proposition 3.21, there is $a \in \mathbb{Z}_2$ such that $(\varphi^\downarrow|_H)^\uparrow_{a,\sigma}$ is $\varphi|_{\tilde{H}}$ up to isomorphism. Now, as in the proof of Theorem 6.14 (in Case 2) $\sigma_* = 0$ and

so we may assume that $\sigma \equiv 0$. Since $\sigma \equiv 0$, we have that H^σ in $([\pi(\mathbf{T})]^\bullet)^\sigma$ consists of two copies of H in two disjoint spheres. So now $(\varphi^\downarrow)^\uparrow_{0,\sigma}$ has order k and $(\varphi^\downarrow)^\uparrow_{1,\sigma}$ has order $2k$ on H^σ and therefore we have the same orders for $(\varphi^\downarrow)^\uparrow_{0,\sigma}$ and $(\varphi^\downarrow)^\uparrow_{1,\sigma}$ on $\widehat{H}^\sigma \cong \tilde{H}$ in $\mathbf{T}$. Thus $\varphi|_{\tilde{H}}$ is $(\varphi^\downarrow)^\uparrow_{1,\sigma}$ up to this isomorphism and $(\varphi^\downarrow)^\uparrow_{1,\sigma}$ must be $(\mathcal{OCRR}_{4t+2,\mathbf{T}})^i$ for $k = 2t+1$.

Case 2 Let O be the single oval of φ; we get that $\varphi(O) = O$ and so k is odd by Proposition 2.8. Let O_1 and O_2 be the cycles obtained from O in $G^\circlearrowleft$ embedded in $[\mathbf{T}^\circlearrowleft]^\bullet = \mathbf{S}$. Since $\varphi^\circlearrowleft$ is pseudofree and takes O_1 to O_2, Theorem 4.1 implies that $\varphi^\circlearrowleft \rightsquigarrow (\mathcal{R}\mathcal{R}_{2k,\mathbf{S}})^i$ for some i relatively prime to $2k$. Let π be the projection from $\mathbf{S}$ to $\mathbf{S}/\langle\varphi^\circlearrowleft\rangle$ (which is the projective plane as in the proof of Theorem 4.1). In $\pi(G)$ the cycle $O' = \pi(O_1) = \pi(O_2)$ bounds the face containing the only branch point of π. Let T be a spanning tree of $\pi(G)$ that contains all but one of the edges of O'. By contracting T and deleting loops we obtain a surface minor as in Figure 6.20, call it H.

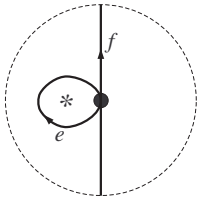

Figure 6.20.

Let σ be the $\mathbb{Z}_{2k}$-voltage assignment on H that reconstructs the surface orbit minor $\tilde{H}$ of $G^\circlearrowleft$. Since the deficiency of the branch point is $2k-2$, we have up to automorphism of $\mathbb{Z}_{2k}$ that $\sigma(e) = 2$. Now since $0 = \sigma_*(e,f,f) = 2 + 2\sigma(f)$ we get $\sigma(f)+1 \in \{0,k\}$ and so $\sigma(f) \in \{2k-1, k-1\}$; however, the connectivity of $G^\circlearrowleft$ implies that $\langle\sigma(e),\sigma(f)\rangle = \mathbb{Z}_{2k}$ which then implies that $\sigma(f) = 2k-1$ because $k-1$ is even. Now $H^\sigma \cong \tilde{H}$ is the embedding as shown on the right in Figure 6.19. Since $\tilde{H}$ is a surface orbit minor of $G^\circlearrowleft$ it corresponds to a surface orbit minor H' of G and the action of $\varphi^\circlearrowleft|_{\tilde{H}} \rightsquigarrow (\mathcal{R}\mathcal{R}_{2k,\mathbf{S}})^i$ corresponds to the action of $(\mathcal{OCRR}_{4t+2,\mathbf{T}})^i$ on H', where $k = 2t+1$. □

7 Cellular automorphisms of the Klein bottle

7.1 A catalogue of cellular automorphisms of the Klein bottle

It is worth noting that because $\mathbf{T}$ double-covers $\mathbf{K}$ it follows that any cellular automorphism of $\mathbf{K}$ lifts to a cellular automorphism of $\mathbf{T}$. However, the lift of an irreducible cellular automorphism in $\mathbf{K}$ need not be irreducible in $\mathbf{T}$. An example of this is $\mathcal{MRR}_{4k+2,\mathbf{K}}$, which is defined below.

Free Automorphisms $\mathcal{LRR}_{2k+1,\mathbf{K}}$, $\mathcal{DRR}_{2k+1,\mathbf{K}}$, $\mathcal{MRR}_{4k+2,\mathbf{K}}$, $\mathcal{ARR}_{4k+2,\mathbf{K}}$, and $\mathcal{ZRR}_{4k+2,\mathbf{K}}$ For any k, define the *loop rotation reflection* $\mathcal{LRR}_{2k+1,\mathbf{K}}$, *diamond rotation reflection* $\mathcal{DRR}_{2k+1,\mathbf{K}}$, *Möbius-exchange rotation reflection* $\mathcal{MRR}_{4k+2,\mathbf{K}}$, *annular rotation reflection* $\mathcal{ARR}_{4k+2,\mathbf{K}}$, and *zigzag rotation reflection* $\mathcal{ZRR}_{4k+2,\mathbf{K}}$, respectively, on the embeddings in Figure 7.1 by $e_i \mapsto e_{i+1}$ and $f_i \mapsto f_{i+1}$. All of these automorphisms are free and irreducible.

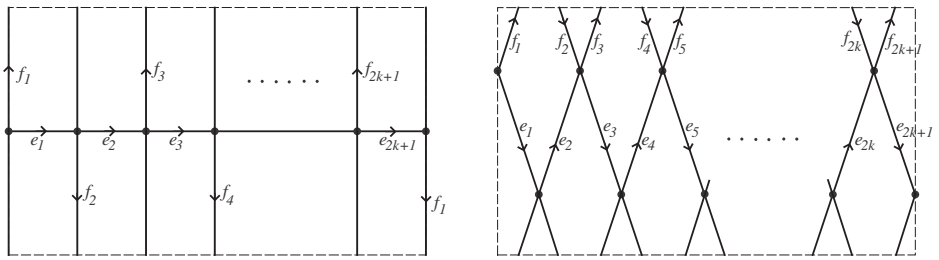

Figure 7.1.

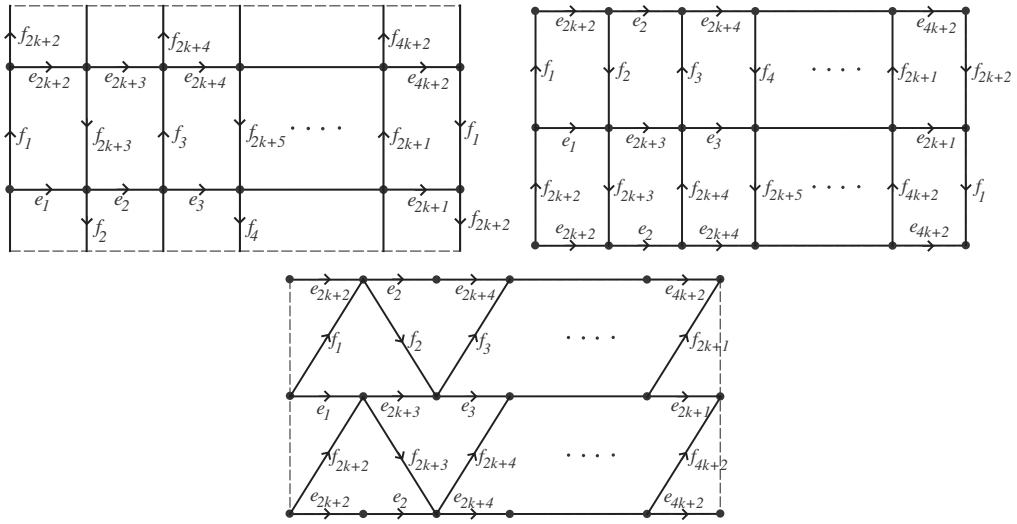

Pseudofree automorphisms $\mathcal{P}_{2,2:1,\mathbf{K}}$, $\mathcal{P}'_{2,2:1,\mathbf{K}}$, $\mathcal{P}''_{2,2:1,\mathbf{K}}$ The first graph in Figure 7.2 depicts the map $\mathcal{P}_{2,2:1,\mathbf{K}}$, the second and third depict $\mathcal{P}'_{2,2:1,\mathbf{K}}$, and the fourth and fifth depict $\mathcal{P}''_{2,2:1,\mathbf{K}}$. Each of these is pseudofree with two fixed points, and in each case the action on each face is rotation by 180°.

Figure 7.2.

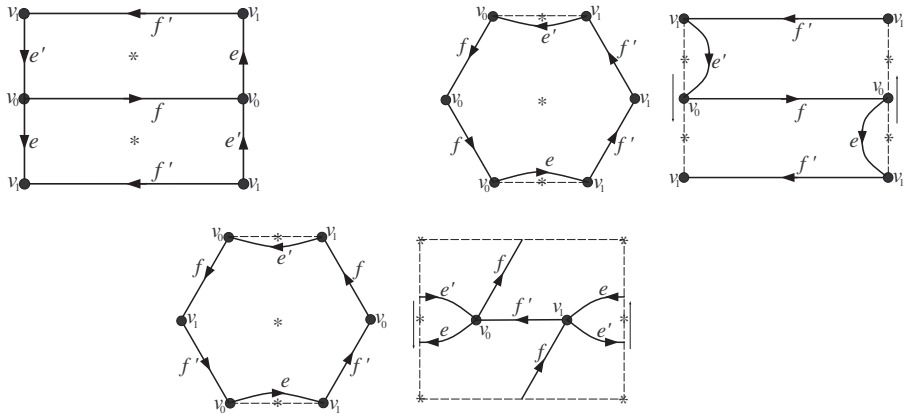

Oval Rotation Reflection $\mathcal{ORR}_{4k+2,\mathbf{K}}$ We define the cellular automorphism $\mathcal{ORR}_{4k+2,\mathbf{K}}$ on the first embedding in Figure 7.3 by $o_t \mapsto o_{t+1}$, $e_i \mapsto d_{i+1}$, and $d_i \mapsto e_{i+1}$, where subscripts are taken mod $2k+1$. This automorphism is non-pseudofree with oval cycle $o_0, \ldots, o_{2k+1}$. On the right we show $\mathcal{ORR}_{2,\mathbf{K}}$.

Figure 7.3.

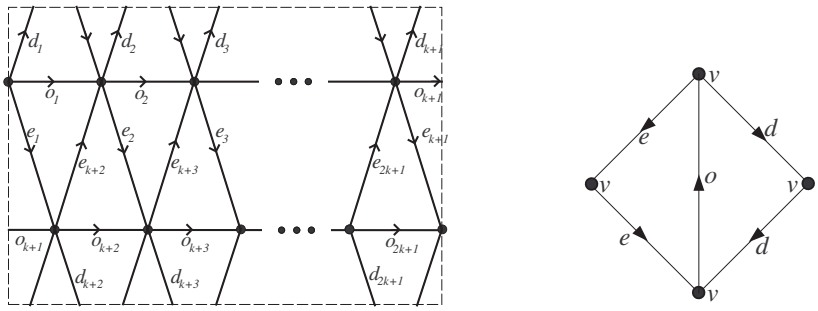

Double Oval Rotation $\mathcal{OOR}_{2k,\mathbf{K}}$ and Double Oval Rotation Reflection $\mathcal{OORR}_{4k,\mathbf{K}}$ The cellular automorphism $\mathcal{OOR}_{2k,\mathbf{K}}$ is defined on the first embedding in Figure 7.4 for any k by $o_i \mapsto o_{i+1}$, $l_i \mapsto l_{i+1}$ (where subscripts for the l_i's and the o_i's are taken mod k) and $e_i \mapsto e_{i+1}$ (where subscripts for the e_i's are taken mod $2k$). Both $o_1, \ldots, o_k$ and $l_1, \ldots, l_k$ are ovals of $(\mathcal{OOR}_{2k,\mathbf{K}})^k$ and $(\mathcal{OOR}_{2k,\mathbf{K}})^k \rightsquigarrow \mathcal{OOR}_{2,\mathbf{K}}$.

The cellular automorphism $\mathcal{OORR}_{4k,\mathbf{K}}$ is defined on the second embedding in Figure 7.4 for any k by $o_i \mapsto o_{i+1}$ (where subscripts for the o_i's are taken mod $2k$) and $e_i \mapsto e_{i+1}$ (where subscripts for the e_i's are taken mod $4k$). Both $o_1, o_3, \ldots, o_{2k-1}$ and $o_2, o_4, \ldots, o_{2k}$ are ovals of $\mathcal{OORR}_{4k,\mathbf{K}}$ and $(\mathcal{OORR}_{4k,\mathbf{K}})^{2k} \rightsquigarrow \mathcal{OOR}_{2,\mathbf{K}}$.

The last embedding in Figure 7.4 depicts the involution $\mathcal{OOR}_{2,\mathbf{K}}$.

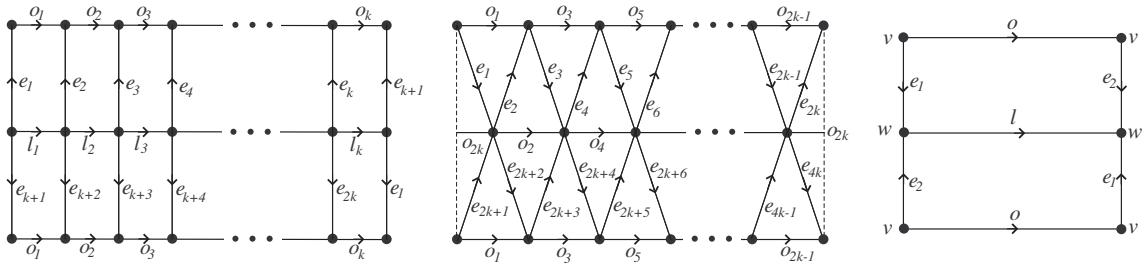

Figure 7.4.

Oval Reflection with Rotations $\mathcal{OR}_{2,2:1,\mathbf{K}}$ The cellular automorphism $\mathcal{OR}_{2,2:1,\mathbf{K}}$ is defined on the graph in Figure 7.5 by $e_0 \mapsto e_1$, $e_1 \mapsto e_0$ and $h \mapsto h$. Here h is the oval cycle and there are two fixed points.

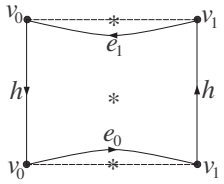

Figure 7.5.

Proposition 7.6. *If φ is a non-pseudofree cellular automorphism of G in $\mathbf{K}$ with $|\varphi| = 2k \geq 4$ and $\overline{G} = G$, then $\varphi^k \not\rightsquigarrow \mathcal{OR}_{2,2:1,\mathbf{K}}$.*

Proof. Suppose that $\varphi^k \rightsquigarrow \mathcal{OR}_{2,2:1,\mathbf{K}}$. Notice that $\varphi^{\circlearrowleft}$ is a pseudofree cellular automorphism of $G^{\circlearrowleft}$ in $[\mathbf{K}^{\circlearrowleft}]^{\bullet} = \mathbf{S}$ with $|\varphi^{\circlearrowleft}| = |\varphi| \geq 4$. However now $\varphi^{\circlearrowleft}$ has four isolated pseudofixed points (two inherited from φ and two in the capped faces) a contradiction of Theorem 4.1. □

7.2 Completeness of the catalogue

Theorem 7.7. *If φ is a free cellular automorphism of G in $\mathbf{K}$, then φ reduces to one of $(\mathcal{LRR}_{2k+1,\mathbf{K}})^j$, $(\mathcal{DRR}_{2k+1,\mathbf{K}})^j$, $(\mathcal{MRR}_{4k+2,\mathbf{K}})^j$, $(\mathcal{ARR}_{4k+2,\mathbf{K}})^j$, and $(\mathcal{ZRR}_{4k+2,\mathbf{K}})^j$ for some j.*

Proof. Note that $G = \overline{G}$ because φ is free. Let $n = |\varphi|$ and let π denote the projection $\mathbf{K} \to \mathbf{K}/\langle\varphi\rangle$. Here $\chi(\pi(\mathbf{K})) = 0/n = 0$ and so $\pi(\mathbf{K})$ is the torus or Klein bottle. However, since a non-orientable surface cannot be a branched cover of an orientable surface, $\pi(\mathbf{K})$ is the Klein bottle.

Since the embedding of $\pi(G)$ in $\pi(\mathbf{K})$ is cellular, we can contract a spanning tree and delete loops to obtain a surface minor H consisting of a vertex v and two loops, say e and f. Without loss of generality either e is in the $(1,0)$-homology class and f is in the $(0,1)$-homology class or e is in the $(1,0)$-homology class and f is in the $(1,1)$-homology class (see Figure 6.9). Let these be Cases 1 and 2. In both cases let $\tilde{H}$ be the surface orbit minor of G corresponding to H as given in Proposition 3.4 and let σ be a voltage assignment on H that recovers $\tilde{H}$ and $\varphi|_{\tilde{H}}$ as given in Proposition 3.1. Also since $\tilde{H}$ is connected we must have that $\mathbb{Z}_n = \langle\sigma(e), \sigma(f)\rangle$.

Case 1 Since φ is free and the facial walk of the single face of H in $\pi(\mathbf{K})$ is $e, f, -e, f$, we get that $0 = \sigma_*(e, f, -e, f) = 2\sigma(f)$. Thus $\sigma(f) = 0$ when n is odd and $\sigma(f) \in \{0, \frac{n}{2}\}$ when n is even. In Case 1.1, say that n is odd and in Case 1.2 say that n is even.

Case 1.1 In this case, $\mathbb{Z}_n = \langle \sigma(e), \sigma(f) \rangle = \langle \sigma(e) \rangle$. So up to automorphism of $\mathbb{Z}_n$, $\sigma(e) = 1$ and $\sigma(f) = 0$. One can show that $H^\sigma \cong \tilde{H}$ is the defining graph for $\mathcal{LR}\mathcal{R}_{2k+1,\mathbf{K}}$ and since $\varphi|_{\tilde{H}}(e_i) = e_{i+j}$ for some j we get that $\varphi|_{\tilde{H}}$ is $(\mathcal{LR}\mathcal{R}_{2k+1,\mathbf{K}})^j$.

Case 1.2 In this case, it actually cannot be that $\sigma(f) = 0$. If we assume that $\sigma(f) = 0$, then $\mathbb{Z}_n = \langle \sigma(e), \sigma(f) \rangle = \langle \sigma(e) \rangle$. So up to automorphism of $\mathbb{Z}_n$, $\sigma(e) = 1$ and $\sigma(f) = 0$. But we also have that any closed Möbius walk w in H has $\sigma_*(w) = \alpha\sigma(e) + \beta\sigma(f) = \alpha$ where α is odd which makes $\sigma_*(w) \neq 0$. Proposition 3.3 now implies that the derived surface given by σ is orientable, a contradiction. It thus must be that $\sigma(f) = \frac{n}{2}$. In Case 1.2.1 say that $\mathbb{Z}_n = \langle \sigma(e) \rangle$ and in Case 1.2.2 say that $\mathbb{Z}_n \neq \langle \sigma(e) \rangle$.

Case 1.2.1 Up to automorphism of $\mathbb{Z}_n$, $\sigma(e) = 1$ and $\sigma(f) = \frac{n}{2}$. Now any closed Möbius walk w in H has $\sigma_*(w) = \alpha\sigma(e) + \beta\sigma(f) = \alpha + \beta\frac{n}{2} \in \{\alpha, \alpha + \frac{n}{2}\}$ where α is odd. Since the derived surface is non-orientable, Proposition 3.3 requires that $\sigma_*(w) = 0$ for some w. It cannot be that $n = 4k$, since then both α and $\alpha + \frac{n}{2}$ would be odd, hence nonzero in $\mathbb{Z}_n$. It follows that $n = 4k + 2$. One can check that $H^\sigma \cong \tilde{H}$ is the defining graph for $\mathcal{MR}\mathcal{R}_{4k+2,\mathbf{K}}$ and since $\varphi|_{\tilde{H}}(e_i) = e_{i+j}$ for some j we get that $\varphi|_{\tilde{H}} = (\mathcal{MR}\mathcal{R}_{4k+2,\mathbf{K}})^j$.

Case 1.2.2 Since $\mathbb{Z}_n \neq \langle \sigma(e) \rangle$ and yet $\mathbb{Z}_n = \langle \sigma(e), \sigma(f) \rangle$, it must be that $\frac{n}{2} \notin \langle \sigma(e) \rangle$. These imply that $|\sigma(e)|$ is odd and also that $\mathbb{Z}_n \cong \langle \sigma(e) \rangle \times \langle \frac{n}{2} \rangle \cong \mathbb{Z}_{2k+1} \times \mathbb{Z}_2$. Thus $n = 4k + 2$ with $\sigma(e) = 2k + 2$ up to automorphism of $\mathbb{Z}_n$. (Note that $\langle 2k + 2 \rangle = \langle 2 \rangle$ in $\mathbb{Z}_{4k+2}$ because the order of $2k + 2$ in $\mathbb{Z}_{4k+2}$ is $(4k + 2)/\gcd(4k + 2, 2k + 2) = 2k + 1$.) One can check that $H^\sigma \cong \tilde{H}$ is the defining graph for $\mathcal{AR}\mathcal{R}_{4k+2,\mathbf{K}}$ and since $\varphi|_{\tilde{H}}(e_i) = e_{i+j}$ for some j we get that $\varphi|_{\tilde{H}} = (\mathcal{AR}\mathcal{R}_{4k+2,\mathbf{K}})^j$.

Case 2 The facial boundary walk of the single face of H in $\pi(\mathbf{K})$ is $e, e, -f, -f$ and so $0 = \sigma_*(e, e, -f, -f) = 2(\sigma(e) - \sigma(f))$. When n is odd this shows that $\sigma(e) - \sigma(f) = 0$ and when n is even it shows that $\sigma(e) - \sigma(f) \in \{0, \frac{n}{2}\}$, that is, $\sigma(e) = \sigma(f)$ or $\sigma(e) = \sigma(f) + \frac{n}{2}$. Let these be Cases 2.1, 2.2.1, and 2.2.2, respectively.

Case 2.1 Since $\sigma(e) = \sigma(f)$ and $\langle \sigma(e), \sigma(f) \rangle = \mathbb{Z}_n$, we get that $\sigma(e) = \sigma(f) = 1$ up to some automorphism of $\mathbb{Z}_n$. On can check that $H^\sigma \cong \tilde{H}$ is the defining graph for $\mathcal{DR}\mathcal{R}_{2k+1,\mathbf{K}}$ and since $\varphi|_{\tilde{H}}(e_i) = e_{i+j}$ for some j we get that $\varphi|_{\tilde{H}} = (\mathcal{DR}\mathcal{R}_{2k+1,\mathbf{K}})^j$.

Case 2.2.1 Since $\sigma(e) = \sigma(f)$ and $\langle \sigma(e), \sigma(f) \rangle = \mathbb{Z}_n$, we get that $\sigma(e) = \sigma(f) = 1$ up to some automorphism of $\mathbb{Z}_n$. Any closed Möbius walk w in H has $\sigma_*(w) = \alpha\sigma(e) + \beta\sigma(f)$ where $\alpha + \beta$ is odd because both e and f are themselves Möbius walks. However now $\sigma_*(w) = \alpha + \beta \neq 0$ because n is even. Proposition 3.3 now implies that H^σ is orientable, a contradiction.

Case 2.2.2 We claim that $n = 4k + 2$. If we assume that $n = 4k$, then $\frac{n}{2} = 2k \in \langle 2 \rangle \neq \mathbb{Z}_n$ and so either $\sigma(e) \notin \langle 2 \rangle$ or $\sigma(f) \notin \langle 2 \rangle$ because $\langle \sigma(e), \sigma(f) \rangle = \mathbb{Z}_n$. So now without loss of generality suppose that $\sigma(e) = a \notin \langle 2 \rangle$ and $\sigma(f) = a + 2k$. Now any closed Möbius walk w has $\sigma_*(w) = \alpha\sigma(e) + \beta\sigma(f)$ where $\alpha + \beta$ is odd. So then $\sigma_*(w) = \alpha a + \beta(2k + a) = (\alpha + \beta)a + \beta 2k \in \{(\alpha + \beta)a, (\alpha + \beta)a + 2k\}$. Now by Proposition 3.3, there must be some w with $\sigma_*(w) = 0$ and $\sigma_*(w) = 0$ implies in turn that $(\alpha + \beta)a \in \{0, 2k\}$; however $\{0, 2k\} \subseteq \langle 2 \rangle$ and since $a \notin \langle 2 \rangle$ no odd multiple of a is in $\langle 2 \rangle$, a contradiction.

Since $n = 4k + 2$, it must be that exactly one of $\sigma(e)$ and $\sigma(f)$ is in the subgroup $\langle 2 \rangle$ of $\mathbb{Z}_{4k+2}$ because the subgroup $\langle 2 \rangle$ has index 2 and $\sigma(e) - \sigma(f) = \frac{n}{2} = 2k + 1 \notin \langle 2 \rangle$. We can assume without loss of generality that $\sigma(f) \notin \langle 2 \rangle$ because there is a homeomorphism of the Klein bottle that exchanges the $(1, 0)$- and $(1, 1)$-homology classes. So now we get that $|\sigma(f)|$ is even and so $\frac{|\sigma(f)|}{2}\sigma(f) = \frac{n}{2}$ and so $\sigma(e) = \sigma(f) + \frac{n}{2} = \left(\frac{|\sigma(f)|}{2} + 1\right)\sigma(f)$ which makes $\langle \sigma(f) \rangle = \mathbb{Z}_n$. Now, up to some automorphism of $\mathbb{Z}_n$ we have $\sigma(f) = 1$ and so $\sigma(e) = \sigma(f) + \frac{n}{2} = 2k + 2$. One can now check that $H^\sigma \cong \tilde{H}$ is the defining graph for $\mathcal{ZR}\mathcal{R}_{4k+2,\mathbf{K}}$ and since $\varphi|_{\tilde{H}}(f_i) = f_{i+j}$ for some j we get that $\varphi|_{\tilde{H}} = (\mathcal{ZR}\mathcal{R}_{4k+2,\mathbf{K}})^j$. □

Theorem 7.8. *If φ is cellular automorphism of $G = \overline{G}$ in $\mathbf{K}$ that is pseudofree but not free, then φ reduces to $\mathcal{P}_{2,2:1,\mathbf{K}}$, $\mathcal{P}'_{2,2:1,\mathbf{K}}$, or $\mathcal{P}''_{2,2:1,\mathbf{K}}$.*

Proof. Let $n = |\varphi|$, let π denote the projection $\mathbf{K} \to \mathbf{K}/\langle \varphi \rangle$, and let Y be the set of branch points of $\pi(G)$ in $\pi(\mathbf{K})$. By Theorem 3.6, $\chi(\mathbf{K}) = n\chi(\pi(\mathbf{K})) - \sum_{y \in Y} \mathrm{def}(y)$ and so $n\chi(\pi(\mathbf{K})) = \sum_{y \in Y} \mathrm{def}(y) \geq 1$ because φ is not free. Thus $\chi(\pi(\mathbf{K})) \in \{1, 2\}$ but since the Klein bottle cannot be a branched covering of the sphere, $\chi(\pi(\mathbf{K})) = 1$ which makes $\pi(\mathbf{K})$ the projective plane.

As explained in Case 1 of the proof of Theorem 6.10, $|Y| = 2$ and each $y \in Y$ has deficiency $\frac{n}{2}$. So, as before we contract a spanning tree and delete loops to get a surface minor H of $\pi(G)$ in $\pi(\mathbf{K})$ with branch points positioned as shown in Figure 6.11. Let σ be a $\mathbb{Z}_n$-voltage assignment that recovers $\tilde{H}$ in $\mathbf{K}$. In the left-hand graph of the figure the possible voltage assignment, up to symmetry, is $\sigma(f) = 0$ and $\sigma(e) = \frac{n}{2}$. Since H is connected, we have $\langle\sigma(e)\rangle = \mathbb{Z}_n$ and thus $n = 2$. It follows that $\varphi_{\tilde{H}}$ is $\mathcal{P}_{2,2:1,\mathbf{K}}$. In the right-hand graph of Figure 6.11 we have $\sigma(e) = \frac{n}{2}$ and either $\sigma(f) = 0$ or $\sigma(f) = \frac{n}{2}$. Again, since H is connected we must have $n = 2$. In the case that $\sigma(e) = \frac{n}{2}$ and $\sigma(f) = 0$ we have that $\varphi_{\tilde{H}}$ is $\mathcal{P}'_{2,2:1,\mathbf{K}}$, and in the case that $\sigma(e) = \frac{n}{2}$ and $\sigma(f) = \frac{n}{2}$ we have that $\varphi_{\tilde{H}}$ is $\mathcal{P}''_{2,2:1,\mathbf{K}}$. □

Theorem 7.9. *If φ is a non-pseudofree involutory cellular automorphism of G in $\mathbf{K}$ with $\overline{G} = G$, then φ reduces to $\mathcal{ORR}_{2,\mathbf{K}}$, $\mathcal{OOR}_{2,\mathbf{K}}$, or $\mathcal{OR}_{2,2:1,\mathbf{K}}$.*

Proof. As in the proof of Theorem 6.14 we get that $(r, s) \in \{(0, 1), (0, 2), (2, 1)\}$. Let π be the projection from $\mathbf{K}$ to $\mathbf{K}/\langle\varphi\rangle$.

If $(r, s) = (0, 1)$, then as in Case 1 of the proof of Theorem 6.14, $\pi(\mathbf{K})$ is the Möbius band. Choose a spanning tree T of $\pi(G)$ in $\pi(\mathbf{K})$ that contains all but one edge of the hole-cycle. After contracting T and deleting loops we can get a surface minor H consisting of two loops e and h where h is the hole cycle (see Figure 6.15). The way that H is obtained satisfies the hypothesis of Proposition 3.14 and so we have the corresponding surface orbit minor $\tilde{H}$ of G in $\mathbf{K}$ and Proposition 3.13 yields a $\mathbb{Z}_2$-voltage assignment σ on H for which $\widehat{H}^\sigma$ in $\mathbf{K}$ is $\tilde{H}$ in $\mathbf{K}$. As shown in Case 1 of the proof of Theorem 6.14, the only possible voltage assignment is then given by $\sigma(h) = 0$ and $\sigma(e) = 0$. Thus the oval cycle h of $\tilde{H}$ in $\mathbf{K}$ separates $\mathbf{K}$ and is noncontractible, so separates $\mathbf{K}$ into two Möbius bands. We get that the corresponding involution $\varphi|_{\tilde{H}}$ is $\mathcal{ORR}_{2,\mathbf{K}}$.

If $(r, s) = (0, 2)$, then as in Case 2 of the proof of Theorem 6.14, $\pi(\mathbf{K})$ is the annulus and there is a surface minor H in $\pi(G)$ consisting of two loops h_1 and h_2 (which are the hole cycles) along with a link e connecting the endpoints of these loops. The construction of the surface minor H satisfies the conditions of Proposition 3.14, so we have a $\mathbb{Z}_2$-voltage assignment σ on H for which $\widehat{H}^\sigma$ in $\mathbf{K}$ is $\tilde{H}$ in $\mathbf{K}$. From the argument in Case 2 of the proof of Theorem 6.14, σ must have $\sigma(h_1) = \sigma(h_2) = 1$. So now the lifts of h_1 and h_2 in $\mathbf{K}$ have Möbius neighborhoods and so, without loss of generality, h_1 is in homology class $(1, 0)$ and h_2 is in homology class $(1, 1)$ and we get that $\varphi|_{\tilde{H}}$ is the involution $\mathcal{OOR}_{2,\mathbf{K}}$ (see Figure 7.4).

If $(r, s) = (2, 1)$, then as in Case 3 of the proof of Theorem 6.14, $\pi(\mathbf{K})$ is the disk and $\pi(G)$ has a surface minor H with a single vertex v, a loop h which is the hole-cycle, and an additional loop e surrounding one of the fixed points, as shown on the left of 6.17; furthermore, H is obtained in a way that satisfies the conditions of Proposition 3.14. As mentioned in Case 3 of the proof of Theorem 6.14, we must have that $\sigma(h) = 0$ and $\sigma(e) = 1$. The embedding shown in Figure 7.5 has the correct facial walks corresponding to the facial walks in H and so $\varphi|_{\tilde{H}}$ is $\mathcal{OR}_{2,2:1,\mathbf{K}}$. □

Theorem 7.10. *If φ is a non-pseudofree non-involutory cellular automorphism of G in $\mathbf{K}$ with $\overline{G} = G$, then φ reduces to one of $(\mathcal{ORR}_{4k+2,\mathbf{K}})^j$, $(\mathcal{OOR}_{2k,\mathbf{K}})^j$, and $(\mathcal{OOR}_{4k,\mathbf{K}})^j$ for some j.*

Proof. By Proposition 2.4, $|\varphi| = 2m$, and by assumption $2m \geq 4$. By Theorem 7.9 and Proposition 7.6, φ^m reduces to $\mathcal{ORR}_{2,\mathbf{K}}$ (Case 1) or $\mathcal{OOR}_{2,\mathbf{K}}$ (Case 2). In each case let π be the projection $\mathbf{K} \to \mathbf{K}/\langle\varphi^m\rangle$ and $\pi^\downarrow$ the projection $[\pi(\mathbf{K})]^\bullet \to [\pi(\mathbf{K})]^\bullet/\langle\varphi^\downarrow\rangle$.

Case 1 Let O be the oval-cycle of φ; note that O has an annular neighborhood. Here $\pi(\mathbf{K})$ is the Möbius band with hole cycle $\pi(O) = O$. We also have (by Theorem 5.1) that $\pi^\downarrow\pi(\mathbf{K})$ is the Möbius band with hole cycle $\pi^\downarrow(O)$. Let C be the edge-set of $\pi^\downarrow(O)$ with one edge excluded and extend C to a spanning tree T of $\pi^\downarrow\pi(G)$. After contracting T and possibly deleting some edge-set D we obtain a surface minor H of $\pi^\downarrow\pi(G)$ with a loop as the hole cycle as in Figure 6.15. By Proposition 3.4, H in $\pi^\downarrow\pi(\mathbf{K})$ corresponds to a surface orbit minor $H' = \pi(G)/(\pi^\downarrow)^{-1}(C)\backslash(\pi^\downarrow)^{-1}(D)$ in $\pi(\mathbf{K})$ with respect to $\varphi^\downarrow$.

Since $\varphi^\downarrow$ is pseudofree, $(\pi^\downarrow)^{-1}(T)$ is a forest in $\pi(G)$ consisting of isomorphic copies of T (as in the proof of Proposition 3.1). Given the way that T and D were chosen, $(\pi^\downarrow)^{-1}(T)$ and $(\pi^\downarrow)^{-1}(D)$ satisfy the conditions of Proposition 3.14. Thus H' corresponds to a surface orbit minor $\tilde{H}$ of G with respect to φ.

By Theorem 5.1(1) $m = |\varphi^{\downarrow}|$ is odd because $\varphi^{\downarrow}$ is pseudofree. Write $m = 2k+1$. By Proposition 3.1 there is a $\mathbb{Z}_m$-voltage assignment σ on H that reconstructs $\varphi^{\downarrow}|_{H'}$. Using the labels in Figure 6.15 and the fact that the branch point in $[\pi^{\downarrow}\pi(\mathbf{K})]^{\bullet}$ has deficiency $m-1$, we get that $\sigma(h) = 1$ up to some automorphism of $\mathbb{Z}_m$. Moreover, since $2\sigma(e) + \sigma(h) = 0$ we get that $\sigma(e) = (m-1)/2 = k$. Thus H' is as in Figure 7.11 and $\varphi^{\downarrow}$ takes vertex i to vertex $i+t$ for some fixed t relatively prime to $m = 2k+1$.

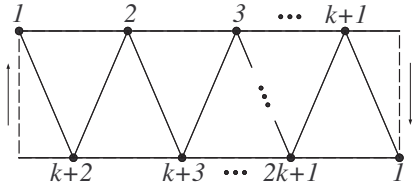

Figure 7.11.

By Proposition 3.13 there is a $\mathbb{Z}_2$-voltage assignment σ' on H' that reconstructs $\tilde{H}$. As in the proof of Theorem 7.9, $\sigma' \equiv 0$. By Proposition 3.21 there is $a \in \mathbb{Z}_2$ such that $(\varphi^{\downarrow})^{\uparrow}_{a,\sigma'}$ is $\varphi|_{\tilde{H}}$. By Proposition 3.17 and the fact that $m = 2k+1$ is odd, exactly one a in $\mathbb{Z}_2$ gives the correct order for $\varphi|_{\tilde{H}}$. Thus $\varphi|_{\tilde{H}}$ must be $(\mathcal{O}RR_{4k+2,\mathbf{K}})^j$ for some $j \in \{t, t+m\}$.

Case 2 Let O_1 and O_2 be the oval-cycles of φ; note that both have a Möbius neighborhood. Here $\pi(\mathbf{K})$ is the annulus with hole cycles O_1 and O_2. In Case 2.1 say $\varphi(O_1) = O_1$ and in Case 2.1 say $\varphi(O_1) = O_2$.

Case 2.1 Since $\varphi(O_1) = O_1$ (and also $\varphi^{\downarrow}(O_1) = O_1$), Theorem 4.1 and Proposition 3.19 imply that $\varphi^{\downarrow} \rightsquigarrow (\mathcal{R}_{k,\mathbf{S}})^j$. Now let γ be a path connecting $\pi^{\downarrow}(O_1)$ to $\pi^{\downarrow}(O_2)$. As in the proof of Theorem 3.1, $(\pi^{\downarrow})^{-1}(\gamma)$ is a disjoint union of k copies of γ whose union with O_1 and O_2, call it H, is a subdivision of the left embedding in Figure 6.19. Note that H is a surface orbit minor of $\pi(G)$ obtained by deletions only, and thus we can apply Proposition 3.14 to obtain a surface orbit minor $\tilde{H}$ of G corresponding to H. By Proposition 3.13 there is a $\mathbb{Z}_2$-voltage assignment σ on H that has $\widehat{H}^{\sigma} \cong \tilde{H}$ and by Proposition 3.21 there is $a \in \mathbb{Z}_2$ such that $(\varphi^{\downarrow})^{\uparrow}_{a,\sigma}$ is $\varphi|_{\tilde{H}}$. Since both O_1 and O_2 have Möbius neighborhoods we have that $\sigma_*(O_1) = \sigma_*(O_2) = 1$ and each facial boundary has total voltage 0. Thus $\widehat{H}^{\sigma} \cong \tilde{H}$ is a subdivision of the defining graph for $\mathcal{OOR}_{2k,\mathbf{K}}$ and so $\varphi|_{\tilde{H}}$ reduces to $(\mathcal{OOR}_{2k,\mathbf{K}})^j$.

Case 2.2 Since $\varphi^{\downarrow}(O_1) = O_2$, $|\varphi^{\downarrow}| = m$ must be even, say $m = 2k$. Since O_1 and O_2 have Möbius neighborhoods they do not separate $\mathbf{K}$, and so we apply the cutting construction to get $[\mathbf{K}^{\circlearrowleft}]^{\bullet} = \mathbf{S}$. Let O_1' and O_2' be the corresponding hole cycles of $G^{\circlearrowleft}$ in $\mathbf{K}^{\circlearrowleft}$. Since O_1' and O_2' each enclose a pseudofixed point of index 2, Theorem 4.1 now implies that $\varphi^{\circlearrowleft} \rightsquigarrow (\mathcal{RR}_{4k,\mathbf{S}})^j$. Let $\pi^{\circlearrowleft}$ be the projection $\mathbf{K}^{\circlearrowleft} \to \mathbf{K}^{\circlearrowleft}/\langle\varphi^{\circlearrowleft}\rangle$. Here $\pi^{\circlearrowleft}([\mathbf{K}^{\circlearrowleft}]^{\bullet})$ is $\mathbf{P}$. As in Case 2 of the proof of Theorem 6.18, we obtain a surface orbit minor of $G^{\circlearrowleft}$ that is a subdivision of the embedding shown on the right in Figure 6.19 where O_1' and O_2' are the inner and outer cycles. If we identify antipodal points on each O_i', then we obtain a subdivision of the defining graph for $\mathcal{OOR}\mathcal{R}_{4k,\mathbf{K}}$ and this is a surface orbit minor of G with respect to φ. The action of φ on this surface orbit minor is thus given by $\varphi^{\circlearrowleft} \rightsquigarrow (\mathcal{RR}_{4k,\mathbf{S}})^j$ and so must correspond to $(\mathcal{OOR}\mathcal{R}_{4k,\mathbf{K}})^j$. □

8 Cellular automorphisms of Dyck's surface

The cellular automorphisms of Dyck's surface $\mathbf{D}$ are much different from the previous four surfaces in that the only possible orders are 2, 3, and 4 and none of the cellular automorphisms are free. We consider three "standard renderings" of $\mathbf{D}$. The three-crosscaps rendering is given by the hexagons in Figure 8.1. We depict the torus with a crosscap and the Klein bottle with a crosscap by the usual renderings of each along with a face removed and its boundary edges identified to form a crosscap; see Figures 8.3-8.5 where the deleted face is shown shaded. For each cellular automorphism we provide a depiction in one of the standard renderings.

8.1 A catalogue of cellular automorphisms of Dyck's surface

The cellular automorphisms $\mathcal{P}_{3,2:1,\mathbf{D}}$, $\mathcal{P}'_{3,2:1,\mathbf{D}}$, and $\mathcal{P}''_{3,2:1,\mathbf{D}}$ are defined, respectively, on the embeddings in Figure 8.1 by $e_i \mapsto e_{i+1}$ with two isolated fixed points as indicated. Each is pseudofree.

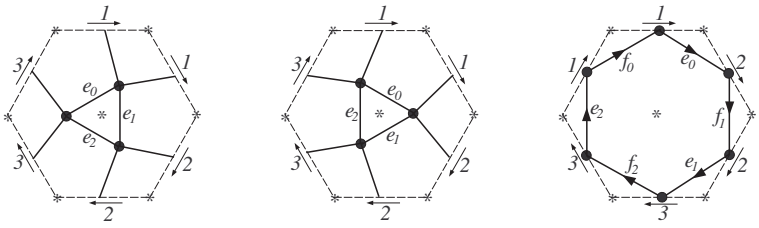

Figure 8.1.

The cellular automorphism $\mathcal{O}_{2,1:1,\mathbf{D}}$ is defined on the first embedding in Figure 8.2 by rotating the single face 180°; it can also be visualized as in the second embedding by reflecting across a. The cellular automorphism $\mathcal{O}'_{2,1:1,\mathbf{D}}$ is defined on the third embedding in Figure 8.2 by rotating the single face 180°; it can also be visualized as in the fourth embedding by reflecting across a. Each cellular automorphism has oval cycle a, which has a Möbius neighborhood, and one isolated fixed point.

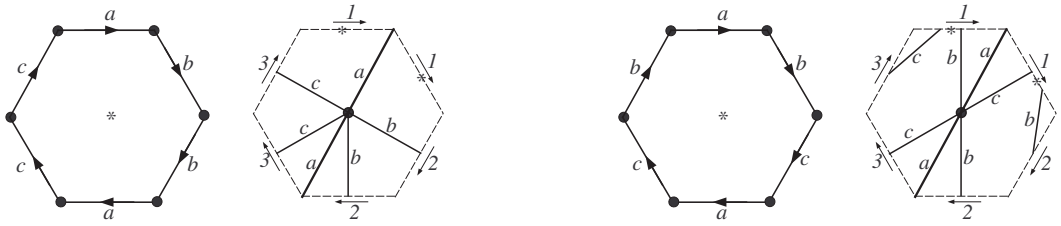

Figure 8.2.

The cellular automorphism $\mathcal{O}_{2,3:1,\mathbf{D}}$ is defined on either of the first two embeddings in Figure 8.3 by rotating the figure by 180°. Similarly, the cellular automorphism $\mathcal{O}'_{2,3:1,\mathbf{D}}$ is defined on either of last two embeddings in Figure 8.3. Each has oval cycle a (which has a Möbius neighborhood) and three isolated fixed points.

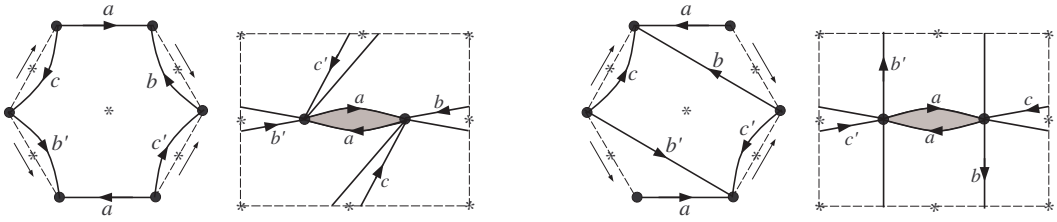

Figure 8.3.

The cellular automorphism $\mathcal{O}_{4,1:1,2:2,\mathbf{D}}$ is defined on either of the first two embeddings in Figure 8.4 by rotating the figure 90°. Similarly, the cellular automorphism $\mathcal{O}'_{4,1:1,2:2,\mathbf{D}}$ is defined on either of the last two embeddings in Figure 8.4. Each has oval cycle ab of length 2 (which has a Möbius neighborhood), one fixed point, and two pseudofixed points of index 2. One can check that $(\mathcal{O}_{4,1:1,2:2,\mathbf{D}})^2 \rightsquigarrow \mathcal{O}_{2,3:1,\mathbf{D}}$ and $(\mathcal{O}'_{4,1:1,2:2,\mathbf{D}})^2 \rightsquigarrow \mathcal{O}'_{2,3:1,\mathbf{D}}$.

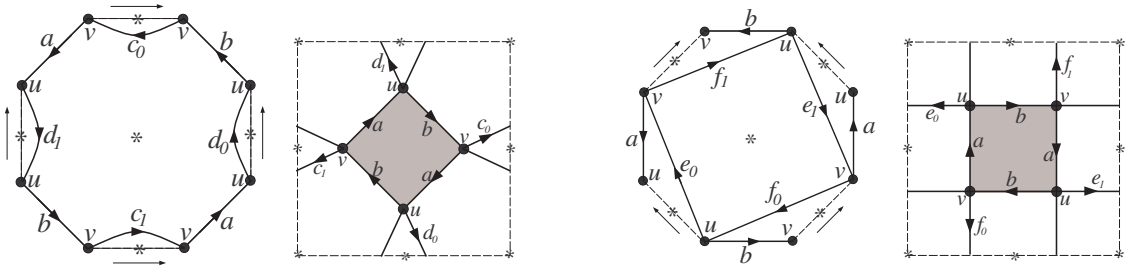

Figure 8.4.

The cellular automorphism $\mathcal{OO}_{2,1:1,\mathbf{D}}$ is defined on either of the embeddings in Figure 8.5 by rotating the single face 180°. It has oval cycles a and b and one isolated fixed point. The oval cycle a has a Möbius neighbohood and the oval cycle b has an annular neighborhood.

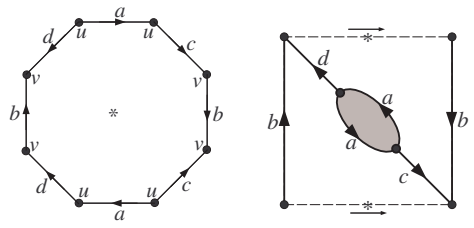

Figure 8.5.

8.2 Completeness of the catalogue

Theorem 8.6. *If φ is a cellular automorphism of G in $\mathbf{D}$ and $\overline{G} = G$, then φ reduces to one of $(\mathcal{P}_{3,2:1,\mathbf{D}})^i$, $(\mathcal{P}'_{3,2:1,\mathbf{D}})^i$, $(\mathcal{P}''_{3,2:1,\mathbf{D}})^i$, $\mathcal{O}_{2,1:1,\mathbf{D}}$, $\mathcal{O}'_{2,1:1,\mathbf{D}}$, $\mathcal{O}_{2,3:1,\mathbf{D}}$, $\mathcal{O}'_{2,3:1,\mathbf{D}}$, $(\mathcal{O}_{4,1:1,2:2,\mathbf{D}})^i$, $(\mathcal{O}'_{4,1:1,2:2,\mathbf{D}})^i$, and $\mathcal{OO}_{2,1:1,\mathbf{D}}$.*

The following Proposition follows from fact that in a closed surface the sum of the voltages on all faces must be 0. It will be used in the proof of Theorem 8.6.

Proposition 8.7. *If G is embedded in closed surface S and σ is a $\mathbb{Z}_2$-voltage assignment on G, then the number of faces whose boundary walks are nonzero under σ_* is even.*

Proof of Theorem 8.6. Let $n = |\varphi|$ and $\pi\colon \mathbf{D} \to \mathbf{D}/\langle\varphi\rangle$ be the corresponding projection. In Case 1 say that φ is pseudofree and in Case 2 say that φ is not pseudofree.

Case 1 Let Y be the set of branch points of π. Applying Theorem 3.6 we get that

$$\chi(\mathbf{D}/\langle\varphi\rangle) = \frac{-1}{n} + \frac{1}{n}\sum_{y\in Y} \mathrm{def}(y) \tag{2}$$

and so (because $\chi(\mathbf{D}/\langle\varphi\rangle)$ is an integer) we get that φ is not free which then makes $\chi(\mathbf{D}/\langle\varphi\rangle) \geq 0$. Since $\mathbf{D}$ is non-orientable, we cannot have that $\chi(\mathbf{D}/\langle\varphi\rangle) = 2$ and so in Case 1.1 we assume $\chi(\mathbf{D}/\langle\varphi\rangle) = 0$ and in Case 1.2 we assume $\chi(\mathbf{D}/\langle\varphi\rangle) = 1$.

Case 1.1 Since $\chi(\mathbf{D}/\langle\varphi\rangle) = 0$, Equation (2) yields $1 = \sum_{y\in Y} \mathrm{def}(y)$ and so $|Y| = 1$ with the single branch point y having order $\frac{n}{n-1}$, which is an integer. Thus $n = 2$ and y is the image of a fixed point. By Proposition 3.1 there is a $\mathbb{Z}_2$-voltage assignment σ on $G/\langle\varphi\rangle$ in $\mathbf{D}/\langle\varphi\rangle$ that recovers φ on G in $\mathbf{D}$ and (because $|Y| = 1$) σ_* is nonzero on the boundary walk of exactly one face. This contradicts Proposition 8.7.

Case 1.2 Since $\chi(\mathbf{D}/\langle\varphi\rangle) = 1$, Equation (2) implies that

$$n + 1 = \sum_{y\in Y} \mathrm{def}(y) \leq (n-1)|Y| \tag{3}$$

and so $|Y| \geq 2$. Applying Theorem 3.7 we have

$$\frac{-1}{n} = 1 - \sum_{y\in Y}\left(1 - \frac{1}{v_y}\right) \leq 1 - \frac{|Y|}{2}$$

and so $|Y| \leq 2 + \frac{2}{n}$. Hence either $|Y| = 3$ with $n = 2$ or $|Y| = 2$. Let these be, respectively, Cases 1.2.1 and 1.2.2.

Case 1.2.1 Because $n = 2$ and $|Y|$ is odd, we contradict Proposition 8.7 in the same way as in Case 1.1.

Case 1.2.2 Using $|Y| = 2$ in (3) we get that $n + 1 \leq 2n - 2$ and so $n \geq 3$. We claim that at least one of the branch points of π has order greater than 2. Assume to the contrary that both branch points have order 2. Let σ be a $\mathbb{Z}_n$-voltage assignment on $G/\langle\varphi\rangle$ in $\mathbf{D}/\langle\varphi\rangle = \mathbf{P}$ that recovers G in $\mathbf{D}$ and φ. We can rechoose σ (without changing σ_*) so that $\sigma(e) = 0$ for edges on some spanning tree T of $G/\langle\varphi\rangle$ and, since both branch

points have order 2, $\sigma(e) \in \{0, \frac{n}{2}\}$ for edges off of T. However, since $n \geq 3$, this contradicts the fact that $G \cong (G/\langle\varphi\rangle)^\sigma$ is connected.

So now write $Y = \{y_1, y_2\}$ and again apply Theorem 3.7 to get

$$\frac{-1}{n} = 1 - \sum_{y \in Y}\left(1 - \frac{1}{v_y}\right) = -1 + \frac{1}{v_{y_1}} + \frac{1}{v_{y_2}} \leq -1 + \frac{1}{2} + \frac{1}{3} = -\frac{1}{6}$$

and so $3 \leq n \leq 6$. Now since each v_{y_i} divides n, the only possibilities are $n = 3$ with $v_{y_1} = v_{y_2} = 3$, $n = 4$ with $v_{y_1} = 2$ and $v_{y_2} = 4$, and $n = 6$ with $v_{y_1} = 2$ and $v_{y_2} = 3$. Let these be, respectively, Cases 1.2.2.1–1.2.2.3.

In each of the three cases, $G/\langle\varphi\rangle$ embedded in $\mathbf{D}/\langle\varphi\rangle = \mathbf{P}$ contains a surface minor H as in Figure 6.11 with the two branch points as indicated. Now let $\tilde{H}$ be the surface orbit minor of G in $\mathbf{D}$ given in Proposition 3.4 and σ be a $\mathbb{Z}_n$-voltage assignment on H that recovers $\tilde{H}$ and $\varphi|_{\tilde{H}}$.

Case 1.2.2.1 If H is the left embedding in Figure 6.11, then up to symmetry and automorphism of $\mathbb{Z}_3$, we may assume that $\sigma(e) = 1$. Now the only way in which $v_{y_1} = v_{y_2} = 3$ is possible is if $\sigma(f) = 0$. One can check that $H^\sigma \cong \tilde{H}$ is the third embedding in Figure 8.1 and so $\varphi|_{\tilde{H}}$ is either $\mathcal{P}''_{3,2:1,\mathbf{D}}$ or $(\mathcal{P}''_{3,2:1,\mathbf{D}})^2$.

If H is the right embedding in Figure 6.11, then up to automorphism of $\mathbb{Z}_3$ we may assume that $\sigma(e) = 1$. Now we need that $\sigma_*(e, f, f) = 2\sigma(f) + 1 \in \{1, 2\}$ and so $\sigma(f) = \{0, 2\}$. If $\sigma(f) = 0$, then one can check that $H^\sigma \cong \tilde{H}$ is the first embedding in Figure 8.1 and so $\varphi|_{\tilde{H}}$ is either $\mathcal{P}_{3,2:1,\mathbf{D}}$ or $(\mathcal{P}_{3,2:1,\mathbf{D}})^2$. If $\sigma(f) = 2$, then one can check that $H^\sigma \cong \tilde{H}$ is the second embedding in Figure 8.1 and so $\varphi|_{\tilde{H}}$ is either $\mathcal{P}'_{3,2:1,\mathbf{D}}$ or $(\mathcal{P}'_{3,2:1,\mathbf{D}})^2$.

Case 1.2.2.2 The branch point of order 2 has facial boundary walk with total voltage $2 \in \mathbb{Z}_4$ and the branch point of order 4 has facial boundary walk with total voltage 1 or 3 in $\mathbb{Z}_4$. Thus, if N is a noncontractible cycle in $G/\langle\varphi\rangle$ in $\mathbf{D}/\langle\varphi\rangle$, then we have orientations of the faces of the embedding so that $2\sigma_*(N) = \sum_i \sigma_*(\theta_i F_i) \in \{1 + 2, 3 + 2\}$, but this is impossible in $\mathbb{Z}_4$.

Case 1.2.2.3 Similar to the previous case, if N is a noncontractible cycle in $G/\langle\varphi\rangle$ in $\mathbf{D}/\langle\varphi\rangle$, then we have orientations of the faces of the embedding so that $2\sigma_*(N) = \sum_i \sigma_*(\theta_i F_i) \in \{3+2, 3+4\}$, but this is impossible in $\mathbb{Z}_6$.

Case 2 In Case 2.1 assume that $n = 2$ and in Case 2.2 assume that $n \geq 4$.

Case 2.1 Applying Proposition 3.9 with $s \geq 1$ we get that

$$\chi([\mathbf{D}/\langle\varphi\rangle]^\bullet) = \frac{-1}{2} + \frac{r}{2} + s \in \mathbb{Z}$$

which implies that $r \geq 1$ and so $\chi([\mathbf{D}/\langle\varphi\rangle]^\bullet) \in \{1, 2\}$. In Case 2.1.1 say that $\chi([\mathbf{D}/\langle\varphi\rangle]^\bullet) = 1$ and in Case 2.1.2 say that $\chi([\mathbf{D}/\langle\varphi\rangle]^\bullet) = 2$.

Case 2.1.1 Here we must have $s = 1$ and $r = 1$ and $\mathbf{D}/\langle\varphi\rangle$ is a Möbius band. Now $G/\langle\varphi\rangle$ in $\mathbf{D}/\langle\varphi\rangle$ contains a surface minor H properly embedded as shown in Figure 8.8 where e is the hole cycle.

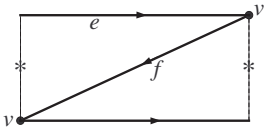

Figure 8.8.

Let $\tilde{H}$ be the surface orbit minor of G in $\mathbf{D}$ given by 3.14 and let σ be a $\mathbb{Z}_2$-voltage assignment on H that recovers $\tilde{H}$ and $\varphi|_{\tilde{H}}$ given by Proposition 3.13. We must have that $1 = \sigma_*(e, f, f) = \sigma(e) + 2\sigma(f) = \sigma(e)$. If $\sigma(f) = 0$, then one can check that the ordinary derived embedding H^σ and basic automorphism β_σ together are $\mathcal{P}'_{2,2:1,\mathbf{K}}$ (see Figure 7.2). So then $\widehat{H}^\sigma \cong \tilde{H}$ and $\varphi|_{\tilde{H}}$ is $\mathcal{O}_{2,1:1,\mathbf{D}}$. If $\sigma(f) = 1$, then one can check that the ordinary derived embedding H^σ and basic automorphism β_σ together are $\mathcal{P}''_{2,2:1,\mathbf{K}}$. So then $\widehat{H}^\sigma \cong \tilde{H}$ and $\varphi|_{\tilde{H}}$ is $\mathcal{O}'_{2,1:1,\mathbf{D}}$.

Case 2.1.2 Here we either have $s = 2$ and $r = 1$ or $s = 1$ and $r = 3$. Let these be Cases 2.1.2.1 and 2.1.2.2, respectively.

Case 2.1.2.1 Here $\mathbf{D}/\langle\varphi\rangle$ is an annulus. Thus $G/\langle\varphi\rangle$ in $\mathbf{D}/\langle\varphi\rangle$ contains a surface minor H that is properly embedded as shown on the left in Figure 8.9 with hole-cycles a and b and isolated branch point as indicated.

Figure 8.9.

Let $\tilde{H}$ be the surface orbit minor of G in $\mathbf{D}$ given by Proposition 3.14 and let σ be a $\mathbb{Z}_2$-voltage assignment on H that recovers $\tilde{H}$ and $\varphi|_{\tilde{H}}$ as in Proposition 3.13. We must have that $1 = \sigma_*(a, e, b, -e) = \sigma(a) + \sigma(b)$. By symmetry we may assume that $\sigma(a) = 1$ and $\sigma(b) = 0$. Given that e is not contained in any cycle, we can choose $\sigma(e) = 0$ without affecting σ_*. One can check that the ordinary derived embedding H^σ (in $\mathbf{S}$) is as shown on the right in Figure 8.9 and the associated basic automorphism reduces to $\mathcal{R}_{2,\mathbf{S}}$. So now $\widehat{H}^\sigma \cong \tilde{H}$ and $\varphi|_{\tilde{H}}$ is $\mathcal{OO}_{2,1:1,\mathbf{D}}$ as shown in Figure 8.5.

Case 2.1.2.2 Here $\mathbf{D}/\langle\varphi\rangle$ is a disk. Thus $G/\langle\varphi\rangle$ in $\mathbf{D}/\langle\varphi\rangle$ contains one of the proper embeddings in Figure 8.10 as a surface minor, call it H. In each embedding a is the hole-cycle. Let $\tilde{H}$ be the surface orbit minor of G in $\mathbf{D}$ given by Proposition 3.14 and let σ be a $\mathbb{Z}_2$-voltage assignment on H that recovers $\tilde{H}$ and $\varphi|_{\tilde{H}}$ as in Proposition 3.13.

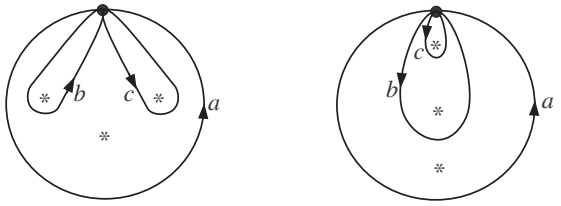

Figure 8.10.

If H is the left embedding from Figure 8.10, we must have that $\sigma(b) = \sigma(c) = \sigma(a) = 1$. One can check that, after relabeling, the ordinary derived embedding of H^σ and the associated basic automorphism together are $\mathcal{P}_{2,4:1,\mathbf{T}}$ (see Figure 6.5). So now $\widehat{H}^\sigma \cong \tilde{H}$ in $\mathbf{D}$ and $\varphi|_{\tilde{H}}$ is $\mathcal{O}_{2,3:1,\mathbf{D}}$.

If H is the right embedding from Figure 8.10, we must have that $\sigma(a) = \sigma(c) = 1$ and $\sigma(b) = 0$. One can check that, after relabeling, the ordinary derived embedding of H^σ and the associated basic automorphism together are $\mathcal{P}'_{2,4:1,\mathbf{T}}$ (see Figure 6.5). So now $\widehat{H}^\sigma \cong \tilde{H}$ in $\mathbf{D}$ and $\varphi|_{\tilde{H}}$ is $\mathcal{O}'_{2,3:1,\mathbf{D}}$.

Case 2.2 Here $n = 2k$ and so by Case 2.1 φ^k reduces to one of $\mathcal{O}_{2,1:1,\mathbf{D}}$, $\mathcal{O}'_{2,1:1,\mathbf{D}}$, $\mathcal{O}_{2,3:1,\mathbf{D}}$, $\mathcal{O}'_{2,3:1,\mathbf{D}}$, and $\mathcal{OO}_{2,1:1,\mathbf{D}}$.

If $\varphi^k \rightsquigarrow \mathcal{O}_{2,1:1,\mathbf{D}}$, then $(\varphi^{\circlearrowleft})^k \rightsquigarrow \mathcal{P}'_{2,2:1,\mathbf{K}}$. By Theorem 7.8 we get that $k = 1$.

If $\varphi^k \rightsquigarrow \mathcal{O}'_{2,1:1,\mathbf{D}}$, then $(\varphi^{\circlearrowleft})^k \rightsquigarrow \mathcal{P}''_{2,2:1,\mathbf{K}}$. By Theorem 7.8 we again get that $k = 1$.

If $\varphi^k \rightsquigarrow \mathcal{OO}_{2,1:1,\mathbf{D}}$, let A be the annular oval cycle and let M be the Möbius oval cycle. We must have $\varphi(A) = A$ and $\varphi(M) = M$. After cutting, A gives rise to two hole cycles A_1 and A_2 and M gives rise to one hole cycle M_1, and $\varphi^{\circlearrowleft}$ exchanges A_1 and A_2 and fixes M_1. If $k > 1$ then $\varphi^{\circlearrowleft}$ must have 4 pseudofixed points, however $[\mathbf{D}^{\circlearrowleft}]^\bullet = \mathbf{S}$, yielding a contradiction to Theorem 4.1. Thus $k = 1$.

If $\varphi^k \rightsquigarrow \mathcal{O}_{2,3:1,\mathbf{D}}$, then the single oval has a Möbius neighborhood and one can check that $(\varphi^{\circlearrowleft})^k \rightsquigarrow \mathcal{P}_{2,4:1,\mathbf{T}}$. By Theorem 6.10 we get that $k \in \{1, 2\}$. Assuming that $k = 2$, Theorem 6.10 also implies that $\overline{\text{fix}}(\varphi)$ consists of an isolated pseudofixed point of index 1 and two isolated pseudofixed points of index two. Let G be the embedded graph for φ and O be the oval-cycle. By Proposition 3.9 we know that $G/\langle\varphi^2\rangle$ is embedded in $[\mathbf{D}/\langle\varphi^2\rangle]^\bullet = \mathbf{S}$ with induced cellular automorphism $\varphi^\downarrow$ which has $\varphi^\downarrow(O) = O$ and maps the capped face to the capped face. Thus $\varphi^\downarrow \rightsquigarrow \mathcal{R}_{2,\mathbf{S}}$ by Theorem 4.1. Now we must have that $G/\langle\varphi^2\rangle$ in $\mathbf{D}/\langle\varphi^2\rangle$ has surface orbit minor H (with respect to $\varphi^\downarrow$) equal to one of the embeddings in Figure 8.11 where a, b is the hole-cycle, the larger asterisk is a fixed point of $\varphi^\downarrow$, and the smaller asterisks are the images of the two index-2 pseudofixed points of φ.

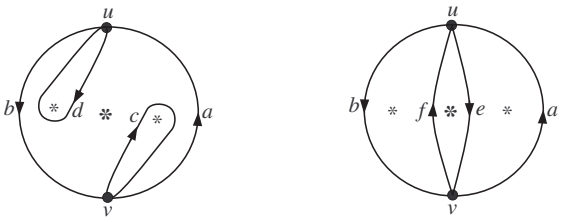

Figure 8.11.

The surface orbit minor H can be obtained in a way that satisfies the conditions of Proposition 3.14 because after deletion of edges we would only have to contract orbits of edges along the hole-cycle and along paths that are subdivisions of c and d or e and f. So now let $\tilde{H}$ be the surface orbit minor of G in $\mathbf{D}$ given by Proposition 3.14 that corresponds to H and let σ be a $\mathbb{Z}_2$-voltage assignment on H given by Proposition 3.13 that reconstructs $\tilde{H}$ and φ^2; Proposition 3.21 ensures that $\varphi|_{\tilde{H}}$ is one of the lifted automorphisms $(\varphi^{\downarrow})^{\uparrow}_{0,\sigma}$ or $(\varphi^{\downarrow})^{\uparrow}_{1,\sigma}$. Now, without loss of generality, we have that $\sigma(a) = 0$ and $\sigma(b) = 1$ because the single oval of φ has a Möbius neighborhood. Since the faces containing branch points must have total voltage 1 along their facial boundary walks we then get that $\sigma(c) = \sigma(d) = 1$ for the first embedding of Figure 8.11 and that $\sigma(e) = 1$ and $\sigma(f) = 0$ for the second embedding. One can now construct the lifted embeddings and automorphisms and get that $\varphi|_{\tilde{H}}$ is one of $\mathcal{O}_{4,1:1,2:2,\mathbf{D}}$, $\mathcal{O}'_{4,1:1,2:2,\mathbf{D}}$, $(\mathcal{O}_{4,1:1,2:2,\mathbf{D}})^3$, and $(\mathcal{O}'_{4,1:1,2:2,\mathbf{D}})^3$. □

9 Self-dual embeddings

Consider a graph G embedded in S and its topological dual embedding G^* in S. If there is a cellular isomorphism φ from G in S to G^* in S, then we say that the embedding of G in S is *self dual*. In this section we will give procedures for constructing all self-dual embeddings in the sphere, projective plane, torus, Klein bottle, and Dyck's surface using our complete catalogs of all irreducible and oval-irreducible cellular automorphisms for those surfaces. In fact, the procedures that we give will work for any given closed surface S for which a complete catalog of all irreducible pseudofree and oval-irreducible cellular automorphisms in S is known.

The techniques we utilize are inspired by those in [7, 8]; indeed our original motivation for this paper was to extend the techniques in [7, 8] to the torus and Klein bottle.

9.1 Radial graphs, cellular automorphisms, and self duality

In [7, 8] self-dual embeddings are related to cellular automorphisms via the observations which we now survey. Given a graph G embedded in a closed surface S, the *radial graph* $R(G)$ is a bipartite graph whose vertex set has partite sets $V(G)$ and $F(G)$ with edges given by the vertex/face incidences of the embedding of G. That is, given an $f \in F(G)$, f is an open n-gon in the embedding of G and the corresponding vertex in $R(G)$ has edges "radiating" out to the corners of this n-gon (see the left of Figure 9.1). As such, the natural embedding of $R(G)$ in S has every face bounded by a walk of length four and in each such face the diagonals correspond to an edge/dual-edge pair of G and G^*. (In Figure 9.1 on the right we have a graph embedded in the projective plane with bold edges and its corresponding radial graph embedding shown in dashed edges.)

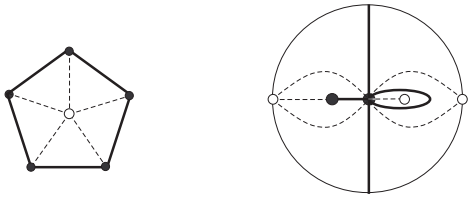

Figure 9.1.

Thus $R(G^*) = R(G)$ and if φ is a cellular isomorphism of G in S to G^* in S, then φ corresponds to a cellular automorphism of $R(G)$ in S that exchanges the partite sets. Conversely, if φ is a cellular automorphism of a

bipartite graph Q embedded in S for which every face has length four and φ exchanges the partite sets of Q, then φ naturally corresponds to a cellular isomorphism of a graph of G in S to G^* in S with $R(G) = Q$. Thus we have Proposition 9.2. Here a *quadrangulation* of S is a graph embedding in which all facial boundaries are of length 4; it does not require any intersection conditions on pairs of boundaries.

Proposition 9.2. *Given a closed surface S, the pairs $(\{G, G^*\}, \varphi)$ where φ is a cellular isomorphism from G to G^* in S are in bijective correspondence with pairs (Q, φ) where φ is a part-reversing cellular automorphism of bipartite quadrangulation Q of S.*

Our procedures for constructing self-dual embeddings are actually procedures for constructing part-reversing cellular automorphisms on bipartite quadrangulations. They are Constructions 9.14, 9.19, and 9.32.

There has been extensive previous work on characterizing quadrangulations of the sphere, projective plane, torus, and Klein bottle (without explicit descriptions of symmetries and pseudofixed points as is done in this paper) by Altshuler [1] and Nakamoto [24, 25, 26, 27]. Altshuler characterizes the 4-regular quadrangulations of the torus; our torus grids of Section 6.1 are very closely related. Nakamoto requires that the embedded graph of the quadrangulation be simple and defines a type of reduction of quadrangulations with respect to which he identifies the minimal quadrangulations. All quadrangulations are then generated by certain expansion operations from the minimal ones. Here we do not require that the embedded graphs be simple and we employ different methods of reduction and construction; in particular, our methods respect the cellular automorphisms of the embedding.

9.2 Basic properties of part-reversing cellular automorphisms on bipartite quadrangulations

Proposition 9.3. *Let φ be a part-reversing cellular automorphism (not necessarily pseudofree) of a bipartite quadrangulation Q in surface S and let x be an isolated pseudofixed point of φ of index m.*

(1) If m is odd, then either

- *x is in the center of a face, the action of φ^m on that face is a 1/4-rotation, and $|\varphi| = 4m$ or*
- *x is in the center of a link, the action of φ^m on that edge is a reflection, and $|\varphi| = 2m$.*

(2) If m is even, then either

- *x is in the center of a face, the action of φ^m on that face is a 1/2-rotation, and $|\varphi| = 2m$ or*
- *x is at a vertex, the action of φ^m on the neighborhood of that vertex is a rotation of order r, and $|\varphi| = mr$.*

Proof. If m is odd, then φ^m is part reversing and so any x of index m must be in the center of a face or link. In the former case, the part-reversing property of φ^m implies that the action of φ^m at x is a 1/4-rotation. In the latter case, the action of φ^m on a small neighborhood of x is a 1/2-rotation. If m is even, then φ^m is part preserving and so x cannot be in the center of a link but may be in the center of a loop, however Q, being bipartite, is loopless. Thus x is either in the center of a face or at a vertex. The remaining assertions follow. □

Notice that for any isolated $x \in \overline{\mathrm{fix}}(\varphi)$ the points in $\mathsf{orbit}_\varphi(x)$ all fall into the same category from Proposition 9.3. Also, the category from Proposition 9.3 that the points fall into is uniquely determined by $|\varphi|/m$ and the parity of m except in the case where m is even and $|\varphi|/m = 2$.

Another interesting fact that arises from Proposition 9.3 concerns pseudofixed points of odd index. In such cases, the possible orders of these cellular automorphisms are severely restricted. For example, in the projective plane, all cellular automorphisms have an isolated pseudofixed point of index 1. So although for any n there is a general cellular automorphism of order n, part-reversing cellular automorphisms on bipartite quadrangulations in the projective plane may have order 2 or 4 only (as shown in [7]).

Proposition 9.4. *Let φ be a part-reversing cellular automorphism of a bipartite quadrangulation Q in surface S with an oval O in $\overline{fix}(\varphi)$.*

(1) If $|\varphi|/2$ is odd, then O intersects Q only at midpoints of links. (See the top of Figure 9.5.) Furthermore,

- *if O has an annular neighborhood, then O intersects an even number of faces and*
- *if O has a Möbius neighborhood, then O intersects an odd number of faces.*

(2) If $|\varphi|/2$ is even, then O intersects Q only at vertices and entire edges. (See the bottom of Figure 9.5.)

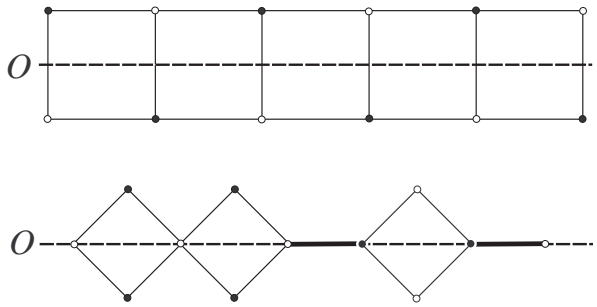

Figure 9.5.

The graph along the oval in the top of Figure 9.5 is called a *ladder* and this ladder is either annular or Möbius . The graph along the oval in the bottom of Figure 9.5 we will call a *necklace*.

Proof of Proposition 9.4. Say that $|\varphi| = 2k$. If k is odd, then φ^k is part reversing on Q and so O must intersect Q as stated. The final two items are implied by the bipartite condition. If k is even, then φ^k is part preserving on Q and so O must intersect Q as stated. □

Since the length of an oval cycle is important for the ladder neighborhoods of ovals in Proposition 9.4, we present Proposition 9.6.

Proposition 9.6. *Let φ be an oval-irreducible cellular automorphism of G in S and let O be an oval-cycle in G.*

(1) If O has an annular neighborhood, then the length of O is odd.

(2) If $|\varphi|/2$ is odd and O has a Möbius neighborhood, then the length of O is odd.

Proof. By Propositions 2.8 and 5.2, $|\varphi| = 2rm$ where m is the index of O and r is the order of the rotation action of φ^m on O. Thus the length of O is rt for some t. We claim that $t = 1$. If $t > 1$, then pick any edge e in O and note that $\mathsf{orbit}_\varphi(e)$ is a collection of edges in the oval-cycles of $\mathsf{orbit}_\varphi(O)$ that are pairwise non-incident. Thus $G/\mathsf{orbit}_\varphi(e)$ satisfies the conditions for a surface orbit minor in S, however, this surface orbit minor is obtained without any deletions and so contradicts the oval-irreducibility of G in S.

In the case that O has an annular neighborhood, Proposition 2.8 implies that r (which is the length of O) is odd. In the case that O has a Möbius neighborhood, the assumption that $|\varphi|/2 = rm$ is odd implies that r is odd. □

Proposition 9.7 is an important property that is used without further mention.

Proposition 9.7. *Suppose G is a connected bipartite graph and $\{A, B\}$ is the unique bipartition of its vertices. Any automorphism φ of G induces a unique bijection on $\{A, B\}$ and this bijection can be determined by checking the parity of the length of a single $v\varphi(v)$-path for any vertex v. Furthermore, all $v\varphi(v)$-paths for all vertices v have the same parity.*

9.3 Quadrangulated Patches

A *quadrangulated patch of length n* is a plane embedding Q with a designated outer face bounded by an n-cycle and each inner face bounded by a walk of length four. Note that a quadrangulated patch is always bipartite and so n is even. One can construct a quadrangulated patch for any even length; in Figure 9.8 we show quadrangulated patches of lengths 2 and 4. It would be worthwhile to know a general construction method for producing all quadrangulated patches of length n, but we do not discuss this here.

Figure 9.8.

In the remainder of this section we will discuss quadrangulated patches with different symmetry types and/or conditions on degrees of vertices. These special patches are important for constructing radial graphs with part-reversing cellular automorphisms.

9.3.1 Patches with rotational symmetry at a vertex

Proposition 9.9. *If n is even and r divides n and Q is a quadrangulated patch of length n with r-fold rotational symmetry about a central vertex, then n/r is even and the rotational symmetry preserves the partite sets of Q.*

Proof. As the central vertex is fixed, the rotational symmetry must preserve the partite sets. The orbit of a vertex on the rim of the patch consists of r vertices on the rim spaced n/r edges apart, and the part-preserving property implies that this distance n/r is even. □

Conversely to Proposition 9.9, for any r dividing n such that n/r is even, a quadrangulated patch of length n having rotational symmetry of order r around a central fixed vertex can always be constructed in the following manner. Take r internally disjoint paths of length $\ell \geq 1$ from the central fixed point to the outer n-cycle at r evenly spaced points. This leaves a planar embedding whose inner faces all have length $n/r + 2\ell$ which is even. Within each inner face paste in copies of a given quadrangulated patch of length $n/r + 2\ell$ in a manner that respects the rotational symmetry.

9.3.2 Patches with 4-fold rotational symmetry around a quadrilateral

Proposition 9.10. *If $n \geq 4$ is divisible by 4 and Q is a quadrangulated patch of length n with 4-fold rotational symmetry around a central quadrilateral face, then $n/4$ is odd and the rotational symmetry exchanges the partite sets of Q.*

Proof. Since the rotational action on the central face is a 90-degree rotation, the rotational symmetry exchanges the partite sets of Q. The orbit of a vertex on the rim of the patch consists of 4 vertices on the rim spaced $n/4$ edges apart. The part-reversing property implies that this distance $n/4$ is odd. □

Conversely to Proposition 9.10, for any n such that $n/4$ is odd, a quadrangulated patch of length n with 4-fold rotational symmetry around a central face can always be constructed in the following manner. Place a 4-cycle inside an n-cycle and connect the vertices of the 4-cycle to the n-cycle by four disjoint paths of length $\ell \geq 0$ whose endpoints on the n-cycle are evenly spaced. Now the four newly formed faces are of length $2\ell + 1 + \frac{n}{4}$ which is even. Fill in these four faces with copies of a given quadrangulated patch of length $2\ell + 1 + \frac{n}{4}$ in a way that respects the 4-fold rotational symmetry.

9.3.3 Patches with 2-fold rotational symmetry around a quadrilateral

Proposition 9.11. *If $n \geq 2$ is even and Q is a quadrangulated patch of length n with 2-fold rotational symmetry about a central face, then $n/2$ is even and the rotational symmetry preserves the partite sets of Q.*

Proof. Given Q, a path of length 2 between opposite vertices may be temporarily inserted into the central quadrilateral and then we obtain our result from Proposition 9.9. □

Conversely to Proposition 9.11, given $n \geq 4$ that is divisible by 4, a quadrangulated patch of length n having 2-fold rotational symmetry around a central face bounded by a 4-cycle can always be constructed in the following way. Place a 4-cycle inside an n-cycle with either 0, 1, or 2 pairs of antipodal vertices of the 4-cycle on the n-cycle.

In the first case, connect one antipodal pair of vertices on the 4-cycle to the n-cycle by two disjoint paths of length $\ell \geq 1$ whose endpoints on the n-cycle are evenly spaced. In the second case take $\ell = 0$. The two newly formed faces are of length $2\ell + 2 + \frac{n}{2}$ which is even. Fill in these two faces with copies of a given quadrangulated patch of length $2\ell + 2 + \frac{n}{2}$ in a way that respects the 2-fold rotational symmetry.

In the third case, the four vertices on the n-cycle must be chosen to separate the n-cycle into paths of lengths a, b, a, b where both a and b are odd. Note that the four newly formed faces all have even length. Fill in these four faces with copies of two quadrangulated patches of the appropriate lengths in a way that respects the 2-fold rotational symmetry.

9.3.4 Patches with 2-fold rotational symmetry around a link

Proposition 9.12. *If $n \geq 2$ is even and Q is a quadrangulated patch of length n with 2-fold rotational symmetry around a central link, then $n/2$ is odd and the symmetry exchanges the partite sets.*

Proof. The symmetry is part reversing because of the rotation around the central link. So now the orbit of any vertex on the rim of the patch consists of 2 vertices spaced $n/2$ edges apart. That the symmetry is part reversing implies that $n/2$ is odd. □

Conversely to Proposition 9.12, given $n \geq 2$ such that $n/2$ is odd, a quadrangulated patch of length n having 2-fold rotational symmetry around a central link can always be constructed in the following way. Place a link inside an n-cycle and connect the endpoints of the link to the n-cycle by two disjoint paths of length $\ell \geq 0$ whose endpoints on the n-cycle are evenly spaced. The two newly formed faces have length $2\ell + 1 + \frac{n}{2}$ which is even. Fill in these two faces with copies of a given quadrangulated patch of length $2\ell + 1 + \frac{n}{2}$ in a way that respects the 2-fold rotational symmetry.

9.3.5 Ladder Patches

Let C be a cycle of even length $n = 2k \geq 4$ with edges of two types, say red and black (monochromatic possible). As such, C decomposes into monochromatic paths that alternate colors along C. A *ladder patch* is a quadrangulated patch P on C in which the endpoints of these monochromatic paths have degree 2 in P, the interior vertices of the red paths have degree 3 in P (the degrees of the interior vertices of the black paths are unrestricted), and no quadrilateral face has a pair of red antipodal edges. When such a P exists for C, we say that C is *ladder patchable*.

Proposition 9.13. *C is ladder patchable iff all black paths in C have length at least two.*

Proof. Suppose P is a ladder patch with outer cycle C. The length of C is even and so is at least two. If C is monochromatic black then we are done. If there is a black path of length one, then there are three consecutive edges on C colored red, black, red. Degree requirements force these three edges to be on a face of P but then this face has a pair of red antipodal edges, a contradiction.

For the converse, suppose all black paths in C have length at least two. If C is monochromatic red, then take the patch P to be an annular ladder along with any arbitrary quadrangulated patch inserted along the

inner face of the ladder (*i.e.*, the face not incident to C). Otherwise we proceed by induction on the number t of red edges in C. If $t = 0$, then pick P as any arbitrarily chosen quadrangulated patch for C. If C has $t \geq 1$ red edges, then take a consecutive red, black pair of edges along C, say e and f. If e is incident to another red edge on C, then add a chordal path of two edges connecting the endpoints of the path e, f and color these edges black. The cycle C' obtained by deleting e, f and appending the chordal path has $t - 1$ red edges and every black path of length at least 2. Inductively, C' is ladder patchable and so C is ladder patchable. If e is incident to two black edges, say f and f' on C, then append a chordal link to the endpoints of the path f, e, f' and color it black. As before, deleting f, e, f' leaves a cycle C' with $t - 1$ red edges that is ladder patchable and thus C is ladder patchable. □

We will also need ladder patches of length n with the types of rotational symmetries described in Sections 9.3.1–9.3.4.

For r-fold rotational symmetry around a central vertex when n/r is even, consider the construction described in Section 9.3.1. The r paths of length $\ell \geq 1$ radiating from the central vertex must be attached to interior vertices of the black paths or red paths on C. (These interior vertices must exist by Proposition 9.13 and the fact that n is even.) Coloring these paths black we then get that each of the r sections of the resulting wheel is ladder patchable by Proposition 9.13. Placing copies of any ladder patch inside these sections of the wheel in a manner respecting the rotational action yields a ladder patch on C with the required rotational symmetry.

For 4-fold rotational symmetry around a central face when $n/4$ is odd, consider the construction described in Section 9.3.2. The four paths of length $\ell \geq 0$ radiating out from the central face must be attached to interior vertices on the black paths or red paths of C. In the case that $\ell = 0$, degree requirements force these paths to be attached to interior vertices of black paths on C. Now color these paths and the edges on the central face black; the resulting 4 regions are all ladder patchable by Proposition 9.13. Placing copies of any ladder patch inside the 4 sections in a manner respecting the rotational action yields a ladder patch on C with the required rotational symmetry.

Ladder patches with 2-fold rotational symmetry around a central face (as in Section 9.3.3) or around a central link (as in Section 9.3.4) are constructed in a similar fashion.

9.4 General constructions

Given a graph H, a *split* of H is a graph G obtained from H by decontractions of links at vertices of degree at least four in H that do not create any new vertices of degree 1 or 2. Given an automorphism ψ of H, a *ψ-orbit split* of H is a split of H for which the automorphism ψ extends and such that the set of decontracted edges is acyclic. That is, at any vertex v of H where a split occurs, all vertices in $\mathsf{orbit}_\psi(v)$ are split in the same manner with respect to ψ. A *ψ-orbit subdivision* of H is a graph G obtained from H by subdivisions of all edges in some set of orbits. Of course, the automorphism ψ extends to any *ψ-orbit subdivision.*

Some important observations about taking minors in graphs are as follows. Given that $H = G\backslash D/C$ for some disjoint sets of edges C and D in G, any loops or pendant edges in G/C may be deleted rather than contracted without affecting H. As such, if we choose D to be a maximal set such that $G\backslash D/C = H$, then the subgraph of G corresponding to C is acyclic and $G\backslash D$ is obtained from H by a sequence of splits and subdivisions. Similarly if φ is an automorphism of G and $H = G\backslash\mathsf{orbit}_\varphi(D)/\mathsf{orbit}_\varphi(C)$ is an orbit minor with $\mathsf{orbit}_\varphi(D) \cap \mathsf{orbit}_\varphi(C) = \emptyset$, then we can move orbits of edges in G from $\mathsf{orbit}_\varphi(C)$ to $\mathsf{orbit}_\varphi(D)$ in order to obtain a maximal deletion set and so that $G\backslash\mathsf{orbit}_\varphi(D)$ is obtained from H by a sequence of orbit splits and orbit subdivisions.

9.4.1 Free automorphisms

Construction 9.14 is a 3-step process that produces free part-reversing cellular automorphisms on bipartite quadrangulations. It takes as input a cellular automorphism φ of G_0 in S and at step i produces a graph G_i in S from G_{i-1} in S to which φ extends. In practice, the input cellular automorphism will be taken from a

complete catalogue of irreducible free cellular automorphisms of S such as what we have determined for the sphere, projective plane, torus, and Klein bottle (there are none for Dyck's surface).

Construction 9.14. Take a graph G that is cellularly embedded in S along with a free cellular automorphism φ of G in S that has even order.

1. Let G_1 be a φ-orbit split of G or let $G_1 = G$.
2. Let G_2 be a φ-orbit subdivision of G_1 such that G_2 is bipartite and φ is part reversing on G_2. If G_1 is already bipartite with φ part reversing, then we may let $G_2 = G_1$.
3. Let $\mathcal{F}_1, \ldots, \mathcal{F}_y$ be the orbits of the faces of G_2 in S under φ. For each $\mathcal{F}_i$ choose a quadrangulated patch of the appropriate length and paste copies of this patch into the faces of $\mathcal{F}_i$ in a way that respects φ.

Each step in Construction 9.14 can always be carried out given the initial assumptions except maybe for Step 2. We will not address the question of when Step 2 is executable, but we do get Theorem 9.15 which tells us that Construction 9.14 along with a complete catalogue of the irreducible free cellular automorphisms of S will be enough to construct all free part-reversing cellular automorphisms on bipartite quadrangulations. The details of the proof of Theorem 9.15 can be found in the proof of Theorem 9.20.

Theorem 9.15. *If φ is a free part-reversing cellular automorphism of a bipartite quadrangulation Q in S, then φ is obtainable by Construction 9.14 from an irreducible free cellular automorphism on G in S.*

An Example As an illustration of Construction 9.14 we will characterize the free part-reversing cellular automorphisms on bipartite quadrangulations that are obtainable by Construction 9.14 from $\mathcal{GR}_{n,a,b,\mathbf{T}}$.

There are two possible outcomes for G_1 in Step 1: the (n,a,b)-torus-grid itself and a 3-regular graph that is an orbit split of the (n,a,b)-torus-grid. Case 1 considers the rest of the construction for the former possibility and Case 2 considers the rest of the construction for the latter possibility.

Case 1 Consider integers r and s such that $ra + sb = \gcd(a,b)$ with $|r| + |s|$ as small as possible, and the path $\gamma_{r,s}$ from v to $\mathcal{GR}_{n,a,b,\mathbf{T}}(v)$ described in Section 6.1 which is of length $|r| + |s|$.

Proposition 9.16. *Let n be even and let O be an orbit subdivision of the (n,a,b)-torus-grid and φ the cellular automorphism on O induced by $\mathcal{GR}_{n,a,b,\mathbf{T}}$. Say that each edge on the $\frac{n}{\gcd(a,n)}$-cycles is subdivided $t_a \geq 0$ times and that each edge on the $\frac{n}{\gcd(b,n)}$-cycles is subdivided $t_b \geq 0$ times.*

(1) O is bipartite iff $(t_a+1)\frac{n}{\gcd(a,n)}$ and $(t_b+1)\gcd(a,n) + (t_a+1)\gcd(b,n)$ are both even.

(2) If O is bipartite, then φ is part reversing iff $(t_a+1)r \not\equiv (t_b+1)s \pmod 2$.

Proof. (1) Let T be a cycle in the (n,a,b)-torus-grid that consists of $\gcd(a,n)$ edges along an $\frac{n}{\gcd(b,n)}$-cycle C_b followed by $\gcd(b,n)$ edges along an $\frac{n}{\gcd(a,n)}$-cycle C_a. Note that T is indeed a cycle since $C_a \cap C_b$ consists of $\frac{n}{\gcd(a,n)\gcd(b,n)}$ vertices that are evenly spaced along each of C_a and C_b. Moreover, T along with any of the horizontal $\frac{n}{\gcd(a,n)}$-cycles generate the first homology group of the torus. Now since every facial walk of O is of length $2(t_a+1) + 2(t_b+1)$ which is even, we get that O is bipartite iff the subdivided $\frac{n}{\gcd(a,n)}$-cycles and subdivided cycle T are both of even length. Thus O is bipartite iff $(t_a+1)\frac{n}{\gcd(a,n)}$ and $(t_b+1)\gcd(a,n) + (t_a+1)\gcd(b,n)$ are both even.

(2) Since O is connected and bipartite, φ is part reversing iff some $v\varphi(v)$-path in O has odd length. The path $\gamma_{r,s}$ of length $|r| + |s|$ in the (n,a,b)-torus-grid corresponds to a path of length $(t_a+1)|r| + (t_b+1)|s|$ in O which is odd iff $(t_a+1)r \not\equiv (t_b+1)s \pmod 2$. □

Of course not all (n,a,b)-torus-grids are bipartite, however those that are bipartite automatically have a part-reversing rotation because of transitivity. One infinite class of bipartite (n,a,b)-torus-grids (whose rotations are thus part reversing) consists of torus grids of the form (n,p,q) where p and q are distinct odd primes and $2pq|n$ (here, we take $t_a = t_b = 0$). Such an example is shown in Figure 6.1.

Case 2 Let G be a 3-regular orbit split of the (n,a,b)-torus-grid and $\psi_{\mathcal{GR}}$ the induced cellular automorphism. The quotient of the (n,a,b)-torus-grid modulo $\mathcal{GR}_{n,a,b,\mathbf{T}}$ in $\mathbf{T}$ is the bouquet of two loops, say ℓ_a and ℓ_b, in $\mathbf{T}$ with the loops in independent homology classes. Thus $G/\langle\psi_{\mathcal{GR}}\rangle$ in $\mathbf{T}/\langle\psi_{\mathcal{GR}}\rangle$ is the triple link with links ℓ_a, ℓ_b and e with facial walk $w = \ell_a, -\ell_b, e, -\ell_a, \ell_b, -e$ or $w = \ell_a, \ell_b, e, -\ell_a, -\ell_b, -e$ along the single face. These two possible facial walks correspond to two possibilities for G in $\mathbf{T}$, which are locally as shown in Figure 9.17. (The (n,a,b)-torus-grid is locally as shown on the left in the figure.)

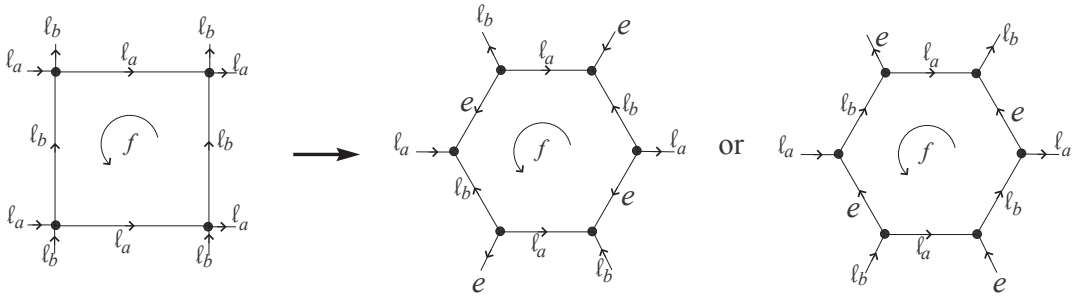

Figure 9.17.

Proposition 9.18. *Let O be an orbit subdivision of G where the e-, ℓ_a-, and ℓ_b-edges are subdivided t_e, t_a, and t_b times and let φ be the induced automorphism.*

(1) O is bipartite iff $(t_a+t_e)\frac{n}{\gcd(a,n)}$ and $(t_b+t_e)\gcd(a,n)+(t_a+t_e)\gcd(b,n)$ are both even.

(2) If O is bipartite, then φ is part reversing iff $(t_e+t_a)r \not\equiv (t_e+t_b)s \pmod 2$.

Proof. (1) Given the cycle T in the proof of Proposition 9.16, there is an analogous cycle, also call it T, in the hexagonal grid that consists of $\gcd(a,n)$ ℓ_b-edges, $\gcd(b,n)$ ℓ_a-edges, and either $\gcd(a,n)+\gcd(b,n)-2$ or $\gcd(a,n)+\gcd(b,n)$ e-edges (depending, respectively, on which possibility in Figure 9.17 is being used). Now since the length of any facial walk in O is $2[(t_e+1)+(t_a+1)+(t_b+1)]$ which is even, it follows that O is bipartite iff the subdivided cycle that is the lift of $\ell_a, -e$ in the quotient and the subdivided T-cycle are both of even length. That is, O is bipartite iff $[(t_a+1)+(t_e+1)]\frac{n}{\gcd(a,n)}$ and $(t_b+t_e)\gcd(a,n)+(t_a+t_e)\gcd(b,n)$ are both even.

(2) Consider the path $\gamma_{r,s}$ from v to $\mathcal{GR}_{n,a,b,\mathbf{T}}(v)$ in the (n,a,b)-torus-grid. Let e_v be the edge decontracted at v and consider $\mathbf{t}(e_v)$. Note that $\psi_{\mathcal{GR}}(\mathbf{t}(e_v)) = \mathbf{t}(\psi_{\mathcal{GR}}(e_v))$ where $\psi_{\mathcal{GR}}(e_v)$ is the edge decontracted at $\mathcal{GR}_{n,a,b,\mathbf{T}}(v)$. Since one of r and s must be positive and the other negative, the path $\gamma_{r,s}$ is either of the form $-\ell_b,\dots,-\ell_b,\ell_a,\dots,\ell_a$ or $\ell_b,\dots,\ell_b,-\ell_a,\dots,-\ell_a$ (where each has $|s|$ copies of ℓ_b and $|r|$ copies of ℓ_a). From Figure 9.17 we see that the path in G from $\mathbf{t}(e_v)$ to $\psi_{\mathcal{GR}}(\mathbf{t}(e_v))$ that projects down to $\gamma_{r,s}$ has one of the following four forms:

$$\begin{array}{l}\ell_b,-e,\dots,\ell_b,-\ell_a,e,\dots,-\ell_a\\ e,\ell_b,\dots,e,\ell_b,e,-\ell_a,\dots,e,-\ell_a\\ e,-\ell_b,\dots,e,-\ell_b,\ell_a,-e,\dots,\ell_a,-e\\ -\ell_b,-e,\dots,-\ell_b,-e,\ell_a,-e,\dots,\ell_a,-e\end{array}$$

Call this path γ'. In the first case, γ' has length $2(|r|+|s|)-2$ and in the remaining cases the length is $2(|r|+|s|)$. The subdivided path γ' in O corresponding to γ in G now has length either

$$[(t_e+1)+(t_a+1)]\,|r| + [(t_e+1)+(t_b+1)]|s| - 2(t_e+1) \quad \text{or}$$
$$[(t_e+1)+(t_a+1)]\,|r| + [(t_e+1)+(t_b+1)]|s|, \quad \text{respectively.}$$

Thus φ is part reversing iff $[(t_e+1)+(t_a+1)]|r| + [(t_e+1)+(t_b+1)]|s|$ is odd which is the case iff $(t_e+t_a)r \not\equiv (t_e+t_b)s \pmod 2$. □

To obtain an infinite class of examples for O in Proposition 9.18, choose n where $2pq \mid n$ for distinct odd primes p and q and choose $a=p$ and $b=q$. Note that $r \not\equiv s \pmod 2$ since p and q are odd and $rp+sq=1$. Letting $t_e=0$ we get that O is bipartite iff t_bp+t_aq is even iff $t_a \equiv t_b \pmod 2$. Then φ is part reversing iff t_a and t_b are both odd.

9.4.2 Pseudofree automorphisms

Construction 9.19 is a 7-step process that produces pseudofree part-reversing cellular automorphisms on bipartite quadrangulations. It takes as input a cellular automorphism φ of $G = G_0$ in S and at step i produces a graph G_i in S from G_{i-1} in S to which φ extends. In practice, the input cellular automorphism will be taken from a complete catalogue of irreducible and non-augmentable cellular automorphisms of S such as what we have determined for the sphere, projective plane, torus, Klein bottle, and Dyck's surface.

Construction 9.19. Take a graph G that is cellularly embedded in S along with a pseudofree cellular automorphism φ of G in S that has even order, has $\overline{G} = G$, and such that if x is an isolated pseudofixed point of odd index $2k+1$ then $\frac{|\varphi|}{(2k+1)} \in \{2, 4\}$.

1. First, let $G_1 = G$ or let G_1 be a φ-orbit split of G. Now if φ is free or there is a pseudofixed point of odd index, then go to Step 2. If there is a pseudofixed point and all pseudofixed points have even index, then either go to Step 2 or do the following.
   i. Let $H = G_1^*$.
   ii. Let G_5 be a φ-orbit split (possibly trivial) of H and skip to Step 6.
2. Let $\mathcal{P}_1, \ldots, \mathcal{P}_z$ be the orbits of the pseudofixed points of even index. For each $\mathcal{P}_i$ either do nothing or for each $x \in \mathcal{P}_i$ place a vertex star with x at the center and pendant vertices attached to the vertices of the facial walk around x in G_1 in such a way that these stars respect the action of φ on $\mathcal{P}_i$. Let G_2 be the graph obtained by this step.
3. There is a set of edges D (possibly empty) in G_2 that is edge disjoint from the stars added in Step 2 and such that the induced embedding of $G_2 \backslash \mathsf{orbit}_\varphi(D)$ in S is a surface orbit minor. Choose a maximal such set D and let $G_3 = G_2 \backslash \mathsf{orbit}_\varphi(D)$.
4. If there are vertices of degree 2 in G_3 whose incident edges are both from stars added in Step 2, then smooth out these vertices. If not, then do nothing. Let G_4 be the graph obtained from this step.
5. For any face of G_4 whose boundary consists of two distinct edges and that has an odd-index isolated pseudofixed point inside, replace the two edges of the face by a single edge through the pseudofixed point. If no such face exists, then do nothing. Let G_5 be the graph obtained by this step.
6. Let G_6 be a φ-orbit subdivision of G_5 such that G_6 is bipartite and φ is part reversing on G_6. If G_5 is already bipartite with φ part reversing, then we may let $G_6 = G_5$.
7. Let $\mathcal{F}_1, \ldots, \mathcal{F}_y$ be the orbits of the faces of G_6 in S under φ. For each $\mathcal{F}_i$ choose a quadrangulated patch of the appropriate length; if there are pseudofixed points in the centers of the faces of $\mathcal{F}_i$ then choose the quadrangulated patch with an appropriate type of symmetry as given in Proposition 9.3. Paste copies of the quadrangulated patch into the faces of $\mathcal{F}_i$ in a way that respects φ.

Each step in Construction 9.19 can always be carried out given the initial assumptions except maybe for Steps 6 and/or 7. We will not address the question of when these steps are executable, but we do present Theorem 9.20 which tells us that Construction 9.19 along with a complete catalogue of the irreducible and non-augmentable pseudofree cellular automorphisms of S are enough to construct all pseudofree part-reversing cellular automorphisms on bipartite quadrangulations in S.

Theorem 9.20. *If φ is a pseudofree part-reversing cellular automorphism of a bipartite quadrangulation Q in S, then φ is obtainable by Construction 9.19 from an irreducible and non-augmentable cellular automorphism of G in S.*

Lemma 9.21. *Let φ be a pseudofree cellular automorphism of G in S such that no isolated point of $\overline{fix}(\varphi)$ is in the center of an edge of G, and let π be the projection $S \to S/\langle\varphi\rangle$. Then*

(1) $\pi(G)$ is a graph that is cellularly embedded in $\pi(S)$ with at most one branch point in the interior of each face and

(2) For each edge e in $\pi(G)$, the induced embedding of $\pi(G)\backslash e$ in $\pi(S)$ is cellular with at most one branch point in each face iff $G\backslash\pi^{-1}(e)$ is a surface orbit minor of G.

Proof. These both readily follow from definitions. □

Lemma 9.22. *Let φ be a pseudofree cellular automorphism of G in S such that no isolated point of $\overline{fix}(\varphi)$ is in the center of an edge of G. If G has no vertex of degree 1 and no pseudofixed vertex of degree $|\varphi|/m$ where m is the index, then G is deletion minimal with respect to φ iff either every face of G in S contains a pseudofixed point or no face of G in S contains a pseudofixed point and φ acts transitively on the faces of G in S.*

Proof. Let π be the projection from S to $S/\langle\varphi\rangle$. Note that the two conditions on degrees imply that $\pi(G)$ has no vertices of degree 1.
($\Leftarrow$) Suppose that every face of G in S contains a pseudofixed point or φ acts transitively on the faces of G in S.

In the first case, the cellular embedding of the graph $\pi(G)$ in the closed surface $\pi(S)$ has a branch point in every face. If $e \in \pi(G)$ bounds two distinct faces, then $\pi^{-1}(e)$ cannot be deleted from G because $\pi(G)\backslash e$ will have a face with more than one branch point in its interior, contradicting Lemma 9.21. If e is on the same face twice, then either the induced embedding of $\pi(G)\backslash e$ will be non-cellular or one endpoint of some edge has degree 1 (which contradicts our assumptions). In the second case, the cellular embedding of $\pi(G)$ in $\pi(S)$ has a single face. Now any edge e of $\pi(G)$ appears twice in the boundary walk of this face. The removal of e will result in a non-cellular embedding unless some edge has one endpoint of degree 1 in $\pi(G)$.
($\Rightarrow$) Suppose that G is deletion minimal with respect to φ. If there are face(s) of G in S with, and faces without, pseudofixed points in their interiors, then $\pi(G)$ in $\pi(S)$ has face(s) with, and faces without, branch points in their interiors. Thus there is an edge e in $\pi(G)$ bounding two distinct faces, one with a branch point and one without, and so the removal of e from $\pi(G)$ leaves a cellular embedding in $\pi(S)$ with at most one branch point in each face. Deleting $\pi^{-1}(e)$ from G in S now gives a surface orbit deletion. We see that either every face of G contains a pseudofixed point or no face of G contains a pseudofixed point. In the former case we are done. In the latter case, if $\pi(G)$ has more than a single face, then there is an edge e in $\pi(G)$ bounding two distinct faces without branch points and so $G\backslash\pi^{-1}(e)$ is a surface orbit deletion. Thus $\pi(G)$ has one face and so φ is transitive on the faces of G in S. □

Lemma 9.23. *Let φ be a pseudofree cellular automorphism of G in S such that no isolated point of $\overline{fix}(\varphi)$ is in the center of an edge of G and such that G is deletion minimal with respect to φ.*

(1) If G has a vertex v of degree 1, then G has exactly $|\varphi|$ edges and S is the sphere.

(2) If G has a pseudofixed vertex v of degree $|\varphi|/m$ where m is the index of v, then G has a pseudofixed point in the interior of each face or G has exactly $|\varphi|$ edges.

Furthermore, in both parts, either each face of G in S has a pseudofixed point or φ acts transitively on the faces of G in S.

Proof. Let π be the projection $S \to S/\langle\varphi\rangle$. Note that in each part of the Lemma $\pi(v)$ has degree 1 in $\pi(G)$ and so $\pi(G)\backslash\pi(v)$ is cellularly embedded in $\pi(S)$ unless $\pi(G)$ is a single link in the sphere. In this case the embedding of $\pi(G)$ in $\pi(S)$ has a single face and so φ acts transitively on the faces of G in S.

(1) Since G is deletion minimal, Lemma 9.21 implies that $\pi(G)$ is a single link. Thus cellularity implies that $\pi(S)$ is the sphere. Since the degree-1 endpoint $\pi(v)$ of $\pi(G)$ cannot be a branch point, G is a star. Cellularity of G in S now implies that S is the sphere.

(2) Assume that G has more than $|\varphi|$ edges, so that $\pi(G)$ has more than one edge. Because $\pi(v)$ has degree 1, $\pi(G)\backslash\pi(v)$ in $\pi(S)$ is cellular with a branch point in the face f where $\pi(v)$ had been. Lemma 9.21 now implies that f contains more than one branch point, so the face of $\pi(G)$ whose boundary contains $\pi(v)$ has a branch point. If there would also be a face of $\pi(G)$ in $\pi(S)$ without a branch point, then there would also be an edge e bordering two faces, one with a branch point and one without. By Lemma 9.21, $G\backslash\pi^{-1}(e)$ in S is a surface orbit minor, contradicting deletion minimality. □

Lemma 9.24. *Let φ be a pseudofree cellular automorphism of G in S such that no isolated point of $\overline{fix}(\varphi)$ is in the center of an edge of G. If G is deletion minimal with respect to φ and H is a φ-orbit subdivision of G, then H is deletion minimal with respect to φ unless G has $|\varphi|$ edges and S is the sphere.*

Proof. Let π be the projection $S \to S/\langle\varphi\rangle$ and note that $\pi(H)$ is a subdivision of $\pi(G)$. Assume that G is deletion minimal and H is not. Since G is deletion minimal, Lemma 9.21 implies that there is no edge e in $\pi(G)$ for which $\pi(G)\backslash e$ in $\pi(S)$ is both cellular and has at most one branch point in each face. As such if e is an edge of $\pi(H)$ for which $\pi(H)\backslash e$ in $\pi(S)$ is both cellular and has at most one branch point in each face, then e is an edge that arose from subdivision. Let $\hat{e}$ be the edge of $\pi(G)$ that was subdivided to form the branch[2] in $\pi(H)$ containing e. Now one of the endpoints, call it v, of e in $\pi(H)$ has degree 1 in $\pi(H)\backslash e$ and, by assumption, is not a branch point of π. Thus all vertices in $\pi^{-1}(v)$ have degree 1 in $H\backslash\pi^{-1}(e)$. Now as in the proof of Lemma 9.23(1) we can delete $\pi^{-1}(v)$ from $H\backslash\pi^{-1}(e)$ unless $H\backslash\pi^{-1}(e)$ is a star of $|\varphi|$ edges in the sphere. This deletion will again leave another vertex of degree 1 that can be deleted until all of $\pi^{-1}(\hat{e})$ is deleted from G, a contradiction, or until we obtain a star in the sphere. □

Proof of Theorem 9.20. There is some $D \subset E(Q)$ (possibly empty) such that $Q\backslash\mathsf{orbit}_\varphi(D)$ in S is a surface orbit minor. Choose a maximal such D and let $Q_1 = Q\backslash\mathsf{orbit}_\varphi(D)$. So now if f is a face of Q_1 in S with a facial boundary walk of length n, then n must be even as Q is bipartite and furthermore the edges of $\mathsf{orbit}_\varphi(D)$ in the interior of f along with a cycle of length n form a quadrangulated patch of length n. These patches obtained from Q_1 relative to Q must of course respect the action of φ and so going from Q to Q_1 is a reversal of Step 7.

There is some $B \subset E(Q_1)$ (possibly empty) such that $\mathsf{orbit}_\varphi(B)$ is acyclic and Q_1 is an orbit subdivision of $Q_1/\mathsf{orbit}_\varphi(B)$. Choose a maximal such B and let $Q_2 = Q_1/\mathsf{orbit}_\varphi(B)$. Going from Q_1 to Q_2 is a reversal of Step 6 of the construction. Notice that Q_2 in S is deletion minimal with respect to φ because Q_1 is deletion minimal by definition. Also, note that if v is a pseudofixed vertex of Q_2 then v comes from a pseudofixed vertex of Q_1. We further claim that Q_2 has no non-pseudofixed vertices of degree 2 unless both Q_1 and Q_2 are cycles. If Q_1 is not a cycle, then since Q_1 is connected it is not a disjoint collection of cycles and so has vertices of degree other than 2. These are called the *branch* vertices of Q_1. Now Q_1 decomposes into branch vertices and branches between them. Thus B is necessarily a collection of subpaths consisting of all but one edge from each branch of Q_1 that does not contain a pseudofixed vertex at its center, along with subpaths consisting of all but two edges from each branch that does contain a pseudofixed vertex at its center. In this case Q_2 has no non-pseudofixed vertices of degree 2. So now we split the remainder of the proof into three cases. In Case 1 say that Q_2 has no vertices of degree 2 and φ is either free or has a pseudofixed point not at a vertex, in Case 2 say that Q_2 (and so also Q_1) is a cycle, and in Case 3 say that all pseudofixed points are at vertices of Q_2.

Case 1 There can be no pseudofixed points of even index in the centers of edges since φ is part-reversing on Q_1. If there are pseudofixed points of odd index in the centers of edges of Q_2, then double these edges and leave the pseudofixed points inside the resulting faces of length 2. Let Q_3 be the resulting graph, and so going from Q_2 to Q_3 is a reversal of Step 5 of the construction. Note that Q_3 is still deletion minimal with respect to φ because any such pair of double edges is in a single orbit.

If there are edges in Q_3 whose endpoint(s) are both pseudofixed, then subdivide these edges. Let Q_4 be the graph obtained. Going from Q_3 to Q_4 is a reversal of Step 4 of the construction. From Lemma 9.24 either Q_4 is still deletion minimal or Q_3 consists of $|\varphi|$ edges in the sphere. However, by the argument in the next paragraph, the latter situation does not occur.

Suppose that Q_3 consists of $|\varphi|$ edges in the sphere. Since there are no pseudofixed points of φ on the edges of Q_3, all of the $|\varphi|$ edges of Q_3 are in the same φ-orbit. By Proposition 9.3, the pseudofixed vertices of φ on Q_3 have even index and so Theorem 4.1 implies that φ on $\overline{Q}_3$ reduces to $(\mathcal{R}\mathcal{R}_{2n,\mathbf{S}})^i$ for $2n = |\varphi| \geq 4$ and i relatively prime to $2n$. Thus all pseudofixed points are at vertices of Q_3, a contradiction to being in Case 1.

[2]Given a subdivision S of G, a *branch* of S is a path that corresponds to a single edge in G.

Since Q_4 is deletion minimal with respect to φ and since no pseudofixed point of φ is on the center of an edge of Q_4, Lemmas 9.22 and 9.23 together imply that either Q_4 in S has a pseudofixed point inside each face or φ acts transitively on the faces of Q_4 in S. The latter situation implies that φ is free because in Case 1 we assume that not all of the pseudofixed points are at vertices of Q_4.

If φ is free, then let $Q_5 = Q_4$; this is a reversal of Step 3. If φ is not free, then the only pseudofixed points of φ that are not in the centers of faces of Q_4 in S are at vertices of Q_4 and (by the construction of Q_4 from Q_3) the vertex stars of these pseudofixed vertices do not share edges in common nor do they contain loops. As such, for any facial boundary walk of Q_4 in S, there are no two pseudofixed vertices in successive order along the walk. Now for each face f and each incidence p with a pseudofixed vertex on the boundary of f, place an edge connecting the vertices before and after p as shown in Figure 9.25. Let Q_5 be the graph obtained. Going from Q_4 to Q_5 is a reversal of Step 3 because Q_4 is deletion minimal.

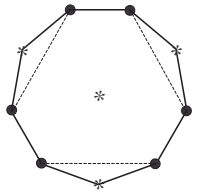

Figure 9.25.

Let W be the set of vertices in Q_5 to which the new edges are attached. Note that the degree of a vertex in W goes up by two for each link it has incident to a pseudofixed vertex. In particular any vertex of W that had degree 2 in Q_4 arose in going from Q_3 to Q_4 and so has degree 6 in Q_5.

If φ is free, then let $Q_6 = Q_5$; this is a reversal of Step 2. If φ is not pseudofree, then each face of Q_5 in S either contains a pseudofixed point and is not incident to any pseudofixed vertex or does not contain a pseudofixed point and is incident to exactly one pseudofixed vertex. Now delete the pseudofixed vertices and their incident links to obtain a graph Q_6 with a pseudofixed point in the center of each face. Going from Q_5 to Q_6 is a reversal of Step 2. Now Q_6 is deletion minimal with respect to φ by Lemma 9.22 as long as Q_6 has no vertices of degree 1. If v is a vertex of degree 1 in Q_6, then $v \notin W$ because the vertices in W have degree in Q_6 strictly larger than their degree in Q_4 which was at least 2. Thus v has degree 1 in Q_4 as well. Since Q_4 is deletion minimal, Lemma 9.23 implies that Q_4 is a vertex star in the sphere. But this has a pseudofixed vertex of index 1, which is a contradiction of Proposition 9.3.

Now we claim that Q_6 has no vertices of degree 2. As above, the vertices of W cannot have degree 2 in Q_6. The other vertices of Q_6 have the same degree that they had in Q_4; these vertices in Q_4 did not have degree 2 because non-pseudofixed degree-2 vertices were smoothed out when going from Q_1 to Q_2, and Q_2 was assumed to have no non-pseudofixed vertices of degree 2 in this case. So then Q_6 is an orbit split of some Q_7 that is irreducible and not augmentable.

Case 2 We may assume that some pseudofixed point of φ is not located at a vertex of Q_2, because otherwise we could refer to Case 3. The action of φ on Q_2 is either rotation or reflection. In the former case, there are no pseudofixed points on Q_2 and so φ is irreducible and not augmentable. Reversing Step 5 to Step 1 involves doing nothing.

In the latter case, there are exactly two pseudofixed points on Q_2. Note that by cellularity S must be the sphere or projective plane. If S is the projective plane, then the fact that pseudofree cellular automorphisms of the projective plane have exactly one pseudofixed point (see Theorem 5.1) would yield a contradiction. Suppose then that S is the sphere. By Theorem 4.1 the two pseudofixed points on are the only pseudofixed points of φ and they have index either 1 or 2. If both points are at centers of edges, then Q_2 has length 2. If one point is at a vertex and the other is in the center of an edge, then Q_2 is a loop.

If Q_2 has both pseudofixed points in the centers of links, then by Proposition 9.3 the index of these pseudofixed points is 1 and so Q_2 in S is not deletion minimal, a contradiction.

If Q_2 is a loop, then φ fixes the vertex of Q_2. This is a contradiction, since φ is part-reversing on Q_1.

Case 3 We may assume that φ has a pseudofixed point, since otherwise we could refer to Case 1. By Proposition 9.3 all pseudofixed points have even index.

We will now show that we can reverse the duality option in Step 1, and thus we need not consider reversals of Steps 2 – 5. There is some set C of edges such that $Q_2/\mathsf{orbit}_\varphi(C)$ in S is a surface orbit minor. Choose C to be a maximal such set, possibly empty, and let $Q_2' = Q_2/\mathsf{orbit}_\varphi(C)$. Note that Q_2' is irreducible with respect to φ because Q_2 is deletion minimal. Going from Q_2 to Q_2' is a reversal of Step 1.ii.

We claim that all vertices of Q_2' are pseudofixed. If not, there is an edge e connecting some pseudofixed vertex x with some non-pseudofixed vertex y. Let $\pi\colon S \to S/\langle\varphi\rangle$; the embedding of $\pi(Q_2')$ in $\pi(S)$ is cellular with $\pi(x) \neq \pi(y)$. Contracting $\pi(e)$ in the quotient leaves a cellular embedding and does not bring two branch points together. Also, we get that $\mathsf{orbit}_\varphi(e)$ is acyclic because the facts that $\mathsf{orbit}_\varphi(x) \cap \mathsf{orbit}_\varphi(y) = \emptyset$, $|\mathsf{orbit}_\varphi(x)| = |\varphi|/m$ where m is the index of x, $|\mathsf{orbit}_\varphi(y)| = |\varphi|$, and $|\mathsf{orbit}_\varphi(e)| = |\varphi|$ together imply that $\mathsf{orbit}_\varphi(e)$ is a vertex-disjoint union of stars. Thus we can contract $\mathsf{orbit}_\varphi(e)$ in Q_2, contradicting the maximality of C.

Now let $Q_3 = (Q_2')^*$; going from Q_2' to Q_3 is a reversal of Step 1.i. Since each vertex of Q_2' is pseudofixed, each face of Q_3 in S contains a pseudofixed point. Thus Q_3 is deletion minimal with respect to φ by Lemma 9.22 as long as Q_3 has no vertices of degree 1. If Q_3 has a vertex of degree 1, then Q_2' has a contractible loop, which would contradict the irreducibility of Q_2'. Now Q_3 is φ-orbit split of some irreducible and non-augmentable Q_4, as required, as long as Q_3 has no vertices of degree 2. However, a degree-2 vertex of Q_3 would come from a length-2 contractible face of Q_2' in S, which again would contradict the irreducibility of Q_2'. □

Example 1 Let us determine all of the possible results of Construction 9.19 starting with the pseudofree cellular automorphism $\mathcal{RR}_{2n,\mathbf{S}}$. Since there are two pseudofixed points of index 2 each, we may choose the duality option in Step 1. There is no first splitting possible in Step 1. After dualizing, however, we may split in Step 1.ii as shown in Figure 9.26. (The resulting graph is the alternating double wheel of length $2n$.)

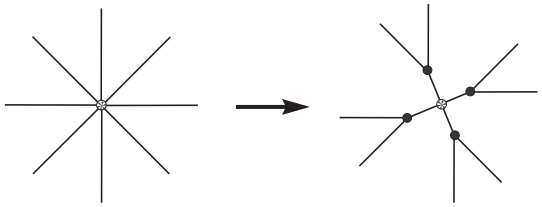

Figure 9.26.

In Step 6, if the above orbit split was not done, then each edge must be subdivided an even number of times so that φ is part-reversing; the bipartite property is automatic. If the above orbit split was done, then each of the old edges must be split an even number of times so that that φ is part-reversing but each of the new edges may be split any number of times. The bipartite property is again automatic. Patching now occurs in Step 7.

If the duality option is not chosen in Step 1, then again no splitting is possible in Step 1. We need not consider Steps 2 – 5 because the only possible results of these steps may be achieved using the duality option in Step 1. In Step 6 each edge must be subdivided an even number of times so that φ is part-reversing; the bipartite property is automatic. Patching can now occurs in Step 7 by the results in Sections 9.3.3 and 9.3.1.

Example 2 Let us determine all of the possible results of Construction 9.19 starting with the pseudofree cellular automorphism $\mathcal{P}_{4,2:1,2:2,\mathbf{T}}$ (see Figure 6.5). First, the possible results from Step 1 are shown in Figure 9.27 (the duality option is not available).

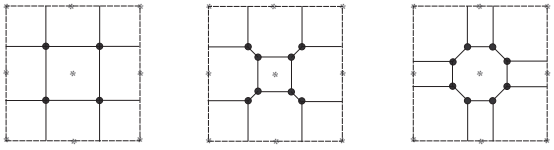

Figure 9.27.

If we are to add any stars to pseudofixed points of even index in Step 2, then the possible results are shown in Figure 9.28.

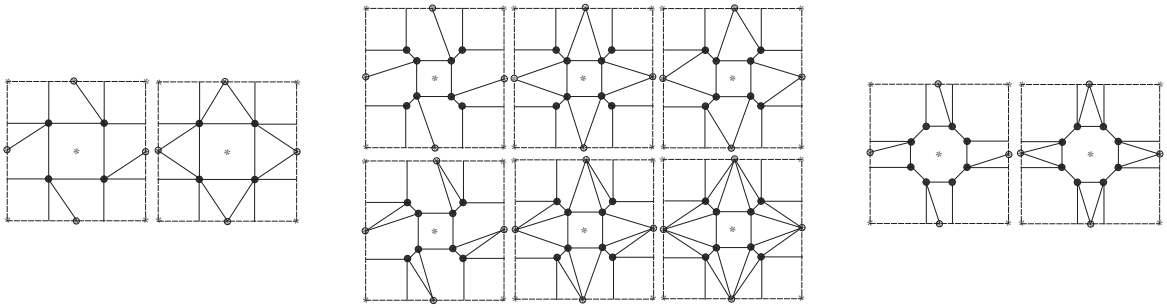

Figure 9.28.

All possible results of Steps 3 and 4 on the graphs in Figure 9.28 are shown in Figure 9.29 up to deletion of vertices of degree 1, deletion of an edge from pairs of double edges not enclosing a pseudofixed point, and subdivisions. We need not consider any of these three possibilities because these deletions and smoothings of subdivisions can be reversed in subsequent steps of the construction.

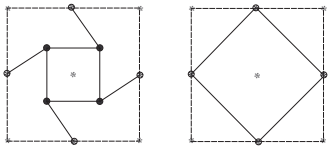

Figure 9.29.

So now at the completion of Step 5, we are left with one of the five embeddings from Figures 9.27 and 9.29. All of these embeddings are already bipartite and φ is part reversing on them save for the rightmost embedding in Figure 9.27. We will now describe all possible results for Step 6. In each case, patching can occur in Step 7 by the results in Sections 9.3.1, 9.3.2, and 9.3.3.

The leftmost embedding in Figure 9.27 has two separate orbits of edges. For each orbit the edges are subdivided an even number of times. The middle embedding in Figure 9.27 has three separate orbits of edges. The edges along the square faces must be subdivided an even number of times and the spoke edges can be subdivided any number of times. The rightmost embedding in Figure 9.27 has three separate orbits of edges: the diagonal edges, the vertical and horizontal edges on the inner octagon, and the vertical and horizontal edges on the outer octagon. Subdivide edges in these orbits a, b, and c times, respectively; we need $a+b$ to be odd and $2a+b+c \equiv b+c \mod 2$ to be even. (These conditions on a, b, c also imply that $a+c$ is odd.)

The first embedding in Figure 9.29 has two separate orbits of edges. The orbit of edges on the central square must be subdivided an odd number of times and the edges in the other orbit can be subdivided any number of times. The second embedding in Figure 9.29 has just one orbit of edges and these must be subdivided an even number of times.

9.4.3 Non-pseudofree automorphisms

Our procedure for constructing non-pseudofree part-reversing cellular automorphisms on bipartite quadrangulations requires the following rather technical proposition about orbit deletions. When φ is a non-pseudofree cellular automorphism of G in S, we denote the augmentation of G along the ovals (but not at the isolated pseudofixed points) by $\widetilde{G}$; call this the *oval augmentation* of G.

Proposition 9.30. *Let φ be a non-pseudofree, part-reversing cellular automorphism on a bipartite quadrangulation Q in S. Properly 2-color the vertices of Q with blue and green. Let $R = \widetilde{Q} \backslash \mathsf{orbit}_\varphi(D)$ be a surface orbit deletion in which none of the edges of $\mathsf{orbit}_\varphi(D)$ are edges of oval cycles of $\widetilde{Q}$ (include the case that $D = \emptyset$).*

(1) If $|\varphi|/2$ is odd, then color the oval edges red and the remaining edges black. The following holds for R in S.

i. All facial boundary walks are ladder patchable.

ii. All oval-cycles with Möbius neighborhoods have odd length.

iii. All oval-cycles with annular neighborhoods have even length.

iv. $\varphi|_R$ exchanges blue and green vertices.

*(2) If $|\varphi|/2$ is even, we have the following for R in S. Call the edges of the oval-cycles that are interior to the diamonds of the necklaces in Q "*diamond chords*."*

i. The length of any closed walk w in R and the number of appearances of diamond chords on w are equivalent mod 2.

ii. $\varphi|_R$ exchanges blue and green vertices.

Proof. (1) By Proposition 9.4, the neighborhood of any oval in Q is a ladder. As such, the facial boundary walks of $\tilde{Q}$ in S are all of length 4. Thus the facial boundary walks of R are all of even length and are ladder patchable. The lengths of the oval cycles follow from Proposition 9.4 and the color-exchange property comes from the fact that φ is part-reversing on Q.

(2) By Proposition 9.4, the neighborhood of any oval in Q is a necklace. If w is a closed walk in $\widetilde{Q}$, then any appearance of a diamond chord in w may be replaced by two of the edges of that diamond to obtain a corresponding closed walk w_0 in Q. Since Q is bipartite, the length of w_0 is even and so the parity of the length of w is equal to the parity of the number of appearances of diamond chords on w. The color-exchange property comes from the fact that φ is part-reversing on Q. □

Construction 9.32 is an 8-step process that produces non-pseudofree part-reversing cellular automorphisms on bipartite quadrangulations. It takes as input a non-pseudofree cellular automorphism φ of $G = G_0$ in S and at step i produces an embedding G_i in S from G_{i-1} in S to which φ extends. In practice, the input cellular automorphism will be taken from a complete catalogue of oval-irreducible and non-augmentable cellular automorphisms of S such as what we have determined for the sphere, projective plane, torus, Klein bottle, and Dyck's surface.

Two special φ-orbit splits that we will utilize are the following. Given φ on G in S, a φ-orbit split of G *away from the ovals of* φ is a φ-orbit split in which none of the new edges are oval edges and all of the old oval edges are still oval edges. The left-hand side of Figure 9.31 shows a split away from an oval vertex. The right-hand side of the figure shows an *oval thickening*. This is obtained by replacing each oval edge of G by a face of length two and then splitting transversely across the oval as shown.

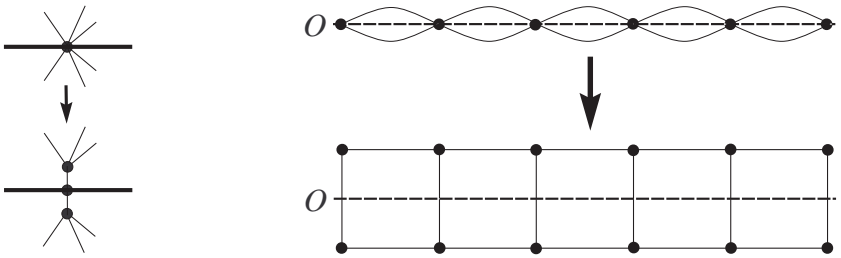

Figure 9.31.

Construction 9.32. Take a graph G that is cellularly embedded in S along with a non-pseudofree cellular automorphism φ of G in S that has $\overline{G} = G$ and whose isolated pseudofixed points satisfy the conditions for Construction 9.19.

1. Let G_1 be a φ-orbit split of G such that $\overline{G}_1 = G_1$ or let $G_1 = G$. If there are no isolated pseudofixed points or there is an isolated pseudofixed point of odd index, then skip to Step 2. If there is an isolated pseudofixed point and all isolated pseudofixed points have even index, then either skip to Step 2 or do the following:
   i. Let H_1 be the oval thickening of G_1.
   ii. Let T be a collection of edges of H_1 (possibly empty) which are transverse to the ovals such that $H_2 = H_1 \backslash \mathsf{orbit}_\varphi(T)$ in S is a surface orbit minor of H_1 in S and such that H_2 has minimum degree 3.

iii. Let $H_3 = H_2^*$. (Note that $\widetilde{H_2^*} = H_2^*$.)

iv. Let G_6 be a φ-orbit split away from the ovals of H_3. If $|\varphi|/2$ is odd, then the φ-orbit split must be such that all oval vertices have degree 4. Now skip to Step 7.

2. Let $\mathcal{P}_1, \ldots, \mathcal{P}_z$ be the orbits of the isolated pseudofixed points of even index. For each $\mathcal{P}_i$ either do nothing or for each $x \in \mathcal{P}_i$ place a vertex star with x at the center and with its pendant vertices attached to the vertices of the facial walk around x in G_1 in such a way that these stars respect the rotational action of φ around x. Let G_2 be the graph obtained by this step.

3. There is a set of edges D (possibly empty) in G_2 that is edge disjoint from the oval-cycles and stars added in Step 2 and such that the induced embedding of $G_2 \backslash \mathsf{orbit}_\varphi(D)$ in S is a surface orbit minor. Choose a maximal such set D and let $G_3 = G_2 \backslash \mathsf{orbit}_\varphi(D)$.

4. If there are vertices of degree 2 in G_3 whose incident edges are both from stars added in Step 2, then smooth out these vertices. If not, then do nothing. Let G_4 be the graph obtained from this step.

5. For any face of G_4 whose boundary consists of two distinct edges that are not on oval cycles and that has an odd-index isolated pseudofixed point inside, replace the two edges of the face by a single edge through the pseudofixed point. If no such faces exist, then do nothing. Let G_5 be the graph obtained by this step.

6. If $|\varphi|/2$ is even, then let $G_6 = G_5$. If $|\varphi|/2$ is odd, the vertices of G_5 on its oval-cycles that have degree greater than 4 must be split so that the edges of oval-cycles remain in the ovals and the vertices along the new oval-cycles have degree 2 or 4. Let G_6 be the graph obtained.

7. - If $|\varphi|/2$ is odd, then color the edges of the oval-cycles of G_6 red and the remaining edges of G_6 black. Let G_7 be a φ-orbit subdivision of G_6 such that: all facial boundary walks of G_7 have even length; facial boundary walks containing oval edges have all maximal black paths of length at least two; all oval-cycles of G_7 with Möbius neighborhoods have odd length; all oval-cycles of G_7 with annular neighborhoods have even length; and the vertices of G_7 that are not on the oval cycles may be 2-colored blue and green so that no two vertices of the same color are adjacent and so that φ exchanges the colors.
   - If $|\varphi|/2$ is even, then let G_7 be a φ-orbit subdivision of G_6 along with a designation of some (or none) of the edges on the oval-cycles as diamond chords such that: the assignment of diamond chords respects the action of φ; the length of any closed walk w and the number of appearances of diamond chords along w are equivalent mod 2; and the vertices of G_7 may be 2-colored blue and green so that adjacent vertices along diamond chords have the same color, adjacent vertices along non-diamond-chord edges have different colors, and φ exchanges the colors.

8. Let $\mathcal{F}_1, \ldots, \mathcal{F}_y$ be the orbits of the faces of G_7.
   - If $|\varphi|/2$ is odd, then for each $\mathcal{F}_i$ the colored facial boundary walks of $\mathcal{F}_i$ correspond to ladder patchable cycles C by Proposition 9.13. Choose an appropriate ladder patch and paste copies of it into the faces of $\mathcal{F}_i$ in a manner respecting the action of φ. Delete the edges of the oval cycles and smooth out the resulting vertices of degree 2.
   - If $|\varphi|/2$ is even, then for each $\mathcal{F}_i$ let ℓ be the length of the faces in $\mathcal{F}_i$ plus the number of appearances of diamond chords along such a facial boundary walk. (Note that ℓ must be even.) Choose a quadrangulated patch whose length is ℓ. If there are pseudofixed points in the centers of the faces of $\mathcal{F}_i$ then choose the patch to have an appropriate type of symmetry as given in Proposition 9.3. Paste copies of the quadrangulated patch into the faces of $\mathcal{F}_i$ in a way that respects φ and so that diamond chords are covered by paths of length 2. Now delete the diamond chords.

Each step in Construction 9.32 can always be carried out given the initial assumptions except maybe for Steps 7 and/or 8. We will not address the question of when these steps are executable, but we do present Theorem 9.33 which tells us that Construction 9.32 along with a complete catalogue of the oval-irreducible and non-augmentable cellular automorphisms of S will be enough to construct all non-pseudofree part-reversing cellular automorphisms on bipartite quadrangulations.

In Step 8 we need not account for patches with reflectional symmetry because of the following argument. Any oval-cycle intersecting a face $f \in \mathcal{F}_i$ does so along its boundary because the ovals are covered by cycles. So then the existence of any reflectional symmetry caused by an oval edge appearing twice along the boundary walk of $f \in \mathcal{F}_i$ implies that there is an isolated pseudofixed point of index m dividing $|\varphi|/2$ at the center of f. Thus rotational symmetry around this isolated point will account for any such reflectional symmetry.

A somewhat awkward aspect of Construction 9.32 is Step 6. This step is *a priori* necessary because of degree constraints on vertices in oval cycles given by Proposition 9.4; however, in the proof of Theorem 9.33 it is not necessary to reverse this step. As such, it should be possible to modify the construction in a way that omits this step. It seems that such a change, however, would make the construction more complicated.

Theorem 9.33. *If φ is a non-pseudofree part-reversing cellular automorphism of a bipartite quadrangulation Q in S, then φ is obtainable by Construction 9.32 from an oval-irreducible cellular automorphism on G in S that is not augmentable.*

Proof. Properly 2-color the vertices of Q with blue and green. Color the edges of the oval cycles of $\widetilde{Q}$ red and the remaining edges of $\widetilde{Q}$ black. If $|\varphi|/2$ is even, then designate the edges of $\widetilde{Q}$ inside the diamonds of the necklaces as diamond chords.

There is some set of black edges $D \subset E(\widetilde{Q})$ (possibly empty) such that $\widetilde{Q}\backslash\mathsf{orbit}_\varphi(D)$ in S is a surface orbit minor. Choose a maximal such D and let $Q_0 = \widetilde{Q}\backslash\mathsf{orbit}_\varphi(D)$. We now have that Q_0 satisfies Proposition 9.30. Let f be a face of Q_0 in S of length ℓ. In the case that $|\varphi|/2$ is even, the parity of ℓ is the same as the parity of the number, say $\hat{\ell}$, of diamond chords appearing along the boundary walk of f. Proposition 9.4 now implies that the edges of $\mathsf{orbit}_\varphi(D)$ in the interior of f taken with an additional cycle of length $\ell+\hat{\ell}$ (not necessarily in $\widetilde{Q}$ because the boundary walk of f may not be a cycle in $\widetilde{Q}$) form a quadrangulated patch of length $\ell+\hat{\ell}$ perhaps with rotational symmetry around some central isolated pseudofixed point. In this case, going from Q to Q_0 is a reversal of Step 8. In the case that $|\varphi|/2$ is odd, Proposition 9.4 implies that the edges of $\mathsf{orbit}_\varphi(D)$ in the interior of f taken along with an additional cycle of length ℓ (with appropriate colors) form a ladder patch perhaps with rotational symmetry around some central isolated pseudofixed point. In this case as well, going from Q to Q_0 is a reversal of Step 8. By the maximality of D, there are no black edges in Q_0 in S whose orbits may be deleted. We thus say that Q_0 in S is black-deletion minimal with respect to φ.

There is some set of edges $B \subset E(Q_0)$ (possibly empty) such that $\mathsf{orbit}_\varphi(B)$ is acyclic and Q_0 is an orbit subdivision of $Q_0/\mathsf{orbit}_\varphi(B)$. Choose a maximal such B and let $Q_1 = Q_0/\mathsf{orbit}_\varphi(B)$; going from Q_0 to Q_1 is a reversal of Step 7 of the construction because Q_0 satisfies Proposition 9.30. By construction, Q_1 in S is still black-deletion minimal with respect to φ because Q_0 is. As in the proof of Theorem 9.20 we also get that either Q_1 has no vertices of degree 2 except possibly isolated pseudofixed vertices of degree 2 or Q_0 and Q_1 are both cycles. In Case 1 say that φ has no isolated pseudofixed points or has an isolated pseudofixed point not at a vertex of Q_1. In Case 2 say that φ has an isolated pseudofixed point and all isolated pseudofixed points are at vertices of Q_1. Additionally in Cases 1 and 2 say that Q_1 is not a cycle. In Case 3 say that Q_0 and Q_1 are both cycles.

Case 1 To reverse Step 6, we need not do anything. Since φ is part reversing on Q, no isolated pseudofixed point in the center of an edge of Q_1 has even index. If there are such isolated pseudofixed points of odd index, then each such edge is black and we can replace each with two black edges forming a digon around the pseudofixed point. Let Q_2 be the graph obtained. Going from Q_1 to Q_2 is a reversal of Step 5 of the construction. Note that Q_2 is still black-deletion minimal with respect to φ because the doubled edges are in the same orbits under φ.

If there are black edges in Q_2 whose endpoint(s) are both isolated pseudofixed points of even index, then subdivide these edges. Let Q_3 be the graph obtained. Going from Q_2 to Q_3 is a reversal of Step 4 of the construction.

Claim 1. *Q_3 is black-deletion minimal.*

Proof of Claim: Note that Q_3 is connected and is assumed to not be a cycle and so must have black edges. Thus Q_3 has at least two orbits of edges, one of each color. As such Q_3 has at least $2|\varphi|$ edges because ovals do not intersect edges transversely and there are no isolated pseudofixed points in the centers of edges. Now the details of the proof of Lemma 9.24 actually focus on individual non-deletable edges and so we can apply the same reasoning here to the black edges of Q_3 to get that Q_3 in S is black-deletion minimal with respect to φ. ♣

The only isolated pseudofixed points of φ that are not in the centers of faces of Q_3 in S are at vertices of Q_3. Such a pseudofixed vertex is, of course, not on an oval-cycle and no two such pseudofixed vertices share edges in common nor do they have incident loops.

Claim 2. *Either every face of Q_3 in S has a pseudofixed point at its center or φ acts transitively on the faces of Q_3 in S and no face has a pseudofixed point at its center.*

Proof of Claim: The proof is the same as one direction of the proof of Lemma 9.22, with the following caveat. Two faces sharing a red edge are in the same orbit under φ and so any edge bounding two faces in different orbits is black. ♣

Based on Claim 2 and the assumptions of Case 1 we have two subcases. In Case 1.1 every face of Q_3 in S has an isolated pseudofixed point at its center and in Case 1.2 φ acts transitively on the faces of Q_3 in S and φ has no isolated pseudofixed points.

Case 1.1 Given a face f of Q_3 in S, there can be no two pseudofixed vertices in consecutive cyclic order along the facial boundary walk of f. For each f and each incidence of a pseudofixed vertex v with f, place a black edge in f connecting the vertices around the incidence of v in the boundary walk of f (see Figure 9.25). Let Q_4 be the graph obtained and note that φ extends to Q_4 and preserves the red and black colors of edges. Going from Q_3 to Q_4 is a reversal of Step 3. Let W be the vertices of Q_4 (and also Q_3) to which the new edges are attached. Note that the degree of each vertex in W goes up by two (in going from Q_3 to Q_4) for each adjacency with a pseudofixed vertex. As such the non-pseudofixed vertices of degree 2 in Q_3 have degree 6 in Q_4.

Now delete the pseudofixed vertices and their incident edges from Q_4 to obtain Q_5. This is an orbit deletion and is a reversal of Step 2. Note that every face of Q_5 in S has a pseudofixed point in its center. The degree of a vertex of Q_5 not in W is the same as its degree in Q_3. The degree of a vertex of Q_5 in W is at least 1 greater than its degree in Q_3. As such Q_5 has no vertices of degree 2.

Claim 3. *Q_5 is black-deletion minimal.*

Proof of Claim: By construction every face of Q_5 in S has an isolated pseudofixed point at its center and these are all of the isolated pseudofixed points of φ. By way of contradiction let e be a black edge such that $\mathsf{orbit}_\varphi(e)$ may be deleted from Q_5. If e borders two distinct faces, then deleting e violates the condition on more than one pseudofixed point in the interior of a face, a contradiction. If e borders the same face twice, then deletion will either violate cellularity (a contradiction) or e has an endpoint v of degree 1, also a contradiction. ♣

Now since Q_5 is black-deletion minimal, there is a maximal set of edges that we may contract to obtain an oval-irreducible surface orbit minor that is not augmentable. This is a reversal of Step 1 because Q_5 has no vertices of degree 2, as noted above.

Case 1.2 In this case, Q_3 is actually equal to Q_1. Since φ has no isolated pseudofixed points we need not do anything to reverse Steps 2 and 3.

Now since $Q_3 = Q_1$ is black-deletion minimal, there is a maximal set of edges that we may contract to obtain an oval-irreducible surface orbit minor that is not augmentable. This is a reversal of Step 1 because $Q_3 = Q_1$ has no vertices of degree 2, as noted above.

Case 2 Let C be a maximal collection of black edges (possibly empty) such that $Q_2 = Q_1/\mathsf{orbit}_\varphi(C)$ in S is a surface orbit minor of Q_1 in S. Going from Q_1 to Q_2 is a reversal of Step 1.iv. In particular this is a valid reversal when $|\varphi|/2$ is odd because the oval vertices of Q_2 have degree 4. Note that since Q_1 is black-deletion

minimal, so is Q_2. Since there are no pseudofixed points in the centers of faces, we also get that φ acts transitively on the faces of Q_2 in S.

Now we get that each vertex of Q_2 is an either an oval vertex or is pseudofixed. If v is a non-pseudofixed vertex of Q_2 in S, then there is a black edge e connecting v to a vertex w that may be pseudofixed. We must have that $\mathsf{orbit}_\varphi(e)$ is a vertex-disjoint union of stars and so $\mathsf{orbit}_\varphi(e)$ may be contracted from Q_2, a contradiction of the maximality of C.

Claim 4. *The length of the faces of Q_2 in S is at least 4.*

Proof of Claim: Since φ acts transitively on the faces of Q_2 in S, at least one edge on the boundary of each face is an oval edge. If there is a face of Q_2 in S that has length less than three, then all vertices of Q_2 are on ovals, contradicting the assumptions of Case 2. If there is a face f of Q_2 of length three, then since at least one vertex v on the boundary of f is not on an oval, f has exactly one oval edge on its boundary and two non-oval edges. Since v is pseudofixed and φ is transitive on the faces of Q_2 in S, we get that Q_2 is a double wheel in the sphere with the rim of the double wheel being the oval cycle. This contradicts the black-deletion minimality of Q_2 in S. ♣

Now let $Q_3 = Q_2^*$ and so going from Q_2 to Q_3 is a reversal of Step 1.iii. By the properties of Q_2 in the last paragraph each face of Q_3 either contains an isolated pseudofixed point at its center or contains a segment of an oval which connects the centers of a pair of antipodal edges along its boundary walk, but not both of these possibilities. Furthermore, each edge of Q_3 that transversely crosses an oval is a link (*i.e.,* not a loop). This is because the presence of such a loop would imply that some face of Q_2 has an oval edge appearing twice along its boundary walk. Such a face must then contain an isolated pseudofixed point at its center; however, all isolated pseudofixed points of φ appear at vertices of Q_2, a contradiction. Moreover, Claim 4 implies that Q_3 has minimum degree 4.

Now for each face of Q_3 containing a segment of an oval and having length greater than 4, subdivide the face into quadrilaterals with edges transversely crossing the ovals. Let the graph obtained be denoted by Q_4. Going from Q_3 to Q_4 is a reversal of Step 1.ii. So we can now let Q_5 in S be obtained from Q_4 in S by a reversal of the oval thickening operation, hence reversing Step 1.i. Now $\widetilde{Q}_5 = Q_5$ and each face of Q_5 contains an isolated pseudofixed point at its center and so Q_5 is minimal with respect to deleting edges off of the ovals. Furthermore, Q_4 has minimum degree 4 and thus Q_5 has minimum degree 3. It follows that Q_5 is a φ-orbit split of some oval-irreducible Q_6 in S.

Case 3 Note that Q_1 must be an oval-cycle and so S is the sphere or projective plane. By Theorems 4.1 and 5.1, φ reduces to a power of $\mathcal{OR}\mathcal{R}_{4k+2,\mathbf{S}}$ or a power of $\mathcal{R}_{2k,\mathbf{P}}$. In each case Q_2 is oval irreducible and so reversal of the remaining steps involves doing nothing. □

Example 1 We will determine all of the possible results of Construction 9.32 starting with $\mathcal{OR}_{2,2:1,\mathbf{K}}$ (see Figure 7.5).

First, the possible results from Step 1 are shown in the first row of Figure 9.34. Since the isolated pseudofixed points have odd index, Steps 2, 3, and 4 are omitted. The necessary applications of Step 5 to the first and third embeddings in the first row of Figure 9.34 are shown in the second row. Step 6 is now not necessary.

For all three of the embeddings to be considered in Step 7 (*i.e.,* the middle embedding of the first row and the two embeddings of the second row) the oval cycle must subdivided so that its length is even because $|\varphi|/2$ is odd and the oval cycle has an annular neighborhood.

For the embeddings shown in the second row, the path off of the oval cycle must be subdivided so that its length is odd (because the index-1 isolated pseudofixed point at its center must be in the center of a link) and at least three (for patchability). The desired 2-coloring of the vertices off of the oval cycle is now possible and the single face of the orbit subdivision has length $4t + 2$ for some t and so patching may occur in Step 8 by the results in Section 9.3.4.

For the middle embedding of the first row, the original two vertices on the oval cycle partition the subdivided oval cycle into two subpaths of lengths a and b where $a \equiv b \pmod 2$. The two paths off of the oval cycle must be subdivided at least once (for patchability) and with parity opposite to that of a and b to ensure that the resulting faces have boundaries of length $4t+2$. The desired 2-coloring is possible and now patching may occur in Step 8 by the results in Section 9.3.4.

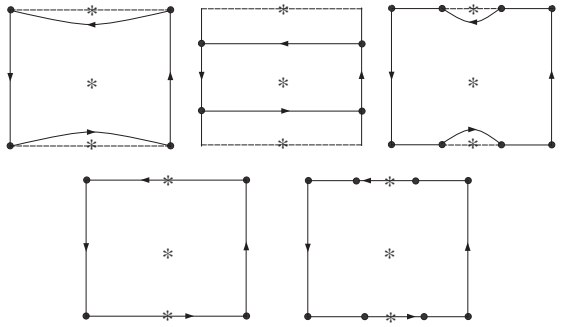

Figure 9.34.

Example 2 Let us determine all of the possible results of Construction 9.32 starting with $\mathcal{O}'_{4,1:1,2:2,\mathbf{D}}$ (see Figure 8.4). The first three embeddings in Figure 9.35 show $(\mathcal{O}'_{4,1:1,2:2,\mathbf{D}})^{\circlearrowleft}$ (the shaded region represents the hole resulting from the cut) and all of the possible results of Step 1. If we take advantage of Step 2, then the possibilities are all shown in Figure 9.28 (after shading in the central face as in Figure 9.35). Now we need only consider the results of Steps 3 and 4 that are minimal with respect to deletion off of ovals and orbit subdivisions. The only such result is shown on the right in Figure 9.35. Now Steps 5 and 6 are unnecessary (the latter is because $|\varphi|/2$ is even).

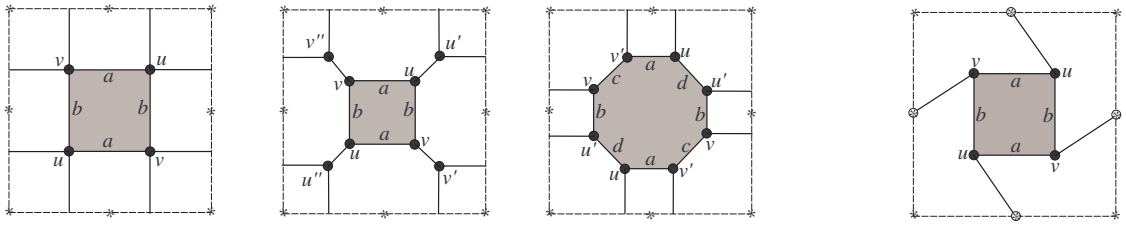

Figure 9.35.

We now describe all of the possible ways in which Steps 7 and 8 may happen.

Consider the leftmost embedding in Figure 9.35. The vertices u and v must be colored different colors so that φ will reverse the blue and green colors. So now the oval edge a must be subdivided to have length ℓ_o along with any d_o edges designated as diamond chords such that $d_o \not\equiv \ell_o \pmod 2$ (see Proposition 9.30). Do the same to the oval edge b. The non-oval edges are all in the same orbit and must be subdivided so that their lengths ℓ_v are odd in order that the 2-coloring of u and v extends. Now every closed walk satisfies the parity condition of Step 7. Now by the results of Sections 9.3.1, 9.3.2, and 9.3.3 we can find patches with the proper symmetry for Step 8.

Consider the second embedding in Figure 9.35. Again color u and v different colors and subdivide the oval edges a and b to have lengths ℓ_o along with any d_o diamond chords such that $d_o \not\equiv \ell_o \pmod 2$. The diagonal edges are subdivided to have length ℓ_s and the remaining edges, which are all in the same orbit, are subdivided to have length ℓ_v. In order to extend the 2-coloring we need that $\ell_v + 2\ell_s$ is odd. Thus ℓ_v is odd and ℓ_s is arbitrary. Now every closed walk satisfies the parity condition of Step 7 and the 2-coloring of u and v extends as well. Now by the results of Sections 9.3.1, 9.3.2, and 9.3.3 we can find patches with the proper symmetry for Step 8.

Consider the third embedding in Figure 9.35. Again color u and v different colors so that φ exchanges blue and green colors. Either color u' the same color as u or the other color. In the first case, v' must have the same color as v so that φ exchanges colors. Thus the length ℓ_o of a and b and the number of diamond chords d_o must satisfy $\ell_o \not\equiv d_o \pmod 2$ and the length of the diagonal edges on the oval, say ℓ_s, and the

number of diamond chords d_s on the diagonal edges must satisfy $\ell_s \equiv d_s \pmod 2$. If the remaining four edges of the embedding are subdivided so that their length ℓ_v is odd, then the subdivision satisfies the parity condition. The 2-coloring of the vertices will extend as well. Similarly, in the second case we need $\ell_o \equiv d_o \pmod 2$, $\ell_s \not\equiv d_s \pmod 2$, and ℓ_v even. In both cases, by the results of Sections 9.3.1, 9.3.2, and 9.3.3 we can find patches with the proper symmetry for Step 8.

For the rightmost embedding in Figure 9.35, color u and v different colors and the pseudofixed vertices p_u (adjacent to u) and p_v (adjacent to v) different colors. Either the colors of p_u and u are the same or different. The rest follows as in the previous paragraph.

Acknowledgements

The authors thank John Wierman for bringing to their attention the question of self-duality in the torus and its connection to percolation theory, and also thank Chris Bishop for offering useful suggestions in the writing stage. Finally, they thank John B. Conway for his support and encouragement.

References

[1] A. Altshuler, *Construction and enumeration of regular maps on the torus*, Discrete Math. **4** (1973), 201–217.

[2] M. S. Anderson and R. B. Richter, *Self-dual Cayley maps*, European J. Combin. **21** (2000), no. 4, 419–430.

[3] D. Archdeacon, *A survey of self-dual polyhedra*, Fourth Czechoslovakian Symposium on Combinatorics, Graphs and Complexity (Prachatice, 1990), Ann. Discrete Math., vol. 51, North-Holland, Amsterdam, 1992, pp. 5–12.

[4] ———, *Self-dual embeddings of complete multipartite graphs*, J. Graph Theory **18** (1994), no. 7, 735–749.

[5] D. Archdeacon, P. Gvozdjak, and J. Širáň, *Constructing and forbidding automorphisms in lifted maps*, Math. Slovaca **47** (1997), no. 2, 113–129.

[6] D. Archdeacon and N. Hartsfield, *Self-dual embeddings of complete bipartite graphs*, J. Combin. Theory Ser. B **54** (1992), no. 2, 249–256.

[7] D. Archdeacon and S. Negami, *The construction of self-dual projective polyhedra*, J. Combin. Theory Ser. B **59** (1993), no. 1, 122–131.

[8] D. Archdeacon and R. B. Richter, *The construction and classification of self-dual spherical polyhedra*, J. Combin. Theory Ser. B **54** (1992), no. 1, 37–63.

[9] J. S. Birman, *Braids, links, and mapping class groups*, Princeton University Press, Princeton, N.J., 1974, Annals of Mathematics Studies, No. 82.

[10] B. Bollobás and O. Riordan, *Percolation*, Cambridge University Press, New York, 2006.

[11] T. Breuer, *Characters and automorphism groups of compact Riemann surfaces*, London Mathematical Society Lecture Note Series, vol. 280, Cambridge University Press, Cambridge, 2000.

[12] S. A. Broughton, *Classifying finite group actions on surfaces of low genus*, J. Pure Appl. Algebra **69** (1991), no. 3, 233–270.

[13] J. H. Conway, H. Burgiel, and C. Goodman-Strauss, *The symmetries of things*, A K Peters Ltd., Wellesley, MA, 2008.

[14] J. H. Conway and D. H. Huson, *The orbifold notation for two-dimensional groups*, Structural Chemistry **13** (2002), no. 3/4, 247–257.

[15] H. S. M. Coxeter and W. O. J. Moser, *Generators and relations for discrete groups*, fourth ed., Ergebnisse der Mathematik und ihrer Grenzgebiete [Results in Mathematics and Related Areas], vol. 14, Springer-Verlag, Berlin, 1980.

[16] M. Dehn, *Die Gruppe der Abbildungsklassen*, Acta Math. **69** (1938), no. 1, 135–206, Das arithmetische Feld auf Flächen.

[17] P. Giblin, *Graphs, surfaces and homology*, third ed., Cambridge University Press, Cambridge, 2010.

[18] J. L. Gross and T. W. Tucker, *Topological graph theory*, Wiley-Interscience Series in Discrete Mathematics and Optimization, John Wiley & Sons Inc., New York, 1987, A Wiley-Interscience Publication.

[19] A. Kuribayashi and H. Kimura, *Automorphism groups of compact Riemann surfaces of genus five*, J. Algebra **134** (1990), no. 1, 80–103.

[20] I. Kuribayashi and A. Kuribayashi, *Automorphism groups of compact Riemann surfaces of genera three and four*, J. Pure Appl. Algebra **65** (1990), no. 3, 277–292.

[21] W. B. R. Lickorish, *A finite set of generators for the homeotopy group of a* 2*-manifold*, Proc. Cambridge Philos. Soc. **60** (1964), 769–778.

[22] A. Malnič, R. Nedela, and M. Škoviera, *Lifting graph automorphisms by voltage assignments*, European J. Combin. **21** (2000), no. 7, 927–947.

[23] W. S. Massey, *A basic course in algebraic topology*, Graduate Texts in Mathematics, vol. 127, Springer-Verlag, New York, 1991.

[24] A. Nakamoto, *Irreducible quadrangulations of the Klein bottle*, Yokohama Math. J. **43** (1995), no. 2, 125–139.

[25] ———, *Diagonal transformations in quadrangulations of surfaces*, J. Graph Theory **21** (1996), no. 3, 289–299.

[26] ———, *Irreducible quadrangulations of the torus*, J. Combin. Theory Ser. B **67** (1996), no. 2, 183–201.

[27] ———, *Generating quadrangulations of surfaces with minimum degree at least* 3, J. Graph Theory **30** (1999), no. 3, 223–234.

[28] D. Pellicer and A. I. Weiss, *Uniform maps on surfaces of non-negative euler characteristic*, Symmetry Culture Science **22** (2011), no. 1-2, 159–196.

[29] B. Servatius and P. R. Christopher, *Construction of self-dual graphs*, Amer. Math. Monthly **99** (1992), no. 2, 153–158.

[30] B. Servatius and H. Servatius, *Self-dual maps on the sphere*, Discrete Math. **134** (1994), no. 1-3, 139–150, Algebraic and topological methods in graph theory (Lake Bled, 1991).

[31] ———, *The* 24 *symmetry pairings of self-dual maps on the sphere*, Discrete Math. **140** (1995), no. 1-3, 167–183.

[32] ———, *Self-dual graphs*, Discrete Math. **149** (1996), no. 1-3, 223–232.

[33] ———, *Symmetry, automorphisms, and self-duality of infinite planar graphs and tilings*, International Scientific Conference on Mathematics. Proceedings (Žilina, 1998), Univ. Žilina, Žilina, 1998, pp. 83–116.

[34] J. Širáň, *Coverings of graphs and maps, orthogonality, and eigenvectors*, J. Algebraic Combin. **14** (2001), no. 1, 57–72.

[35] J. Širáň and T. W. Tucker, *Symmetric maps*, Topics in topological graph theory, Encyclopedia Math. Appl., vol. 128, Cambridge Univ. Press, Cambridge, 2009, pp. 199–224.

[36] S. Stahl, *Self-dual embeddings of Cayley graphs*, J. Combin. Theory Ser. B **27** (1979), no. 1, 92–107.

[37] J. Stillwell, *Classical topology and combinatorial group theory*, second ed., Graduate Texts in Mathematics, vol. 72, Springer-Verlag, New York, 1993.

[38] D. B. Surowski, *Lifting map automorphisms and Macbeath's theorem*, J. Combin. Theory Ser. B **50** (1990), no. 2, 135–149.

[39] C. Thomassen, *Tilings of the torus and the Klein bottle and vertex-transitive graphs on a fixed surface*, Trans. Amer. Math. Soc. **323** (1991), no. 2, 605–635.

[40] W. Thurston, *The geometry and topology of 3-manifolds*, Tech. report, Princeton University, 1980, Chapter 13, electronic version available at http://library.msri.org/books/gt3m.

[41] T. W. Tucker, *Finite groups acting on surfaces and the genus of a group*, J. Combin. Theory Ser. B **34** (1983), no. 1, 82–98.

[42] A. T. White, *Orientable imbeddings of Cayley graphs*, Duke Math. J. **41** (1974), 353–371.

[43] H. Whitney, *2-Isomorphic Graphs*, Amer. J. Math. **55** (1933), no. 1-4, 245–254.

[44] J. C. Wierman, *Construction of infinite self-dual graphs*, Proceedings of the 5th Hawaii International Conference on Statistics, Mathematics and Related Fields, 2006.

[45] T. Zaslavsky, *Biased graphs. I. Bias, balance, and gains*, J. Combin. Theory Ser. B **47** (1989), no. 1, 32–52.

[46] R. M. Ziff and C. R. Scullard, *Exact bond percolation thresholds in two dimensions*, J. Phys. A: Math. Gen. **39** (2006), 15083–15090.